A Framework For Representing Objects in Cellular Automata

by

Cody Tischler

A thesis submitted in partial fulfillment of the requirements for the degree of

Master of Science

in

Chemical Engineering

Department of Chemical and Materials Engineering
University of Alberta

Abstract

Cellular automata consistently grow in relevance to engineering and science as computation becomes more important for design and theoretical analysis. Although cellular automata have been used for a variety of tasks a means of representing objects has not yet been devised. This is a severe limitation for cellular automata as objects are the ultimate means for systematically describing physical systems. In an effort to construct objects in cellular automata a discrete structure called an event-lattice was developed. It refines the definition of an event to have explicit extension in time and space. Using Alfred North Whitehead's conception of what distinguishes an actual entity from an object a framework for objects could be devised under the assumption that a finite volume of space-time contains a finite amount of information. An external binary operation uses a finite set of symbols to give the event-lattice its structure and also acts as a set used to construct objects. The set of occurrences of all objects in the lattice is representable as the free group generated by the set of symbols. This particular structure was inspired by the Lattice Gas Automaton. This conception of objects has a number of agreeable properties beyond the applications of simulation.

As the point particle is arguably the most important object for description a point particle model was developed and investigated. An algorithm is identified such that particles may maintain their identities by having unique spatial coordinates at all times. Interactions amongst these particles were generalized and studied using a momentum balance. A discretized form of the Navier-Stokes equation was obtained. When the generalized interactions are organized as a vector the evolution of the system closely resembles the collision step of the Lattice Boltzmann Method which was then retrofitted and used to study the point particle model further. The most important directions for further research are in the compact representations of objects as sequences.

Acknowledgements

First and foremost I would like to express gratitude for my supervisor Dr. Qingxia Liu. None of this work could have come to fruition had Dr. Liu not provided me the time necessary for free enquiry into many diverse subjects. His support, interest, and feedback provided valuable impetus. Secondly, my gratitude goes to my friends and family who have offered endless support. In particular discussions with André-Marie Lumanglas, Chao Qi, Carl Corbett, Jonathan Malainey, and Joshua Ianes have been most productive. I thank my father for challenge and inspiration, my mother for reassurance and support, my step-father for interest and inquiry, and my step-mother for guidance and understanding. Lastly, I would like to mention the names of those intellectual giants I most greatly admire, Alan Watts, Alfred North Whitehead, and Alfred Korzybski. Their works have been a constant source of inspiration and suggestion throughout this process.

Contents

List of Figures

Chapter 1

Introduction

This thesis concerns itself with the task of representing objects in computers for the purpose of simulating physical systems. What is meant by a physical system is a system that can be described in terms of time, space, and matter. [1] Motivation for this research arose from the challenges associated with simulating nanoscale fluid systems. Many important industrial and biological processes are carried out in environments which are best described as nanofluidic. The objects of investigation are on the order of nanometers and interact within a solvent basin larger than themselves but by no means macroscopic. The self assembly of colloidal materials, reaction-diffusion at and around catalyst sites, and the folding of proteins are important examples. Construction and design of technology at this order of magnitude presents wonderful opportunities along with serious engineering challenges. Computer simulation, so long as it can be efficiently applied provides an indispensable technique of design, analysis, and investigation in this area of research. However, many systems are beyond the reach of current simulation techniques due to the shear magnitude of entities involved and the complexity of their interactions.

The work of Toffoli provides interesting ideas for how to approach these problems from a pragmatic standpoint. [2] Toffoli's main dilemma was that physical description has always been influenced by the nature of the available computational tools for its formulation and expression and that as computational technology evolves so too should the means of physical description. The most pernicious feature of the past formulations being the use of continuums. Although appropriate for analytic derivation, mathematical descriptions which utilize continuums must undergo discretization in order to be expressed in a computational environment. As the overwhelming majority of cases are only solvable numerically, i.e. very few systems admit analytic solutions, Toffoli analyzed

cellular automata as an alternative rather than an approximation of differential equations. He questioned whether differential equations should be the starting point for computer simulation of physical systems noting that differential equations are already an abstraction of the underlying reality as a continuum, abstracted again in discretization to create a system of linear equations, and then abstracted a third time in projecting real valued variables onto finite computer words. The central question underlying Toffoli's work is how can we innovate upon then means of physical description such that the framework of physical description is itself isomorphic to the framework and structure of the computer. This framework of course being of a discrete nature. The bet is that a discrete framework naturally attuned to the discrete computational environment will be orders of magnitude faster and more effective with no rounding error, such that simulations will stand with the authority of mathematical theorems yet maintain a direct relevance to physical systems as they were devised in that framework.

Toffoli's dilemma was of pragmatic character but the general concern was not new. For instance Feynman in his later years inquired about the nature of computation as a means for understanding quantum mechanics. [3] He analyzed consequences of the proposition that there is a simulation that behaves exactly like the contents of a finite space-time volume with a finite number of logical operations. Cellular automata find their way into his enquiry by nature of their local behaviour thereby satisfying his condition that the number of logical operations should grow proportionally, not exponentially, to the volume of space-time under consideration. Similar ideals of a finite amount of information in a finite volume of space-time have been espoused by 't Hooft although on entirely different lines of thought. By finding success with non-local probabilistic quantum mechanical predictions applied to results of local, determnisitic cellular automata 't Hooft has begun to question the generally accepted interpretations of quantum mechanics. [4]

All three, Toffoli, Feynman, and 't Hooft have been influenced by Fredkin and his continuous efforts to create a cellular automaton which can be programmed to act like physics. [5] Fredkin developed his digital mechanics in companion with his digital philosophy which centers around the fundamental assumption that all physical processes are discrete by nature, and accordingly have a fundamental representation as information processes. The motivating issue is that the use of continuums in physical description require that a volume of space-time, no matter how small, will always contain an infinite amount of information. One can very well suspect that the main

subject of these ideas of finite information in a finite space-time volume are following a thematic trend of our era in the information age. [6] Ideas about the equivalence between information and physical processes obtained concreteness by the mathematical theory of communication of Shannon in finding that the measure of average information and Boltzmann's formulation of entropy have identical form. [7] This relation was long anticipated by Maxwell and his Demon. [8, 9] Yet, there was something different about Toffoli's work that was implicit in his exposition and also shared by 't Hooft. Namely that frameworks for physical description are tools and that they should be understood and innovated as such.

Frameworks for physical description or frameworks in short are for describing, not explaining physical processes. Even if Fredkin's program reaches perfection in that a universal cellular automaton is found which can exhibit all of the abilities of matter and predict new features of the microscopic world that no other mechanical theory has yet obtained there will still be doubt in regards to it as having any absolute truth. In the same way that a camera being able to create images of a variety of disparate objects is not evidence that the world is pixelated so too symbolic physical theories are unable to assert their own absolute truths by agreement with empirical facts. This does not mean they are not useful and valuable. It is simply that a mechanical theory is a framework for description which in itself enforces the general rules or at least has the potential to enforce the general rules which have been deemed true of objects. Conservation of energy and momentum, the finite speed of light and uncertainty are examples of the general rules of objects which a framework must have the capacity to exhibit in order for use in physical description. When a framework of description can maintain these rules it can be used to describe a multiplicity of systems without concern of violating what is agreed upon as physical law. Since these laws generally apply and the framework follows these laws it can then be predictive about the behaviour of actual objects, useful for simulation, and aid in the efforts of engineering. The task of finding finite representations of objects suitable for computers is then a pragmatic effort but it cannot be avoided that any advances on this front have theoretical content.

Automata, as direct models of computation, could not be better suited to solving Toffoli's dilemma. The potential of automata for physical simulation and modelling has long been recognized even before their cellular conception by von Neummann and have proved to be powerful means of simulating complicated systems. [10] Their theoretical merits have also been affirmed by the

work of Nobel Laureate's Feynman and 't Hooft. However, as literal models of complexity their general application to physical simulation is far from trivial. [11] Aside from single particles with unit velocities, objects in all their usefulness and practicality, as physical entities or as conceptual conveniences constituting the basis of physical description, are not yet liable to formulation in cellular automata. This thesis addresses this problem directly in an effort to find a framework for representing objects within cellular automata, not as emergent entities but as discrete computable structures.

Such a framework can be constructed. It begins first with an understanding of what simulation constitutes for science, why automata can play a profound role, and why the inclusion of objects is important. Secondly one must know what is really meant by an object as opposed to an entity or an event. The process metaphysics of Whitehead has proved to be an in-exhaustible mine of suggestion on this front. Thirdly, knowing which features of cellular automata have proved useful in the past is necessary for success in the present. With this background in hand we can then embark on the task of constructing a framework for representing objects in cellular automata.

Chapter 2

Background

2.1 The Appeal of Cellular Automata

Science as a practice is concerned with the objective understanding of the actual world. Objective signifying that science comprises of an understanding we can all agree on. The empirical aspect of science demands that the understanding itself be liable to falsification through experiment. In order that a given understanding of a phenomenon be falsifiable it must in some way be compared to the phenomenon itself. The first task is to give a description of the phenomenon such that the description can be used to make predictions. These descriptions are to be exact as possible but are not definitions. A description in this sense is to be understood as a symbolic representation of the phenomenon. But the representation itself as ink on paper is a completely separate and independent thing in the actual world which allows it to be an object of agreement. The fact that it may ever be considered a representation results from a structural similarity shared between the actual phenomenon and the symbolic description. The process of description in science is to give a symbolic representations of phenomena and is a means of expressing a given hypothesis in objective form. This symbolic form cannot be just any old squiggle of ink on paper. A systematic framework of description is necessary. In particular what is required is some description which exists in a framework such that alterations in the description correspond to alterations in experiment which lead to testable consequences that are reflected in the description as indicated by the framework. An example of a description of a phenomenon would be the truth value of the sentence of 'if $\boldsymbol{p}$ then $\boldsymbol{q}$,' compactly, $\boldsymbol{p} \rightarrow \boldsymbol{q}$. Suppose $\boldsymbol{p} \rightarrow \boldsymbol{q}$ to be a hypothesis or theory. By itself $\boldsymbol{p} \rightarrow \boldsymbol{q}$ is

nothing but ink on paper or a contrast of pixels. It is only in the framework of logic that this becomes a scientific description of some sort. Supposing the scientific description to be $\boldsymbol{p} \rightarrow \boldsymbol{q}$ then it follows that if $\boldsymbol{p}$ is made to be true then $\boldsymbol{q}$ should be observed. If there is indeed $\boldsymbol{p}$ and then $\boldsymbol{q}$ is not observed the framework of logic says the description is false, and indeed the scientist would conclude the hypothesis or theory is false. It is the framework of logic that allowed the description as description to be falsified.

Newtonian mechanics is a framework to describe the motion of point particles, statistical mechanics is a framework to describe ensembles of particles, thermodynamics to describe work and energy, relativity to describe energy and space-time curvature, and quantum mechanics to describe wavefunctions. The descriptive power of a framework can always be increased through addition or improvement of the supposed objects. For instance, the transition of classical mechanics to quantum mechanics is like the transition from a black and white television to a color television. Naturally a complex probability amplitude has more descriptive power for expressing the position of an object than the Newtonian binary conception that the particle is either there or not there. In the same way color pictures have more descriptive power than binary black and white images. However it is often times much more preferable to use a black and white image just as it is often much better to use Newtonian mechanics as opposed to quantum mechanics for describing some objects.

One may inquire as to what framework is the true framework. None of them. They are not truths, they are frameworks for describing physical systems to a degree of accuracy. The effectiveness of a framework is just as much constituted by what the framework can include as well as what it can leave out. Consider the following circumstances: (i) an electron fired in a cathode ray tube, (ii) an electron on a nano scale crystal surface, (iii) a person being fired from a cannon, and (iv) a person choosing a seat in a café. All of these cases can be found in the external world and on the basis of the fallacy of misplaced concreteness none can be taken as more fundamental than any other. [12] Cases (i) and (iii) are liable to the Newtonian framework. Newtonian mechanics can give a good prediction where the human will end up given the angle of the cannon, mass of the human, initial velocity and so forth. Similarly a cathode ray tube can be designed to project the electron at a screen to such a degree of accuracy that you could use the system to watch a video. Cases (ii) and (iv) however are beyond the Newtonian framework's domain. Neither the exact position of the

electron on the surface, nor the final seating choice in the café can be predicted with certainty or even be well defined for that matter.

As computers can express a great variety of descriptions and enforce their associated frameworks it is natural to inquire about a common framework inherent in computers which all these other frameworks are expressed in terms of. Certainly if this framework can be instantiated as any other framework than it has a universal character.

Fundamentally computers process information. Automata, or finite state machines, are mathematical models of devices which process information by giving responses to inputs. [13] Hence their appeal. Formally one may consider an automaton as a tuple consisting of a set of states Q, inputs X, outputs Y, and a transition function $\delta : X \times Q \to Y \times Q$. [14, 15] When the automaton is in a given state and receives an input it produces an output and selects a new state as determined by the transition function. Most often the state of the automaton is identical to its output such that the automaton consists solely of the tuple (Q, X, δ). When many automata are working in concert with each other it is necessary to have a clock such that the automata all update their states at the same time. Automata have much in common with semi-groups and formal languages and were intensively studied as models of computation. [16] It is no surprise that the computer, granted this general framework, can replicate a wide variety of frameworks.

The basic applicability of automata can be elucidated by describing a system at multiple orders. Take flowing water as an example. In one case the water may be divided into elements extended in space and considered over a duration. The states of the various fluid elements become velocity and pressure. The next state of the fluid element is determined by its current state and the state of surrounding elements guided by some transition function such as the Navier-Stokes equation. Further the water molecules may be identified as the elements with states of position and momentum. The next state being a function of its state and the states of the other molecules guided by some transition function such as Newton's Laws of motion in molecular dynamics. Automata are absolute generalizations of this basic notion. So long as the system may be divided into things and states may be specified for the things the system can be viewed in terms of automata. This is supported by the wide variety of uses automata have found in scientific applications. The most prominent automata for physical description have been cellular automata.

Cellular automata are a type of automata where all the automatons are organized in space like a

grid of cells. Thus the cellular structure constitutes a spatial basis where automaton events can take place. [17] Each automaton uses the states of the neighboring automata as inputs for determining its next state. The set of all the neighbors comprise the neighborhood of the automaton, and accordingly the set of inputs X is then the total set of states the neighborhood can be in. If there are N neighbors and each automaton can be in k states then there are $k^N = |X|$ possible inputs. Von Neumann first used cellular automata for his basic theory of self-reproduction. [10] The cellular arrangement was suggested to him by Ulam who was interested in the interaction of finite sets of particles, too many for analytical methods but too few for probabilistic analysis to be meaningful. [18, 19] Creating self-reproducing systems out of cellular automata were further conducted by Codd, Devore, and Langton. [20–22]

Aside from the natural implementation of automata in computation cellular automata have proved useful for the physical modeling of polymer conformation and dynamics [23, 24], complex reaction-diffusion schemes [25–27], urban growth prediciton [28–30], the dynamics of how diseases spread in the study of pandemics [31,32], biological modelling for pattern formation [33–35], molecular self assembly [36–38], traffic flow simulation and dynamics [39–41], the behaviour of pedestrians and crowds [42, 43], artificial life [44], and population dynamics. [45–47] The largest resource for cellular automata applications is found in the proceedings of the ACRI International Conference on Cellular Automata for Research and Industry. The major topics included are cellular automata theory and implmentation, computational theory, population dynamics, physical, urban, environmental, traffic, crowd, swarm, and social modeling, boolean networks, multi-agent systems, robotics, crypotgraphy, dynamical systems, cellular automata based hardware, natural computing, and pattern classification [48–54].

The wide application of this framework to diverse areas speaks to the potential of cellular automata for physical description but only a handful of models, namely traffic simulation and hydrodynamics, have reached a level of practical use. A seemingly endless search is ahead for finding transition functions which are universally applicable to physical systems without generating an unbearable degree of complexity. In fact cellular automata are widely noted for exhibiting extremely complex behaviour with very simple rules. [11, 55, 56]

In the early 20th century Einstein generated the field equations which describe the geometry of space-time given the energy and momentum distributed within it. That is, given a distribution of

energy in space, Einstein's field equations yield the geometry of the space-time which in turn yields gravity. Aside from these relations, the general theory of relativity does not provide any basis as to how the energy distribution evolves in and of itself. The task of determining the evolution of the energy distribution in itself has its natural home in the subject of mechanics. Prior to the application of a mechanical theory the existence of a something somewhere is posited. It then proceeds to derive the evolution of the state of this something as it goes somewhere as per the rules of the mechanical theory. This something is an object, and this somewhere is in space-time. As objects are representations for the energy and momentum in the system, mechanics effectively provides a way for describing the evolution of an energy distribution in space-time through objects. Advances in mechanical theories are often accompanied by an innovation in the nature of the object that was posited, for example point particles, waves, fields, ethers, and probability amplitudes are examples of objects which have different descriptive powers, advantages and disadvantages, pending the system undergoing description.

In the theoretical development of cellular automata much focus has been placed on trying to make physics emerge and not enough has been focused on expanding the range of its applicability to already known problems. Although cellular automata utilize a powerful and general framework their current formulation does not allow for the easy and ready implementation of objects i.e. those things which have proved so productive since the inception of science centuries ago and enjoy an ultimate generality of application. Ultimately some synthesis between the notion of objects and the framework of cellular automata will be necessary to extend this framework to the larger purpose of physical description.

2.2 The Process Conception of Objects

A brief survey of the environment may suggest objects are forms taken by substance. But if substance is investigated and described it is found to be composed of objects. Watts provides a useful thought experiement for elucidating the dilemma of what constitutes an object. [58] Consider a string made of a blue string, green string, and red string tied together such that one end of the green string is tied to an end of the blue string and the other end of the green string is tied to an end of the red string. If we were to tie a knot into the blue string, and then wiggle it across the

string without undoing the knot until it was completely in the red part of the string we can ask "is it the same knot?" It is by virtue of it having the same form and so it is recognizable as the knot throughout the wiggling process. But the knot at the beginning was composed of blue string and only blue string, in the middle it was made of green and only green string, and in the end it is made of red and only red string. We can then untie the knot and it no longer exists. The object of the knot was not substance but we do not find ground to deny its existence. In the same way that a whirlpool in a river does not consist of any particular set of water molecules but instead is a flux of water, or a university is a flux of students, teachers, bricks, and books, the knot was recognizable as the knot and it was convenient to call it so. Watts makes the case an object is a noun, i.e. it is a name given to a recognizable form for convenience of description and communication.

On a further basis our language as a system which we participate in requires identification of objects. For instance Quine recognized that language as a social institution requires physical objects as common denominators of individual sense experiences. [59] What is not so well indicated by Quine is that we did indeed invent the objects as they are understood. A tree leaf does not exist as a thing separate from a tree but it is readily considered in common speech as an individual object. We cannot define a single entity without artificially, albeit conveniently, separating it from the rest of actuality. The leaf may indeed be plucked from a branch and called individual, but the leaf never springs alone. Korzybski describes this viewpoint in wider scope. In his general semantics Korzybski cautions against mistaking the map for the territory in that the real objects which make up the actual world are on an un-speakable objective level. He claims that the only link between the objective and verbal world is of structural content i.e. a complex of relations, concluding that objects may be considered as names for relations among microscopic events. [60] From this point of view the name leaf is indeed the relationship between a collection of plant cells amongst themselves and equally a relationship between them and our experience of that collective. This in turn requires the description of the plant cells as molecules in the same way *ad infinitum*. The result of this is that we cannot describe or attribute any properties to an individual object without specifying other entities to describe it in terms of because the only inherent knowledge in the description is the structure.

Whitehead, whom no doubt influenced Watts, Quine, and Korzybski on this matter, admits as a fundamental truth that objectification is abstraction and bears the important role of blocking out

unwanted detail. [61, p. 154] Whitehead's process metaphysics provides an interesting means of getting a hold of the knot in Watts' thought experiment. It is also appealing in that the cosmology of the process metaphysics has an algorithmic character. Process philosophy recognizes the difference between the instances of the knot as bare experiential fact but yet all participating in a recognizable form. Throughout the wiggling process the knot was at one time composed purely of blue string, another time purely of green string and another time as purely red string. Each of these instances of the knot Whitehead terms an actual entity or an actual occasion. They are undeniable truths of happening in the world, each unique and independent of one another. In this sense they are events with extension in time and extension in space. Each of these three events is enveloped by the total event of the knot from being tied to untied and each of the three events envelope other events of the knot. For instance over a duration where the knot was composed of green and only green string there was still a flux of air into and out of the threads of the string, and Brownian motion of the molecules making it up causing it to be in different states, each of these being an actual occasion or an actual entity in their own right. In terms of actual entities there is not the blue knot turning into a green knot turning into a red knot. There was a blue knot and then a green knot and then a red knot. When the red knot is, the green knot isn't. To borrow from Watts, spring does not become summer - there is spring and then there is summer. It is important to realize it is these actual occasions as determinate matters of fact i.e. things that have happened, which are the only content of subjective experience and thus the only data of empirical investigation. Beyond the subjective experience there is bare nothingness. [61, p. 254]

Accordingly in the present actual entities are perishing and others are in becoming. In becoming, actual entities are always novel as they arise in the present which is a state of objective facts never hitherto experienced. In their perishing they add their novelty to the objective facts. [61, p. 134] Objects are then the recognizable forms which are constituted by actual occasions. That is an object is a series of actual entities which all participate in the objective form of that object. Accordingly objects are persistent while actual entities are fleeting. Whitehead actually calls them eternal objects due to their similarity with Platonic forms.

A vortex in a stream is a useful image. Vortexes form and are persistent but there is no definite persistent substance that forms the vortex for the duration of its existence. In process philosophy all persistent things are objects and not composed of substance but arise from recognizable patterns of

actual occasions which are events. A full elucidation of the process philosophy cannot be undertaken here. Actual entities along with eternal objects play many more roles then those ascribed above and are necessary for Whitehead's full conception. But the details given are sufficient for a satisfactory notion of objects that can be realized in practice. The discrete character of actual occasions participating in succession as the basis for objects relieves us of having to define substance before defining objects as they may be solely given as collections of events which are recognizable over durations beyond the actual occasions. We now turn to the Lattice Gas Automaton in search of the feature from which it derives its utility.

2.3 Useful Features of Lattice Gas Automata

In 1973, Hardy, Pomeau, and de Pazzis introduced a fully deterministic two-dimensional cellular automata model to better understand hydrodynamic relaxation processes [62]. This model was the original Lattice Gas Automaton (LGA). The model consists of cells organized as a grid on a plane. Each cell has four sites and each site may be in one of two states thus the state of each cell may be represented by four bits. Each cell is an automaton. The neighborhood consists of the four cells sharing an edge with the given cell known as the von Neumann neighborhood. Each site has an associated velocity. The four velocities corresponding to the four sites are $(1, 0)$, $(0, 1)$, $(-1, 0)$, and $(0, -1)$ for the standard (x, y) plane. If a site in a cell is 'occupied' then the interpretation is that there is a particle at that cell with the velocity associated with that site. Particles being in the same cell with the same velocity are not allowed and so long as the initial state of the LGA does not violate this condition it will never violate it thereafter. The model is endowed with an evolution mapping which consists of a streaming process and a collision process. In the streaming process a particle moves from its cell into the adjacent cell as given by the velocity. But there are no actual particles, only cells with sites and their occupancy states. Thus the streaming process is actually the activation of states. Take any given cell (an automaton). If the cell below that i.e. in the $(0, -1)$ direction from it, has the site with associated velocity $(0, 1)$ occupied then through the streaming process the given cell's $(0, 1)$ site will become occupied. If the cell below the given cell does not have the same situation i.e. there is not a cell below it that has the $(0, 1)$ site occupied then it will become unoccupied. Thus when a cell has the site with velocity $(0, 1)$ occupied the

streaming consists in causing the $(0,1)$ site in the $(0,1)$ direction to become occupied and then accordingly the $(0,1)$ site which was occupied turns to become unoccupied.

Thus a single particle would appear to propagate in the direction in accordance with the unit velocity of the site it occupies. But there is no particle, only the progression of states which may be interpreted as a particle. In this way the LGA achieves the appearance of an object without ever referencing an object. After each streaming process a collision process occurs. If on a given cell two sites with opposite velocity are occupied and the other sites are unoccupied then the occupied states become unoccupied and the unoccupied states become occupied. As an interpretation in terms of particles the collision process results in the velocities of two particles directed at one another in the same cell being rotated by 90 degrees. A visual aid is found in Figure 2.1. Three time steps are indicated. From t_1 to t_2 is a streaming process, from t_2 to the second t_2 is a collision process which is instantaneous, and from t_2 to t_3 is another streaming process. A white dot with black outline acts as a reference for each time step. The streaming process and collision process together form a

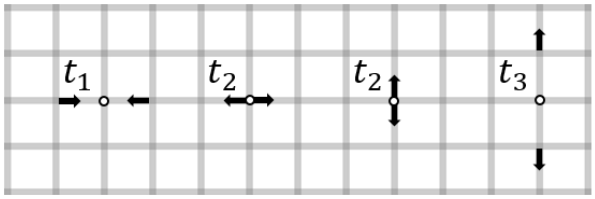

Figure 2.1: A demonstration of streaming and collision steps in the Lattice Gas Automaton

single evolution of the system. It is clear that each evolution operation conserves linear momentum, kinetic energy, and mass. This conservation is afforded by the highly discretized velocities and 90 degree rotation. Although intuitive and conceptually simple to explain, the mathematical formulation of the model does not take a form familiar to the differential equations normally encountered in hydrodynamics. However the set-theoretic formulation allows for investigation of infinite systems, which the creators of the LGA were highly interested in. However it could not be ignored that the LGA had salient computational features, namely that it was a completely discretized formulation which made it highly appropriate for the finite architecture which all computers are endowed with and the locality of the interactions made it trivial to parallelize. The same authors further investigated the model by deriving Navier-Stokes hydrodynamical equations, modes, and numerically

calculated the time correlations corresponding to the transport coefficients obtained by the Navier-Stokes equation and Green-Kubo formulas [63]. Aside from its defects of lack of Galilean invariance and rotational symmetry the model was a great success and marks a milestone in computational fluid dynamics.

Approximately a decade later Frisch, Hasslacher, and Pomeau named the orignal lattice gas automaton the HPP model and presented the the FHP model [64]. The FHP model used a triangular lattice such that the neighborhood of any point is hexagonal. This simple change allowed the momentum flux tensor to become isotropic and give the correct form for the Navier-Stokes equation at low Mach number in two dimensions. There were then six sites, one for each direction on the hexagonal neighborhood. In this work the authors stressed the power of the finite models potential for parallel simulation. In the same year Orzag and Yakhot argued the computational requirements for these cellular automata models are much more severe than for solutions of the continuum equations themselves [65]. These challenges were at the same time being met with improvements in hardware. [66] While analytical interest continued the numerical challenge was quickly met by the efforts of McNamara and Zanetti in 1988 [67], and Higuera, Jiménez, and Succi in 1989 [68, 69]. In these works the authors implemented the Lattice Boltzmann Equation (LBE) as collision rules for the LGA. The LBE as it was then used was already obtained by Frisch et al in 1987. [70] In this alteration the occupancy of a lattice site changed from being boolean to a continuous value. The shift was that instead of the state of the cells representing a given particle or not the state of the cell would represent the velocity distribution of particles at that point in the domain. The Boltzmann equation could then be applied directly to the evolution of these distributions. This move broke away from the finite tradition thus far but it maintained the inherent locality of interaction and thus the parallelism of the method. Still it was a lattice model and there remained a degree of freedom in each cell for every neighboring cell.

After this point two schools of thought emerged. In 1992 Qian, d'Humières, and Lallemand presented a single relaxation time model where the Bhatnagar-Gross-Krook collision process is used to relax the velocity distribution values to the equilibirum velocity distribution. [71,72] A near identical model by was presented Chen et al. at the same time [73]. In the same year d'Humières strove to remove the constraints of the standard equilibrium distribution function by adding new degrees of freedom thereby creating the multiple relaxation times model which was originally called

the generalized lattice-boltzmann equations. [74] The multiple relaxation times model is superior to the single relaxation time model but the latter is more popular due its simplicity. [75]

The LBM single relaxation time may be directly derived from the Boltzmann Equation to obtain the Lattice Boltzmann Equation which is then separated into a streaming process and a collision process. [76] The cells are related by velocity vectors $\boldsymbol{c}_k$, $k = 0, 1, 2...K$ where $k = 0$ refers to the zero vector or the vector from a cell to itself. These $\boldsymbol{c}_k$ velocity vectors have a simple interpretation. Suppose there to be a cell with position x and at that cell at time t a particle has velocity $\boldsymbol{c}_k$. Then at the next time step $t + \Delta t$ the particle will be at the cell located at $\boldsymbol{x} + \boldsymbol{c}_k \Delta t$. This cell which the particle arrives at is the k^{th} cell relative to the first cell. The discrete distribution function of particles in a cell is a set f_k, $k = 0, 1, 2...K$ where each member of the distribution function f_k is the number of particles in the cell with velocity $\boldsymbol{c}_k$. The streaming step can then be stated as

$$f_k(\boldsymbol{x} + \boldsymbol{c}_k \Delta t, t + \Delta t) = f_k(\boldsymbol{x}, t) \tag{2.1}$$

A natural consequence is that the lattice has a maximum velocity $\Delta x/\Delta t$ often taken to be the speed of sound. Whereas the streaming process handles the particle-space relations, the collision process handles the particle-particle relations. The collision process causes the distribution function, the set f_k, to tend towards an equilibrium distribution f_k^{eq} in accordance with the average velocity of the fluid in the cell. The collision step is computed as

$$f_k(\boldsymbol{x}, t + \Delta t) = f_k(\boldsymbol{x}, t)[1 - \frac{\Delta t}{\tau}] + \frac{\Delta t}{\tau} f_k^{eq}(\boldsymbol{x}, t) \tag{2.2}$$

and occurs at a single cell. It does not alter the net velocity at the cell but redistributes the amount of particles in each f_k due to collision. The LBM marked a great innovation of the LGA and has become a powerful technique of computational fluid dynamics. [77] Accordingly it has caused a great deal of attention to be paid to cellular automata models in general and speaks to the potential which was implicit in the LGA formulation.

It is however not so much what has changed in the evolution of the LGA into the LBM that matters here. The more important question to ask is what feature the LGA and LBM share. For instance this feature was necessary when Succi and Benzi extended the Lattice Boltzmann Method

to non-relativistic quantum mechanics. [78] It was also useful for Meyer in building upon the works of Grössing and Zeilinger for making cellular automaton based quantum algorithms [79–82].

The critical feature of the LGA is that each state has specific relevance to the members of the neighborhood. Recognizing the value and productivity of this feature it became the appropriate place to begin developing a means for representing objects in cellular automata. It manifests itself in the following work through an external binary operation $\sigma : S \times \Gamma \to \Gamma$ where S is a finite set of symbols and Γ is a set of cells. The set S plays the dual role of giving spatial relations amongst cells via σ and also acting as a set of states for the cells. The result is a direct relation between the states of the cells and the members of the neighborhood.

Chapter 3

Objects as Action Sequences

In preparation for the ensuing discussion it is worthwhile to point out some basic forms of spatial abstraction so as to give an idea as to what is meant in the following. In the most basic form of physical space the point is the fundamental yet undefined feature. A point is the ideal of absolutely no spatial extension and is given by a set of coordinates. A set of points is the basis of a space. Since no object is like a point, they are spatially extended, the point does not actually refer to an object directly but instead refers to a derivative notion of it such as a center of mass or center of charge. The use of a distance dependent interaction such as an interaction potential is necessary for points as objects since regardless of how close two points may be they are not in contact until they are given the exact same coordinate. If the entities are nothing but points then the condition of contact relinquishes to the points being identical. When an entity is not well represented by a single point it can be represented as a collection of points. The interaction amongst the collection is carried out so as to maintain the form of the total object. When using a cellular structure such as those commonly used in cellular automata the cell and the object are identified such that the state of the cell implies the existence of the object. In its most abstract ideal there are no actual objects. The idea of objects arise from the pattern of states which the cells may take. The framework developed here works to leverage these notions. The object being associated with the cell is not the claim that the object is within the cell nor is it the claim that the center of mass of the object resides within the cell. It is that a derivative notion of the object may be associated with a single well defined unit of space-time, namely an event. The object is expressed as a pattern of events designated by the states of the cells expressible within but beyond the assumed lattice structure.

An event-lattice consists of a set of cells Γ and a set of actions S with an external binary operation such that $\sigma : S \times \Gamma \to \Gamma$. Thus an event-lattice is a tuple $\mathcal{L} = (\Gamma, S, \sigma)$. The event-lattice is the underlying framework for constructing cellular automata which can utilize objects. A naive event-lattice will be presented first to develop an intuition for the event-lattice structure. This event-lattice has the virtue of being easily displayed as an image with a normal coordinate system. It bears many similarities to a less naive event-lattice to be presented following the first. This second event-lattice has less assumptions and a smaller action set. A metaphorical diagram can be given but in the end it requires a greater leap of imagination than the first event-lattice. Afterwards the event-lattice is left as is and the representation of objects in cellular automata is formulated using the event-lattice as a basis. The remainder of the thesis after this chapter is concerned with interpreting these objects with the available tools and algorithms in a classical case to see if this framework has any merit.

3.1 Event-Lattices

Envision a real line partitioned into equal segments called cells such that Γ refers to the set of all cells. For a system with one spatial dimension, space-time may be envisioned as a typical grid where each square of the grid is a cell over a duration. Let an event refer to a cell over a duration. Thus the grid is composed of events. If the horizontal axis is taken as space and the vertical axis as time then each row refers to the set of cells Γ over the same duration while rows above and below refer to those same cells but in the past and future durations. Any given column is then the same cell $\gamma \in \Gamma$ over many durations. In the way that the cells partition space, events can be thought of as partitioning space-time. Let the ratio of the spatial extension of the event, dx, to the temporal extension of the event, dt, be equal to the speed of light such that in natural units

$$\frac{dx}{dt} = c = 1 \tag{3.1}$$

It follows that if there is an object which is within a cell $\gamma \in \Gamma$ at an instant t then there is a finite set of cells, Γ', after a duration dt which the object may be be found within. This set Γ' consists of the same spatial cell $\gamma \in \Gamma$ and the cells directly adjacent to that cell. It cannot be in any other cells because to do so would require a velocity greater than the speed of light. The

transition of the object from cell $\gamma \in \Gamma$ at t to $\gamma' \in \Gamma'$ at $t + dt$ is called the action of the object over the duration dt. Now the action set S and the binary operation σ are such that there is an action $s \in S$ where

$$\gamma'(t + dt) = \sigma^s(\gamma(t)) \tag{3.2}$$

Thus the action set defines the finite set which the object may be found within as

$$\Gamma' = \{\gamma' | \forall s \in S : \gamma' = \sigma^s(\gamma)\} \tag{3.3}$$

It is the action set, and the binary operation together which give the space its structure such that

$$\forall \gamma_0 \in \Gamma \ \& \ \forall x, y \in S : \left(\exists \gamma_x, \gamma_y \in \Gamma : \gamma_x = \sigma^x(\gamma_0),\ \gamma_y = \sigma^y(\gamma_0) \ \& \ \gamma_x = \gamma_y \iff x = y \right) \tag{3.4}$$

To make it more concrete, in a one dimensional space let there be a lattice which divides the line into a set of cells $\gamma_i \in \Gamma, i = 1, 2, 3, ...$ such that γ_3 is to the right of γ_2 and to the left of γ_4. Now, if an object is covered by the cell γ_j in the duration $t_0 \leq t \leq t_0 + dt$ then one duration later i.e at $t = t + dt$ the object is either in γ_{j-1}, γ_j, or γ_{j+1}. It cannot be in γ_{j-2} nor in γ_{j+2} because to do so would require a velocity greater than the speed of light. Thus the action of the object over the duration dt is

$$\gamma_{j+s}(t + dt) = \sigma^s(\gamma_j(t)) \tag{3.5}$$

and the total action set has three members such that $S = \{1, 0, -1\}$ or as $S = \{+, 0, -\}$.

In this way the world line of any object in an event-lattice can be represented as a sequence of a finite set of actions. Figure 3.1 is a pictorial representation of the lattice just discussed. The black line represents a world-line of some object. The grid of squares represent events. A line of events parallel to the horizontal axis are events which occur in the same duration. The vertical axis denotes time such that a column of cells parallel to the time axis denote the same cell over multiple durations. Under the world-line a set of events have been shaded. The left sequence is proper in that only one event occurs for the object over a duration. The events shaded in the right sequence are improper. Figure 3.2 displays relations between the only possible event patterns and

the action set for the one dimensional lattice. With this identification the object is representable as an action sequence. For the object in the left side of Figure 3.1 $s = \{+\ 0\ +\ 0\ +\ 0\ 0\ 0\ 0\ 0\ 0\ -\ -\ 0\ ...0\ +\ +\}$ represents the path of the object in the event-lattice.

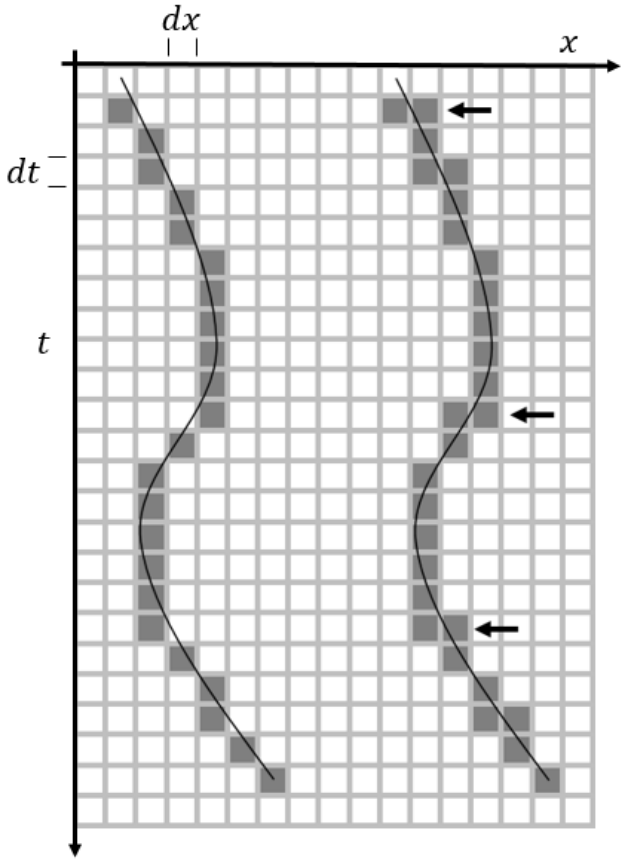

Figure 3.1: The world line of an object in an event-lattice with shaded squares indicating events which the object participates in. The left line shows this process when carried out in agreement with the resolution of the event-lattice. The right line shows an improper sequnce where an object participates in multiple events in a single duration.

A central issue of this lattice is that it has a definite limit of resolution as can be understood in terms of the following. Consider the world line travelling through a duration of $t_0 < t' < t_0 + dt$. At some exact instant $t_0 + \Delta t$ it is decided which cell the object resides in by virtue of which cell covers the object at that time i.e. which cell the world line is in at $t_0 + \Delta t$ where $0 \leq \Delta t \leq dt$. Regardless of what Δt is selected, in the next duration it must be decided at that same instant relative to the duration i.e at $t_0 + dt + \Delta t$. For example if $\Delta t = 0$ the proper cell for the event in the duration is the cell which the the world line entered the event from the previous duration.

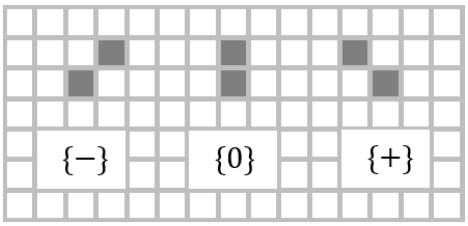

Figure 3.2: Notation relating the members of the action set to actions of an object as a world line in an event-lattice.

Equivalently it could be taken as the cell which the world-line exits from given the duration in which case $\Delta t = dt$. The former case is shown in the Figure 3.1. In this way the proper event is determined by the temporal resolution of the lattice and the instant of when it was determined i.e. it references time externally.

Objects are extensions in time and in space. The idea of an object with perfect extension in time and none in space is as fictitious as the idea of an object with perfect extension in space and no extension in time. The latter is characterized by the idea that light had infinite velocity and so had pure spatial extension. Similarly the former is characterized by the idea of a pure rest mass point particle with no velocity representing an object with perfect extension in time and no extension in space. The finite velocity of light of order c and the uncertainty principle of the order of Plank's constant h confirm the falsity of these abstract notions.

Although this lattice does not commit the fallacy of perfect extension in space by using a finite velocity of light it does allow perfect extension in time where a sequence can have the form $s = \{000...0\}$ for any resolution. In the limit as $dx \to 0$ i.e. as the spatial resolution of the lattice approaches zero the sequence becomes a poor representation of any real object as the object has an exact position and no translation thus no velocity nor momentum thereby violating the uncertainty principle. Secondly the notion of time and space were separately assumed and used to define an event. As has been thoroughly argued by Whitehead neither time nor space make up direct experience, both are abstractions from the events which are the basic substance of experience as readily available fact. [83] Thus it should instead be the opposite that the notion of an extension in time and an extension in space are derived from the definition of the event itself, which is in turn derived from the tuple which constitutes the event-lattice.

Consider now the following, an event-lattice consists of a set of cells Γ and a set of actions S

with an external binary operation such that $\sigma : S \times \Gamma \to \Gamma$. In the previous event-lattice an event was defined as a cell over a duration. Now, let two cells related by an action $s \in S$ denote an event. Under this definition an event does not obtain extension or duration through the cell and an absolute time respectively, but obtains extension and duration as an action. We maintain that

$$\forall \gamma_0 \in \Gamma \ \& \ \forall x, y \in S : \left(\exists \gamma_x, \gamma_y \in \Gamma : \gamma_x = \sigma^x(\gamma_0),\ \gamma_y = \sigma^y(\gamma_0) \ \& \ \gamma_x = \gamma_y \iff x = y \right) \quad (3.6)$$

This definition of an event imposes a direct relation between space and time. It is a manifestation of the following facts. Let the predicate $\Delta(x, x')$ denote a change in x such that if $x \neq x'$ then $\Delta(x, x')$ is true and false otherwise. Now let r represent position of an object, and t denote an instance in time. Granted an object changes position i.e $\Delta(r, r')$, and velocity is finite it implies that there was a change in time thus

$$\Delta(r, r') \to \Delta(t, t') \quad (3.7)$$

However, if one were to scientifically measure the passage of time they must look into the environment to see if something has moved e.g. observing the movement of a clock hand. We cannot scientifically affirm a passage of time i.e. $\Delta(t, t')$ without referencing a change in position of an object $\Delta(r, r')$. If all the sudden everything stopped moving a logical conclusion would be that time has stood still. Thus a change in time implies a change in position such that

$$\Delta(t, t') \to \Delta(r, r') \quad (3.8)$$

But, 3.7 and 3.8 together are by logical definition equivalent to the statement of "$\Delta(t, t')$ if and only if $\Delta(r, r')$" which is symmetric such that "$\Delta(r, r')$ if and only if $\Delta(t, t')$" is an identical statement. In conclusion there can only be a change in time if a corresponding change in position is observed. Take the well known thought experiment of an object alone in free space. Most agree that if there is only one object in free space it is impossible to tell if the object is moving or not, because there is nothing for the object to move relative to. However if there is only one object and this idea is maintained then it is not only impossible to tell if it is moving but also impossible to determine if time is passing. The observer is the object in this condition which implicitly grants the passage of

time such that the object can be conceived as stationary or moving.

This is principally concerned with the idea of a free object of any mechanical theory. A free object is an object which is not interacting with any other object. Yet observation is itself a definite form of interaction. Thus there cannot be an observed free object, because the observation of the object is a form of interaction, and if the object is interacting the object is not free. That does not imply the non-existence of a free object. It implies that a free object is always in a process of change to exist in space-time. Thus if an object is a series of events they must be extended in space and time. This amounts to the restriction on the action set that

$$\nexists s \in S \text{ such that } \gamma = \sigma^s(\gamma) \tag{3.9}$$

Since actions such as $\gamma = \sigma^s(\gamma)$ lack spatial extension, or a change in position they also lack temporal extension and thus do not constitute events in space-time. Two metaphorical diagrams of this event-lattice are shown in Figure 3.3. The left event-lattice is four times smaller than the right event-lattice. Unlike the previous event-lattice the grid is rotated so that cells appear as diamonds and do not refer to events. For each event-lattice a set of dotted lines are shown. The path of an object is depicted as black disks in the small event-lattice and shaded diamonds in the larger event-lattice. The crossing of an object from cell to cell comprises an event and in each event-lattice an event has been circles with a small black oval. As has been discussed no free object can exceed the speed of light nor can it remain stationary of its own accord. This diagram achieves this by not allowing an object to pass from diamond to diamond without them having adjacent edges but no diamond shares an edge with itself. Also objects can only go backwards in time if they have a velocity faster than the speed of light. Secondly the duration of an event is derivative from the event itself by the fact that definite durations can be allotted in the time axis such that for a given object each duration only contains one event. To make this clear the smaller event-lattice is superimposed on the larger lattice as shown in Figure 3.4. This is easiest seen by observing the world line of the object in the small event-lattice in the region of the large event-lattice which has durations indicated over it with dotted lines. A black line linking two black discs indicates the event in the larger lattice. With the durations allotted one event occurs for one duration such that events determine duration. In the top of the figure durations can also be defined for the

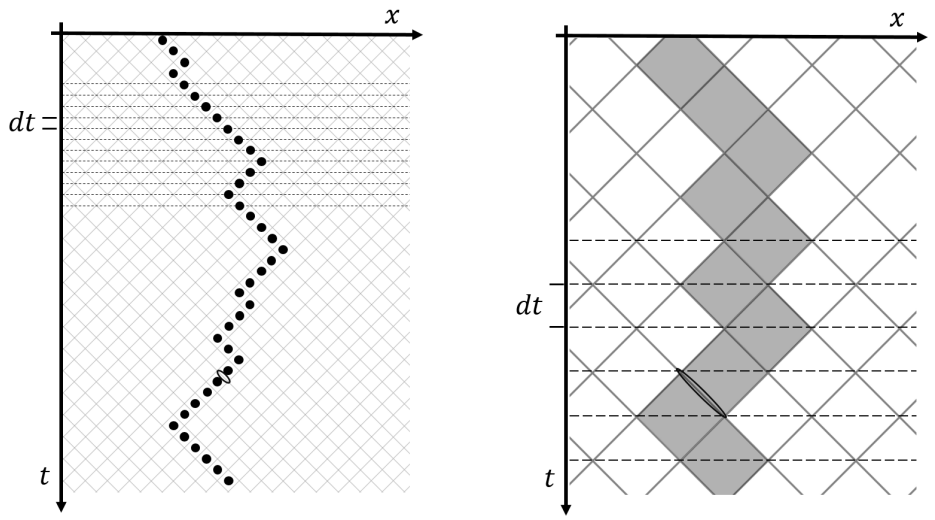

Figure 3.3: Metaphorical diagram on a event lattice which utilized relations between cells as the definition of events. Two separate lattices are shown one four times smaller than the other. Disks portray active cells in the path of an object for the smaller lattice, while shaded cells show the path of another object in the larger lattice. The circled edge joining two cells is the event between the two cells. Indications on the time axis show that the time may be partitioned such that only one event occurs per duration.

smaller event-lattice where each action constitutes an event. It will also be noted that for each duration outlined the full set of cells are present although in an obtuse way, hence the diagram as metaphorical. It exhibits an interesting property that the space-time itself can be tessellated but it does not give consistent reference to a tessellation in space or a tessellation in time as the elements of the space-time tessellation overlap when projected onto either the space or the time axes. An additional property of objects is that they can have no net translation i.e be at rest. Since objects are always participating in events in order to be existent and have no net translation it is required that

$$\forall x \in S : \left(\exists y \in S \text{ such that } \gamma = \sigma^x \sigma^y(\gamma) = \sigma^y \sigma^x(\gamma) = \sigma^{x+y}(\gamma) \right) \tag{3.10}$$

We shall call y the inverse of x and most often write y as x^{-1}. This condition is also a symmetry condition on the event-lattice that if γ is a neighbor of γ' then γ' is a neighbor of γ. Thus if γ' and γ are neighbors there exists an action x relating γ to γ' and an action x^{-1} relating γ' to γ. The subset $\{x, x^{-1}\} \in S$ will be termed an inverse action pair. Extending this framework to multiple dimensions amounts to adding inverse action pairs.

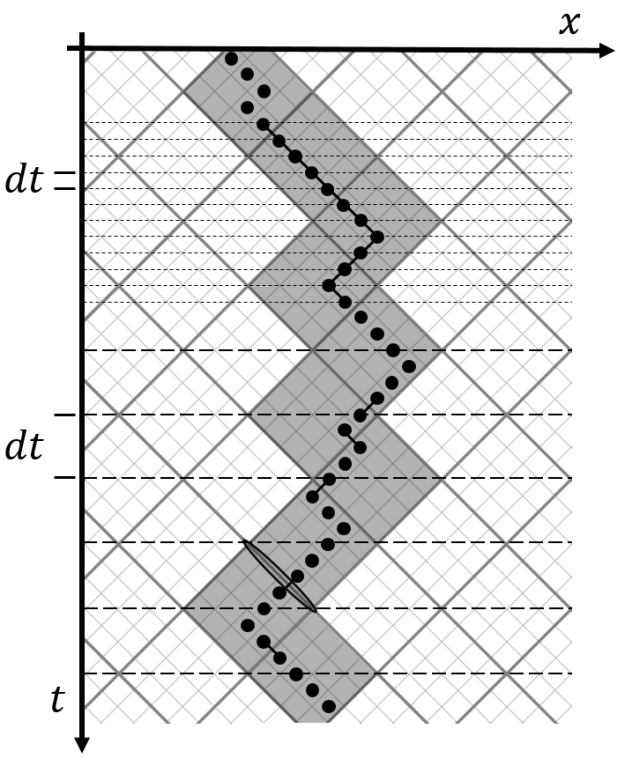

Figure 3.4: The two event-lattices of Figure 3.3 superimposed onto the same axis.

Although the description of this event-lattice may suggest that the fundamental nature of space is a Cartesian lattice geometry with a Manhattan metric it was not stipulated nor required. The only requirement is that each cell in the event-lattice has a neighboring cell given by the external binary operation σ for every member of the action set S, where no two different actions yield the same neighboring cell, every action has an inverse action, and no action maps a cell to itself. For example it is perfectly viable that a cell be missing from where one thinks it should be as in Figure 3.5 where the dots are cells and the lines connecting the dots represent connections through actions. The event-lattice is completely ignorant of this apparent error which arose from embedding the two dimensional event lattice on the Euclidean plane. This loose requirement leaves plenty of room for further development as far as space-time topology is concerned. Still in this event-lattice the world line of any object may be represented as a sequence of actions from the action set.

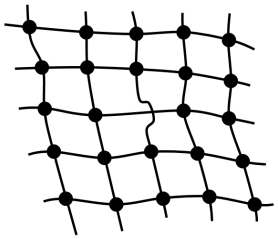

Figure 3.5: Depiction of a structure which satisfies the event lattice condition. Dots indicate cells in the event-lattice and lines connecting dots indicate actions relating cells. Even though the a cell appears to be missing this structure will still make a valid event-lattice.

3.2 Finite Representations of Objects in an Event-Lattice

Before getting into the more abstract definitions let us assume that an object is representable by a finite string of symbols from the action set. Imagine this string of symbols to be a tiny script or tiny program which the object uses to traverse the event-lattice by executing the actions in sequential order. Once the object reaches the end of the script it begins from the beginning again. In a one dimensional event-lattice the action set is simply $S = \{+, -\}$ and so the action sequence of the object is representable as a finite binary action sequence.

Let us now consider an object be given by the action sequence $s = \{+ - + - ++\}$. This sequence is quantifiable in two distinct ways. The first is that of size or length which will be denoted as $\lceil s \rceil$ which is the number of members in the sequence such that $\lceil s \rceil = 6$. The second quantification will be called the sum of the sequence which has the intuitive notion that the sum of s is $\vec{s} = 2$. In more depth, the sum of $s = \{+ - + - ++\}$ is obtained by the replacement of each member of the sequence such that $+ = +1$, $- = -1$ and the sum is then the algebraic sum of the result. Thus $\vec{s} = +1 - 1 + 1 - 1 + 1 + 1 + 1 = 2$. Figure 3.6 shows this particular sequence and indicates precisely what is meant by the length and the sum. The length of s, $\lceil s \rceil$, is akin to a projection of the total sequence on the time axis while the sum of s, $\vec{s}$, is akin to the projection on the space axis. However the length of an object is only indirectly a measure of temporal extension. The length is actually the total number of events from which the all the information of the object can be obtained. The sum is the net cells the object traverses given the length as defined and

related to duration. Thus the velocity which is a parametrization of motion is such that

$$v(s) = \frac{\vec{s}}{\lceil s \rceil} \tag{3.11}$$

in units of the velocity of light. Clearly $\vec{s} \leq \lceil s \rceil$ for any sequence as all motions have velocity less than or equal to that of light and the equality only holds for sequences characteristic of photons. It is clear that by these measures the object s when divided into any number of components preserves these measures. In particular the sequence s may be decomposed into a resting sequence $s_m = \{+ - + -\}$ and a pure sequence $s_p = \{++\}$. Pure sequences will be termed photonic. Given this decomposition of $s \to s_m + s_p$ it follows that $\lceil s \rceil = \lceil s_m \rceil + \lceil s_p \rceil$ and similarly $\vec{s} = \vec{s_m} + \vec{s_p}$.

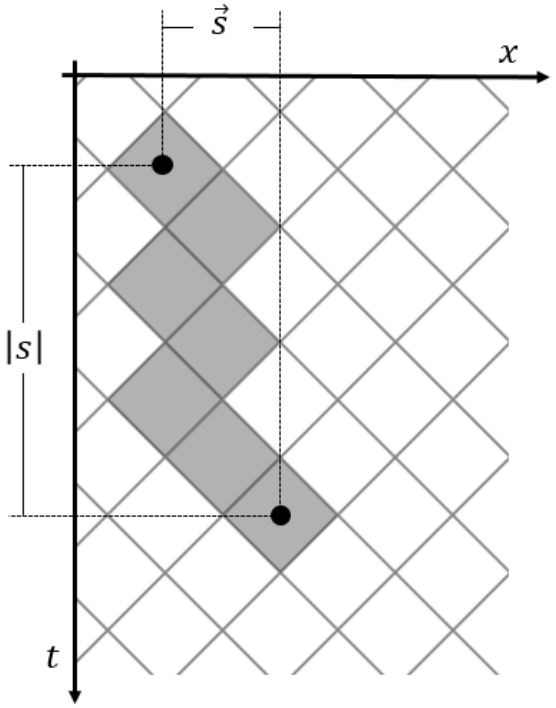

Figure 3.6: Exhibition of the path given by the sequence $s = \{+ - + - ++\}$ quantified by the length of the sequence and the sum of the sequence in one dimension. Shaded in diamonds show the path of the object for one pass through the sequence.

We now consider the notions of length and sum as related to conventional properties of objects namely mass, energy, and momentum. The resting sequence s_m has length but no net sum while the photonic sequence s_p has a length equal to its sum. Thus s_m has a velocity of zero while s_p has a velocity equal to the speed of light. With a little imagination the conversion between the

sequence $s \rightleftharpoons s_m + s_p$ has the basic form of an emission of a photon from a moving particle or the absorption of a photon by a resting particle pending on if the forward arrow or backward arrow is taken as the direction of time. Accordingly the total energy of s equals the total energy of s_m and s_p together. Although this requirement is met by both the sum and the length separately the sum assigns s_m to have a value of zero which is false as a measure of energy. According to special relativity the energy of an object is equivalent to its mass if it has no velocity in the frame of reference. [84] Thus the real mass and equivalently the energy of the sequence is better given by the length of the sequence. By hypothesis, let the length of the sequence be a measure of the energy. Thus length is identified with a scalar non-negative measure of motion. Consider an object with conventional mass. As a massive object the resting mass energy dominates the total energy content. In other words the mass is proportional to the total energy. Then $\lceil s \rceil$ is a measure of the mass and momentum may be taken as

$$p = m \cdot v = E \cdot v = \lceil s \rceil \cdot \frac{\vec{s}}{\lceil s \rceil} = \vec{s} \tag{3.12}$$

in which case the resting sequence s_m has no net momentum $p_m = \vec{s_m} = 0$ while the photonic sequence has a momentum directly proportional to its energy $p_p = \vec{s_p} = \lceil s_p \rceil$. These results agree with the energy-momentum relation of special relativity given in natural units

$$E^2 = p^2 + m^2 \tag{3.13}$$

such that equation 3.13 reduces to $E = m$ when $p = 0$ and reduces to $E = p$ when $m = 0$. The special property of the photonic sequence is such that if a sequence is photonic

$$x \in s_p \rightarrow x^{-1} \notin s_p \tag{3.14}$$

Whereas for a massive object i.e. any object with a velocity less than the speed of light $x \in s_m \rightarrow x^{-1} \in s_m$. Thus massive objects may be represented by sequences which contain inverse action pairs while photons do not. For multiple dimensions the sum produces a vector. For example if there are three dimensions and thus three inverse action pairs and $s = \{\ x\ x^{-1}\ y\ z\ z\ \}$ then $\vec{s} = (0, 1, 2)$. In these cases the same condition holds for photonic sequences in that $x \in s_p \rightarrow x^{-1} \notin s_p$ and the

sum of the components of $\vec{s}$ equals $\lceil s \rceil$.

Before any further effort is spent on analyzing this sequence representation of objects, we must first ask if there is any good reason for doing so? Aside from the obvious reason for which the representation was constructed, i.e. being for cellular automata, the objects entail an utter simplicity. On the philosophical side this is a monism where there is no fundamental difference between the mass, energy, or momentum of an object. An object is a composition of actions while energy and momentum are different means of quantifying the motion of the object in the event-lattice. All objects consist of the same 'substance' which is the action set which comprises the structure of the space. Where an object given by a single symbol of the action set would correspond to a particle moving the speed of light with no mass like a photon. In which case the energy equals the momentum which equals the action. The actual occurrence of an object is what the object does through the sequences of actions. Thus the total object is always in a process of becoming as a recognizable pattern.

If the action of an object in a cell is taken as the action of the cell given by the object then the 'states' of the automaton play the dual role of representing objects and giving the structure of the space. Thus there does not exist a strict differentiation between substance and space. Or as Schrödinger said it "What we observe as material bodies and forces are nothing but shapes and variations in the structure of space." [85]. On the relativistic side of things for objects moving at velocities much slower than the speed of light the mass must dominate the total energy of the object. All objects are acting in events at the speed of light such that there is no proper reference frame to take, as in the sense of special relativity, since the speed of light cannot be taken as the reference frame. If an object has mass, i.e. there is at least one inverse action for a given action in its action sequence then its mass (energy) will tend to infinity before it can reach the speed of light. Furthermore there exists a definite concept of the inertia of an object, or resistance to change of motion, proportional to the mass of an object in a plain way.

On the quantum side these objects never have a definite position nor a definite momentum. Position and momentum are properties of the total object and cannot be realized at an instant and so the relative parameters can be selected to satisfy the Heisenberg uncertainty principle. In that sense an object is said to have a given momentum and position does not require the object to follow a definite path over short intervals but will follow a general path over long intervals. The

basic form of the event-lattice is very similar in likeness to the checkerboard model devised by Feynman in the 1940s in the development of the path integral formulation of quantum mechanics. Feynman showed in his checkerboard model that if at each time step δt the particle moves δtc to the right or left and each turn is weighted by $-im\delta tc^2/\hbar$ then in the limit of infinitesimal time steps which correspond to infinitely small distances between the lattice points the sum over all possible paths gives a propagator which satisfies the one dimensional Dirac equation. [86,87] Thus Feynman directly associated the turns of the object in the sequence, i.e. an inverse action pair, with mass as was found here. Further 't Hooft found that in quantum field theory fermions obtain mass if one allows for leftward propagating massless particles to turn into rightward propagating massless particles when studying fermionic gases on a lattice. [88]

Interestingly if we take the cellular automaton interpretation of Quantum mechanics by 't Hooft seriously and apply it to Feynman's path integral formulation directly then a valid interpretation would not be that the object takes every path but that the object can take any path but we do not know which path due to lack of information about the object. [89] This is nearly identical to this conception. Although Feynman and 't Hooft differ about the interpretation of the quantum mechanical formulation both agree that a finite volume of space-time should contain a finite amount of information and the result of this when applied gives a possible synthesis of their formulations of quantum mechanics. [3, 90]

Objects have interesting properties. For instance this formulation automatically requires that an object which has been deemed to have a certain form must change energy in discrete levels in order to maintain that form. For example in an appeal to intuition if

$$s_1 = \{+-+-+-+-+-+-\} \tag{3.15}$$

let this sequence be represented as $s_1 = \{+-\}^6$. Clearly this sequence differs from

$$s_2 = \{++--++--++--\} = \{++--\}^3 \tag{3.16}$$

as each has a characteristic form. If either s_1 or s_2 were to change energy but maintain their form it would have to occur in an amount in accordance with the form. If frequency is considered a

form then objects must change energy at levels appropriate to their frequency in order to remain at that frequency. Thus there are a number of agreeable properties of the objects which make them worthwhile for analysis. The case of an object as a repeating sequence is only one possibility of formulations that an object could take. In fact a sequence as a string of symbols is a an example of a maximally ordered evolving topology on a set partitioned with the action set S. Objects may instead be defined as a set and evolving topology directly.

Let an object be a set of actions A and a collection of subsets of A called the form of the object A_τ. Each action in A can be mapped to a member of the action set. That is each action in the action set defines an equivalence relation on the set of actions which make up the object. We now borrow Whitehead's terminology to make a clear distinction between an object, its occurrence as an actual entity, and its actions.

An actual entity is the occurrence of a sequence of actions in the event-lattice. Actual entities are unique and exist over a definite extension in time and a definite extension in space. Actual entities are not recognizable by virtue of their novelty as a new occurrence. Further, each actual entity is composed of actions which are themselves actual entities and each actual entity is part of larger actual entities. Since S is a finite set of symbols and

$$(x \in S) \to (x^{-1} \in S) \tag{3.17}$$

a sequence of actions from S may be expressed as the concatenation of symbols of S such that the set of all actual entities as occurrences for single objects is given by the free group, F_S, generated by S. [91]

Let A denote a set of actions composing the object. Note that the elements of A are not directly actions of S but every member of A belongs to an equivalence class given by S so that each member of A has an associated action as given by S. This is necessary because sets are not permitted to have repeated elements and thus a distinction must be made in order to impose a topological structure on the object as a set. The form of the object A_τ is a collection of subsets of A which includes A and the empty set. The form designates which actions can be taken and which actions cannot be taken in order for the actual entities to retain the form of the object. An action a_i can only be

taken by an occurrence of the object A if

$$\forall Z \in A_\tau : (\exists a_i \in Z \text{ and } Z \neq \{\}) \tag{3.18}$$

where $\{\}$ is the empty set. Put another way, A_τ is a topology on A and an action can only be taken if it is an element of every member of A_τ aside from the empty set. Once the action is taken the form evolves. Let T denote an evolution operator corresponding to the object taking the action a_i. Then the new form of the object is the collection of subsets of A such that

$$T(A_\tau) = \{Z' | \forall Z \in A_\tau : (Z' = Z - a_i)\} \cup \{A\} \tag{3.19}$$

Note that it is not A being joined with each Z', A is one of the sets in the collection. This description is very abstract but a simple example which satisfies equations 3.19 and 3.18 should make things clear. Let the object be $A = \{a, b, c, d, e\}$ and let $A_\tau = \{\{A\}, \{c, d\}, \{\}\}$. The next action of the object can only be given by the action of c or d because only c and d are in every member of A_τ aside from the empty set. Suppose the action of c is taken. Then a new A_τ is generated such that the form becomes $A^1_\tau = \{A, \{a, b, d, e\}, \{d\}, \{\}\}$ as per equation 3.19. Now the only action which is in every member of A^1_τ aside from the empty set is d so that is the only action the object can take. In taking action d the form becomes $A^2_\tau = \{A, \{a, b, c, e\}\ \{a, b, e\}, \{\}\}$. Now the object can take actions a, b, or e and so forth.

This formulation of objects ensures that each action which composes the object receives equal use so that momentum is conserved but does not determine the exact path of an object in the event-lattice. An object designated as a repeating sequence also satisfies this conception and is the maximally ordered topology. The maximally order topology is more useful because the next action is always determined. The general topological form was presented for completeness of the Whiteheadian conception of an object as more than a mere string. However, we shall only make use of the maximally order topology, i.e. a repeating sequence. Further, if the maximally ordered topology is taken then objects may be represented by subsets of the free group generated by the action set where members of the subset are related by left and right permutations. To be clear if $abbc \in F_S$ then $bbca$ and $cabb$ are also in F_S and are all actual occurrences of the same object,

where *bbca* is a left permutation and *cabb* is a right permutation of *abbc* respectively.

With the notion of objects in hand the event-lattice can now be used as a basis for a cellular automaton. Each cell in the event-lattice is then an automaton with states being the possible forms of objects which reside at the cell. Thus the states are the free group generated by action set S such that $Q = F_S$. Normally this would be absolutely detrimental to a cellular automata model since the possible set of inputs into the transition function is the number of states raised to power of the neighborhood ${F_S}^N$ which is infinite. But since each automaton can only instantiate one member of the action set the only relevant aspect of the object is the action which will be instantiated next. Thus while the states of the automaton are practically unlimited the cases are finite.

When the automaton updates it executes the next action of the object. Since each action has a designated neighboring cell given by σ which it acts upon the set of inputs X is one-to-one with the power set of the action set $P(S)$. Thus the transition function $\delta : X \times Q \to Q$ may be expressed instead as $\delta : P(S) \times S \to F_S$. Supplementary functions such as $R : F_S \to S$ which reads the next action from the object string and $L : F_S \to F_S$ which permutes the object string such that $L(abc) = bca$ are necessary ingredients in the transition function but are not difficult to select and are application specific.

The objects themselves are liable to interesting mathematical analysis granted their simplistic structures as free groups and topologies but it may be long and arduous before any conclusions or applications may be obtained. Furthermore, the small and simple sequences which we may indeed compute would correspond to objects so foreign to us that our physical intuition would provide no basis for evaluating them. Accordingly we concern ourselves with reformulating these objects in terms of tools available to us so that we can evaluate their merit and determine if further investigation is warranted. A peculiar feature of these objects is that there is implicit in them dual types of momenta as given by the inverse action pair such that for a D dimensional system there are $2D$ degrees of freedom with respect to motion. This has actually arisen before for Succi and Benzi when extending the LBM to the Dirac equation, and was also noted by Meyer in developing quantum lattice gas automata. It is also certainly in the works of Feynman and 't Hooft who did not reject it but found it to be associated with mass. Special attention will be paid to this property as it is not commonly discussed yet not without support from authoritative figures.

Chapter 4

Point Particle Model

There is arguably no object as important and productive as the point particle. The remainder of this thesis, aside from the conclusions is an attempt to evaluate the merit of the sequence representations of objects by developing and analyzing a conception of point particle objects. Point particles have the virtues of (i) retaining their identity via spatial extension, (ii) not disappearing and (iii) interacting with one another. A point particle is completely characterized by its position and motion. The particles retain their identity by virtue of having unique coordinates from every other particle. Classically this is achieved through repulsive potential energy which tends to infinity as particles tend to the same coordinate. In this conception, position is a cell and motion is an action sequence.

In this chapter an algorithm will be presented that is suitable for use with full detail sequence objects in cellular automata. This algorithm is then used as a basis for subsequent investigations. First we generalize two-body the interactions of the objects in a discrete space by integrating interactions over short durations. With these in hand a momentum balance is conducted over a volume element which suggests some general features the objects should exhibit. Lastly these generalized interactions are used as the basis for an algorithm which closely resembles the famous Lattice Boltzmann Method. In the following chapter the Lattice Boltzmann method is retrofitted and an algorithmic implementation is devised. The chapter after that one presents some simulation results from this retrofitted algorithm.

4.1 Sequence Detail Point Particle Algorithm

In this section a sequence detail resolution algorithm is constructed to produce a point particle model. In a typical cellular automaton the next state of the entity is dependent on the states of the surrounding cells. These surrounding cells are termed the neighborhood. It results that the subsequent state of the cell is dependent on the states of all the surrounding cells. For a modest two state system with a neighborhood of 14 members there are $2^{14} = 16384$ required transition rules. In growing the number of states to be sufficiently descriptive for realistic systems, the number of transition rules required grows exponentially with the number of states raised to a power proportionate to the neighborhood size. Accordingly a determinate set of computations is used in continuous valued state models which utilize an infinite variety of states such as in the Lattice Boltzmann Method. In this way the next state is determined by the state of neighboring cells, but each neighbor can be dealt with separately.

The sequence object has this same property in that for each action only two cells are relevant for a given object and has a vector character of always acting from one cell upon another. Accordingly the actions of the objects act on restricted neighborhoods. This is one of the key advantages of the sequence representations of objects that was used in its development. With a restricted neighborhood as given by the state of the object, where state is current action, the cellular automaton framework becomes exceptionally more friendly to problems of a physical nature. The main issue was that if one were to use a cellular automaton to represent a physical system there are strict conservation laws which must be met. The most critical being that of substance or mass which usually takes the form in the cellular automaton as a cell being in an 'ontological' or 'occupied' state. For every transition of a state from an occupied to an unoccupied state requires a corresponding transition of some neighboring cell from an unoccupied state to an occupied state. However since these transition functions are limited to the neighborhood and the neighborhoods are overlapping but not covering each other completely it becomes inevitable that there will be an incident where a cell may be occupied by more than one particle. If this is admitted a new state must be part of the system, which then creates the probability that three may be represented by the same occupied cell and so on *ad infinitum*. Asynchronous automata and alternating neighborhoods are work-arounds for this problem, but these solutions are external to the descriptive framework,

artificial, and ad-hoc.

With a sequence representation available this problem is trivialized. This of course admits that each cell can be in a near infinite set of states, but the existence of the sequence known and defined allows the constructions of algorithms which require a finite set of rules in order to resolve the states of all the objects with each object having a unique cell. Consider a one dimensional event-lattice as a row of zeros acting as cells

$$... \quad 0 \quad 0 \quad 0 \quad 0 \quad 0 \quad 0 \quad 0 \quad ... \tag{4.1}$$

let s_1 indicate the presence of an object in a lattice. The s_1 indicates the base cell from which the next action will be taken.

$$... \quad 0 \quad s_1 \quad 0 \quad 0 \quad 0 \quad 0 \quad 0 \quad ... \tag{4.2}$$

If the next action is a $\{+\}$ then the following is an event

$$... \quad 0 \quad s_1 \quad + \quad 0 \quad 0 \quad 0 \quad 0 \quad ... \tag{4.3}$$

the cell being acted upon, designated with a $+$, becomes the new base cell for the object

$$... \quad 0 \quad 0 \quad s_1 \quad 0 \quad 0 \quad 0 \quad 0 \quad ... \tag{4.4}$$

If the next actions of the sequence were $\{+ + - + ...\}$ then the object would move around the

lattice as follows,

$$\begin{array}{lcccccccccc} t^*: & ... & 0 & 0 & s_1 & 0 & 0 & 0 & 0 & ... \\ t_1: & ... & 0 & 0 & s_1 & + & 0 & 0 & 0 & ... \\ t^*: & ... & 0 & 0 & 0 & s_1 & 0 & 0 & 0 & ... \\ t_2: & ... & 0 & 0 & 0 & s_1 & + & 0 & 0 & ... \\ t^*: & ... & 0 & 0 & 0 & 0 & s_1 & 0 & 0 & ... \\ t_3: & ... & 0 & 0 & 0 & - & s_1 & 0 & 0 & ... \\ t^*: & ... & 0 & 0 & 0 & s_1 & 0 & 0 & 0 & ... \\ t_4: & ... & 0 & 0 & 0 & s_1 & + & 0 & 0 & ... \\ t^*: & ... & 0 & 0 & 0 & 0 & s_1 & 0 & 0 & ... \end{array} \tag{4.5}$$

Note that only those instances in 4.5 of t_i are events while the instances of t^* are not events and are only shown for clarification to identify the base cell and next cell of the object. In the formal conception of an event-lattice 4.5 would appear as

$$\begin{array}{lcccccccc} t_1: & ... & 0 & 0 & s_1 & s_1 & 0 & 0 & 0 & ... \\ t_2: & ... & 0 & 0 & 0 & s_1 & s_1 & 0 & 0 & ... \\ t_3: & ... & 0 & 0 & 0 & s_1 & s_1 & 0 & 0 & ... \\ t_4: & ... & 0 & 0 & 0 & s_1 & s_1 & 0 & 0 & ... \end{array} \tag{4.6}$$

Thus the object is extended in the space by virtue of participating with cells via actions. Two objects interact if the set of cells which constitute each of their events have a non-zero intersect. Thus consider the objects in the circumstance where both take $\{+\}$ as their next action.

$$\begin{array}{lcccccccc} t^*: & ...0 & s_1 & 0 & s_2 & 0 & 0 & 0 & ... \\ t_1: & ...0 & s_1 & + & s_2 & + & 0 & 0 & ... \\ t^*: & ...0 & 0 & s_1 & 0 & s_2 & 0 & 0 & ... \end{array} \tag{4.7}$$

The objects move but they do not interact since their events do not overlap. If they go in

opposite directions they will have overlapping events i.e. contact or a collision.

$$\begin{array}{lccccccc} t^*: & ...0 & s_1 & 0 & 0 & 0 & s_2 & 0 \\ t_1: & ...0 & s_1 & + & 0 & - & s_2 & 0 \\ t^*: & ...0 & 0 & s_1 & 0 & s_2 & 0 & 0 \\ t_2: & ...0 & 0 & s_1 & \pm & s_2 & 0 & 0 \end{array} \tag{4.8}$$

In this case two objects acted on the same cell and thus their events have a non-zero intersect. At this point it can be decided by virtue of the algorithm what will occur. Similarly there can be a collision of the type where one object acts on the base cell of another object. Suppose s_1's next actions are $\{++...\}$ and s_2's are $\{-+...\}$. Such that

$$\begin{array}{lccccccc} t^*: & ...0 & s_1 & 0 & 0 & s_2 & 0 & 0 \\ t_1: & ...0 & s_1 & + & - & s_2 & 0 & 0 \\ t^*: & ...0 & 0 & s_1 & s_2 & 0 & 0 & 0 \\ t_2: & ...0 & 0 & s_1 & -s_2 & + & 0 & 0 \end{array} \tag{4.9}$$

In this case s_1 has acted on s_2 and their events have a non-zero intersect. It follows that with this arrangement many algorithms could be devised such that the objects maintain separate identities thereby satisfying condition (i). Conditions (ii) and (iii) are met by the fact that the algorithm must allow some interactions to result in a transmission of action from object to object and some actions an object has simply cannot be transmitted, respectively. These non-transmittable actions are like the rest mass of the object.

An example of an algorithm which meets these conditions is presented below and supplemented with Figure 4.1. It is in no sense unique. Before proceeding note that the goal of the algorithm over each time step is to resolve every object in terms of action and location. Resolved means that the cell for the object has been determined for the next time step and the action in the current time step is either kept by that object or passed to another object. Even if a given object is resolved, it is still considered present in a cell if it began the time step in that cell. When an object is resolved it can no longer be involved in a cell other than the cell that it acted from i.e. its base cell. The algorithm begins by initializing all the cells and their action sequences. It then iterates through

the objects working to resolve each one. Algorithms such as these can be difficult to conceptualize without relevant images. The following enumeration entails the algorithm to be discussed. Read through it once and then pass directly to the examples following it which work to elucidate its character and function.

Point Particle Sequence Algorithm

1. Initialize all objects in distinct cells with individual sequences and with a next action selected. Go to step 2.

2. The next action of all objects are executed as the current action, and the next action for each is selected. Go to step 3.

3. Select an unresolved object. Go to step 4.

4. Does any other object act on the same cell as the given object or is present in it? Yes: Go to step 6. No: Go to step 5

5. The cell the object acted upon becomes the new base cell for the next action and the object keeps its action. Go to step 15.

6. Do any of the involved objects have an inverse as their next step? Yes: Go to step 7 to resolve each involved object that meets the condition. No: go to step 8.

7. The involved object remains in the cell which it acted from and it keeps its action. Go to step 15.

8. Is there an object present in the cell which the current object is acting on? Yes: Go to step 9. No: go to step 10.

9. The object remains in its cell and gives its action to the object present in the cell it acted on. Go to step 15.

10. Is there more than one other object acting on the cell? Yes: Go to step 12. No: Go to step 11.

11. Each object remains in its cell and gives its action to the other object. Go to step 15.

12. Are there any involved objects with opposite action to one another. Yes: Go to step 13. No: Go to step 14.

13. The objects with opposite action pass their actions to one another and remain in their cells. They are then resolved. Go to step 15.

14. All objects keep their actions and remain in their cells and are resolved. Go to step 15.

15. Are all object resolved for the time step? Yes: Go to step step 2. No: Go to step step 3.

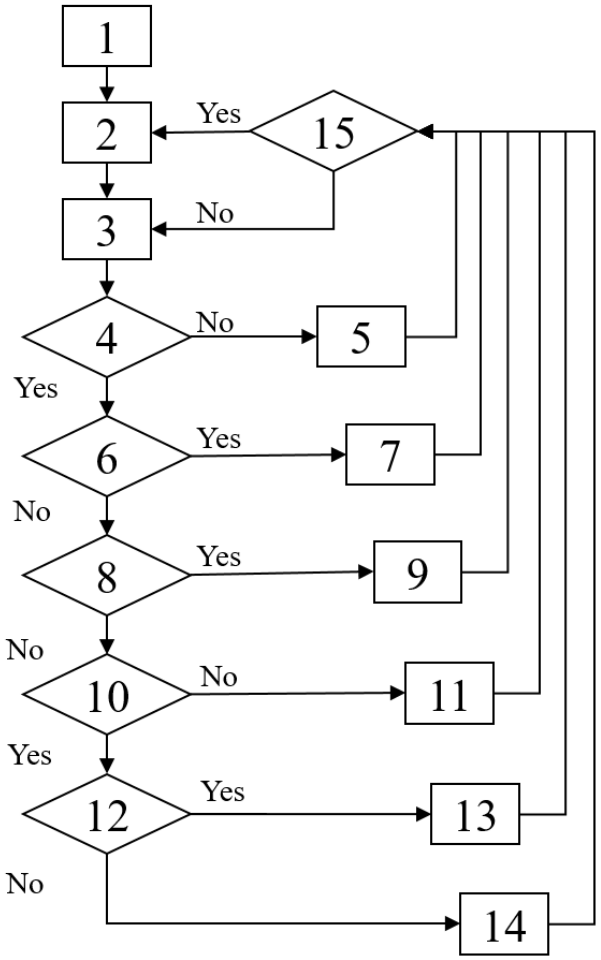

Figure 4.1: A process diagram for the sequence detail algorithm as a visual aid for the algorithm steps outlined in the text.

Figure 4.2 is a pictographic example of the algorithm in a two dimensional lattice structure. There are 8 cases shown each consisting of three images which correspond to a full time step

plus the beginning of the next step. The grids indicate cells and shaded grid squares indicate the presence of an object in the cell. More specifically it indicates that an object will be acting from that cell over the time step. The triangle within the shaded square is the next action. It indicates which cell the object will act on in the time step by pointing to that cell. The action of the object is indicated by the triangle moving from the object into the next cell, but the cell the object acts from remains shaded. At the same time the next action of the object is introduced in the cell the object acts from. Case 1 exemplifies the simple case where two objects move around without collision. Thus the objects span through the algorithm from (2),(3),(4),(5),(15) and back to (2). In case 2, the two objects collide and each object has an inverse action as their next action. Accordingly they keep their actions. Thus the algorithm over the first time step would go (2),(3),(4),(6),(7),(15), and back to (2). Case 3 is similar to case 2 except that only one of the objects has an inverse action as its next action. Thus the algorithm over the first time step would go (2),(3),(4),(6),(7),(15),(3),(4),(5),(15), and back to (2). It does not matter which object was selected first because steps (6) and (7) resolve all objects with an inverse regardless of the object selected. Three objects are involved in case 4. None of the involved objects has an inverse action as their next action. The two objects opposite to one another are resolved first as per step (12), while the other object is not resolved. It then gets resolved by step (5). Thus the algorithm over the first time step would go (2),(3),(4),(6),(8),(10),(12),(13),(15),(3),(4),(5),(15) and back to (2). Note that the two objects opposite to one another exchanged an action with one another. In case 5 an object attempts to move into the cell where another object is present. Thus the algorithm over the first time step would go (2),(3),(4),(6),(8),(9),(15),(3),(4),(5),(15) and back to (2) if the leftmost object was selected first. If the other object was selected first the algorithm over the first time step would go (2),(3),(4),(5),(15),(2),(3),(4),(6),(8),(9),(15) and back to (2) but the end result is the same. Note that the leftmost object transmitted action to the rightmost object in step (9). The order of which objects are selected is immaterial to the outcome. Case 6 shows a similar arrangement to case 5 except that the leftmost object has an inverse. Thus the algorithm over the first time step would go (2),(3),(4),(6),(7),(15),(3),(4),(5),(15) and back to (2). No transfer of action between objects took place in this case. In case 7 the algorithm over the first time step would go (2),(3),(4),(6),(7),(15),(3),(4),(5),(15), and back to (2). Case 8 is similar to case 7, the algorithm over the first time step would go (2),(3),(4),(6),(8),(10),(11),(15) and back to (2).

Note that step (15) acts as a catch all in the algorithm for the case in which three objects act on the same cell but none of them have the inverse actions of the others nor opposites involved. This case arises in three dimensional event-lattice structures and would be a rare occurrence.

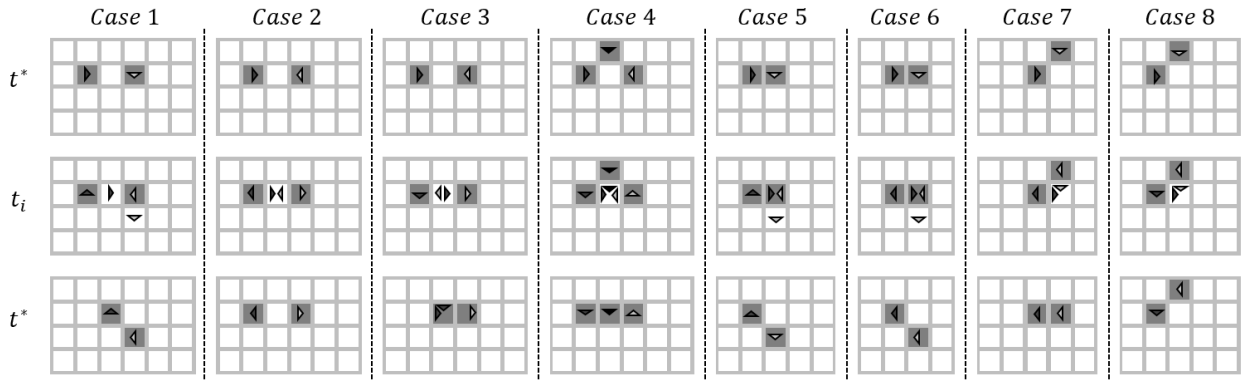

Figure 4.2: A pictographic representation of the example algorithm in a two dimensional lattice structure.

4.2 Generalized Interactions

The example algorithm above is just one in a family of algorithms which satisfy the point particle conditions given at the beginning of the chapter. In this section the interactions of point particle objects are generalized to better represent this family of algorithms. The fundamental character of the objects in the algorithm is how the object retains action i.e. the inverse rule in steps (6) and (7). This rule allows the actions which constitutes the object to be divided into two components, namely a massive component as action that cannot be transmitted and a kinetic component as action that can be transmitted. Thus an object s may be decomposed as $s \to s_m + s_T$. Recall $\lceil s \rceil$ to be the total action comprising the object as before and let s^k be the total amount of actions $k \in S$ comprising the object such that

$$\lceil s \rceil = \sum_{(k,-k) \in S} s^k + s^{-k} \tag{4.10}$$

Thus $\lceil s_m \rceil$ and $\lceil s_T \rceil$ are the amounts of actions in s which have an immediate inverse and those which do not respectively. We will consider massive particles i.e. particles such that $\lceil s_m \rceil >> \lceil s_T \rceil$. Massive in this context does not necessarily mean heavy, massive particles are just not photons and

have velocities $v << c$, and so have many inverse action pairs.

Consider two objects, call them a and b, and let them be adjacent to one another in the lattice such that they are one action away from another of type k and $-k$ respectively. The probability over a given time step dt that object a transfers a unit action of type k to b is

$$P(k|ab) = \frac{a_T^k}{\lceil a \rceil} \tag{4.11}$$

That is, it is the probability that a executes a k action without an inverse action immediately after. Equivalently the probability that b transfers the inverse action $-k$ to a is

$$P(-k|ba) = \frac{b_T^{-k}}{\lceil b \rceil} \tag{4.12}$$

In a similar way, for two objects c and d acting on the same cell but arriving by two different actions, $k1$ and $k2$, the probability of transmission of action $k1$ from c to d is

$$P(k1|cd) = \frac{c_T^{k1}}{\lceil c \rceil} \frac{d^{k2}}{\lceil d \rceil} \tag{4.13}$$

and the probability that d transfers the action $k2$ to c is

$$P(k2|dc) = \frac{d_T^{k2}}{\lceil d \rceil} \frac{c^{k1}}{\lceil c \rceil} \tag{4.14}$$

Since the mass denominates the total action of an object i.e. $\lceil s_i \rceil \approx \lceil s_m \rceil$ because $\lceil s_T \rceil << \lceil s_m \rceil$, and the objects are spherically symmetric it follows that for any object under our consideration

$$\forall k \in S : s^k \approx \frac{\lceil s \rceil}{|S|} \tag{4.15}$$

Where $|S|$ is the cardinality of the action set. Inserting 4.15 into 4.13 and 4.14 we obtain,

$$P(k1|cd) = \frac{c_T^{k1}}{|S| \lceil c \rceil} \tag{4.16}$$

$$P(k2|dc) = \frac{d_T^{k2}}{|S| \lceil d \rceil} \tag{4.17}$$

Thus the transmission probability of adjacent particles differ in magnitude from those which collide by moving into the same cell by a finite constant. Now since the mass dominates the action content of the object then $\lceil s \rceil \approx \lceil s_m \rceil \approx constant$. Thus, irrespective of the collision type the rate at which an object loses transmittable action to another object in a two body interaction may be expressed as

$$\frac{ds_T^k}{dt} = -\frac{1}{\alpha} s_T^k \tag{4.18}$$

Where $\alpha >> 1$ and is an object and relation specific constant. Integrating with respect to time from t_0 to t equation 4.18 becomes

$$s_T^k(t) = [s_T^k(t_0)] \exp\left(-\frac{t}{\alpha}\right) \tag{4.19}$$

For small t we may approximate $\exp(-\frac{t}{\alpha}) \approx (1 - \frac{t}{\alpha})$ and rewrite 4.19 as

$$s_T^k(t) = [s_T^k(t_0)](1 - \frac{t}{\alpha}) \tag{4.20}$$

The amount of action an object would transmit to another object given their specific relation by the lattice over a time step Δt would be the difference in s_T^k at t and s_T^k at $t + \Delta t$ such that

$$s_T^k(t) - s_T^k(t + \Delta t) = \frac{\Delta t}{\alpha} s_T^k(t) \tag{4.21}$$

where α is both object and relation specific.

4.3 Momentum Balance

With these generalized interactions in hand we can analyze the behaviour of a particle in a large group of particles as in a fluid by conducting a momentum balance on a volume element of the particles. Let there be a volume element, Ω of dimensions $\Delta x_1 \Delta x_2 \Delta x_3$. The objects themselves define the boundary so that the only means by which the element gains or looses momentum is through the exchange of actions with objects which are not part of the element. The total momentum of the element is the sum of the momentum of all the objects within the element. The change in the momentum of the element over a duration dt is proportional to the flux of the actions

transmitted through the surfaces of the element to objects outside of the element. For a given dimension k where p_k^Ω denotes the total k momentum of the element Ω,

$$\frac{dp_k^\Omega}{dt} = \sum_{\partial\Omega} J_{\partial\Omega}^k - J_{\partial\Omega}^{-k} \tag{4.22}$$

where $\partial\Omega$ is a boundary of Ω, while k and $-k$ refer to an inverse action pair, and J denotes the flux of transmitted actions through a surface $\partial\Omega$. The summation is only over the boundary as the objects within the boundary will exchange action with other objects within the element and thus do not change the net momentum of the element. For simplicity we let the density of the particles in space be constant such that the probability that an object is in a given cell or acting onto a given cell is ρ.

There are principally two processes of action transmission to be accounted for. Those of a flux direction perpendicular to k and those parallel to k. Let x_k denote the center of Ω such that each boundary is given by the area $\Delta x_i \Delta x_j$ at $x_k \pm \Delta x_k/2$ where $i \neq j \neq k$. Accordingly $x_k \pm \Delta\frac{\Delta x_k}{2} - dx_k$ denotes the region of lattice cells directly within boundary of $\partial\Omega$ over the area $\Delta x_i \Delta x_j$ where $i \neq j \neq k$. Similarly let the region of lattice nodes at $x_k \pm \Delta\frac{\Delta x_k}{2} + dx_k$ denote the set of cells just beyond the boundary $\delta\Omega$ of area $\Delta x_i \Delta x_j$ where $i \neq j \neq k$. A diagram of the cross section of the element is shown with associated notation in Figure 4.3 where the dimension k is perpendicular to the plane of the page.

Thus the exchange of momentum p_k^Ω over the boundary consists of the action transmitted from the objects at $x_i \pm \Delta\frac{\Delta x_i}{2} \mp dx_i$ to objects at $x_i \pm \Delta\frac{\Delta x_i}{2} \pm dx_i$ and the gain of action from objects at $x_i \pm \Delta\frac{\Delta x_i}{2} \pm dx_i$ by objects at $x_i \pm \Delta\frac{\Delta x_i}{2} \mp dx_i$ for $i = 1, 2, 3$. In order to compact the notation let the following identifications be made for use in equations.

$$\begin{aligned}
x_i + \tfrac{\Delta x_i}{2} &\equiv [+]i \\
x_i - \tfrac{\Delta x_i}{2} &\equiv [-]i \\
x_i + \tfrac{\Delta x_i}{2} + dx_i &\equiv [++]i \\
x_i + \tfrac{\Delta x_i}{2} - dx_i &\equiv [+-]i \\
x_i - \tfrac{\Delta x_i}{2} + dx_i &\equiv [-+]i \\
x_i - \tfrac{\Delta x_i}{2} - dx_i &\equiv [--]i
\end{aligned} \tag{4.23}$$

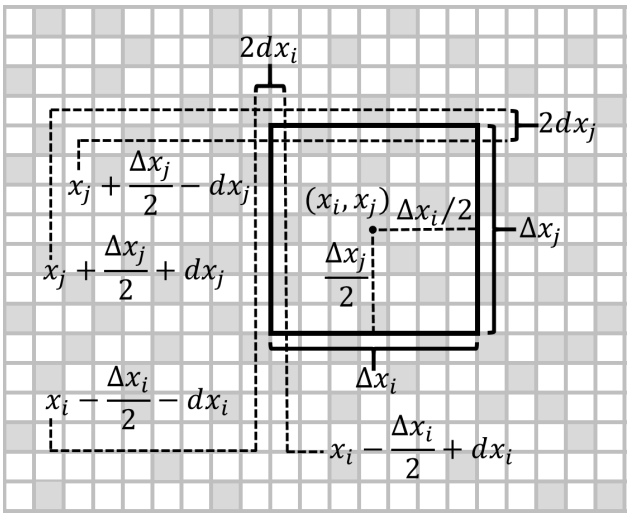

Figure 4.3: Cross section of the volume element Ω in the x_i and x_j plane along with associated notation.

The six surfaces of the element are then denoted as $[+]i$, $[-]i$, $[+]j$, $[-]j$, $[+]k$, and $[-]k$. Let s^k refer to the actions of an object s with respect to dimension k such that the sign of the superscript differentiates the action from its inverse action s^{-k}. Using this k as a form of index notation the momentum of an object s is

$$\vec{s} = s^k - s^{-k} \tag{4.24}$$

Since only some of the actions are transmittable and those which are not transmittable are equally balanced i.e. the actions which constitute the mass the object have no net momentum, the momentum can also be written as

$$\vec{s} = s_T^k - s_T^{-k} \tag{4.25}$$

First consider the case of $i \neq k$ i.e. a surface which is parallel to the dimension k or in another way, the k unit vector is tangent to this surface. For the objects at $x_i + \frac{\Delta x_i}{2} - dx_i$ the change in momentum of the element is given by s_T^k and s_T^{-k} actions resulting in transmission of action to and from objects not in the element. Assuming constant density of objects in the lattice the probability that an object is present for such an interaction is ρ. For each action k and its inverse there is the potentiality for both the gain of actions from other objects and the loss of actions to other objects. In accordance with the algorithm the object can only lose an action granted it executed that action and the action was transmittable i.e s_T^k, and can only gain an action granted another

object executed that action and it was transmittable. Thus for the actions s_T^k the flux is given by the loss of actions by transmission which the object within the element executes and the gain of actions by receiving transmittable actions from another object outside the element.

$$J^k|_{[+]i} = \sum_{\forall s \in [+]i} -\rho\omega_1 s_T^k|_{[+-]i} + \rho\omega_2 s_T^k|_{[++]i} \tag{4.26}$$

Where $\omega_i = dt/\alpha_i$ for α_i defined when generalizing the interactions. The expression under the summation symbols means for all objects s on the boundary of the element at $x_i + \frac{\Delta x_i}{2}$ but within the element. An identical process occurs for s_T^{-k}

$$J^{-k}|_{[+]i} = \sum_{\forall s \in [+]i} -\rho\omega_3 s_T^{-k}|_{[+-]i} + \rho\omega_4 s_T^{-k}|_{[++]i} \tag{4.27}$$

Taking all interactions as equally probably i.e. $\omega = \omega_1 = \omega_2 = ...$ the flux over the surface is then given as

$$J^k - J^{-k}|_{[+]i} = \sum_{\forall s \in [+]i} \rho\omega \left[\left(s_T^k - s_T^{-k}\right)|_{[++]i} - \left(s_T^k - s_T^{-k}\right)|_{[+-]i} \right] \tag{4.28}$$

The total amount of particles on this surface is given as $\rho\Delta x_j \Delta x_k (2dx_i)$. Using the fact that $v_k = s_T^k - s_T^{-k}/\lceil s \rceil$ then the total momentum flux over this side of $\partial\Omega$ can be expressed as

$$J^k - J^{-k}|_{[+]i} = \Delta x_j \Delta x_k (2dx_i)\rho^2\omega\lceil s \rceil \left[v_k|_{[++]i} - v_k|_{[+-]i} \right] \tag{4.29}$$

An identical analysis can be carried out on the opposing surface of $x_i - \frac{\Delta x_i}{2}$ to yield

$$J^k - J^{-k}|_{[-]i} = \Delta x_j \Delta x_k (2dx_i)\rho^2\omega\lceil s \rceil \left[v_k|_{[--]i} - v_k|_{[-+]i} \right] \tag{4.30}$$

Since dimension i was arbitrarily selected 4.29 and 4.30 equally apply if x_i is in the place of x_j and x_j in the place of x_i. Thus there are four equations which describe the action flux over the four sides parallel to the dimension k of the element Ω.

The two boundaries perpendicular to k are different than the others just described. In those boundaries both s_T^k and s_T^{-k} could be transmitted through the surface. However on the perpendic-

ular boundary only the s_T^k can be transmitted from the element to the surrounding at $x_k + \frac{\Delta x_k}{2}$. Similarly only s_T^{-k} can be transmitted from the element to the surrounding at $x_k - \frac{\Delta x_k}{2}$. Accordingly only s_T^{-k} can be transmitted from the surrounding to the element through $x_k + \frac{\Delta x_k}{2}$ and only s_T^k can be transmitted from the surrounding to the element through $x_k - \frac{\Delta x_k}{2}$. Thus the flux at $x_k + \frac{\Delta x_k}{2}$ is given by the loss of s_T^k at $x_k + \frac{\Delta x_k}{2} - dx_k$ which is

$$J^k|_{[+]k} = \sum_{\forall s \in [+]k} -\rho\omega_1 s_T^k|_{[+-]k} \tag{4.31}$$

and the gain of s_T^{-k} at $x_k + \frac{\Delta x_k}{2} + dx_k$ is such that

$$J^{-k}|_{[+]k} = \sum_{\forall s \in [+]k} \rho\omega_2 s_T^{-k}|_{[++]k} \tag{4.32}$$

Thus for the surface at $x_k + \frac{\Delta x_k}{2}$ taking all interactions equally probable

$$J^k - J^{-k}|_{[+]k} = \sum_{\forall s \in [+]k} -\rho\omega(s_T^k|_{[+-]k} + s_T^{-k}|_{[++]k}) \tag{4.33}$$

and similarly the flux at $x_k - \frac{\Delta x_k}{2}$ is given by the loss of s_T^{-k} at $x_k - \frac{\Delta x_k}{2} + dx_k$ as

$$J^{-k}|_{[-]k} = \sum_{\forall s \in [-]k} -\rho\omega_3 s_T^{-k}|_{[-+]k} \tag{4.34}$$

and the gain of s_T^k from $x_k - \frac{\Delta x_k}{2} - dx_k$ such that

$$J^k|_{[-]k} = \sum_{\forall s \in [-]k} \rho\omega_4 s_T^k|_{[--]k} \tag{4.35}$$

Thus for the surface at $x_k - \frac{\Delta x_k}{2}$ taking all interactions equally probable

$$J^k - J^{-k}|_{[-]k} = \sum_{\forall s \in [-]k} \rho\omega(s_T^k|_{[--]k} + s_T^{-k}|_{[-+]k}) \tag{4.36}$$

At this point all of the flux terms in 4.22 over surface $\partial\Omega$ have been obtained. However we desire to express the flux equations in 4.33 and 4.37 as much as possible in terms of velocity in order

to compare with classical fluid concepts. Let the sum of the particles on the surfaces perpendicular to k be equal to $\rho\Delta x_i\Delta x_j(2dx_k)$. Take the sum of the flux on the surfaces perpendicular to k such that

$$\begin{aligned}\psi = (J^k - J^{-k})_{[-]k} + (J^k - J^{-k})_{[+]k} = \Delta x_i\Delta x_j(2dx_k)\rho^2\omega\Big[s_T^k|_{[--]k} + s_T^{-k}|_{[-+]k} \\ - \quad (s_T^k|_{[+-]k} + s_T^{-k}|_{[++]k})\Big]\end{aligned} \tag{4.37}$$

Note that ψ has been introduced for convenience. This expression is resistant to ready formulation in terms of velocity because the inverse action is not present for each term. For example $s_T^k|_{[--]k}$ is present but the inverse action $s_T^{-k}|_{[--]k}$ is absent from the expression. Approximate the complementary exterior terms i.e. the inverse action terms at $x_k + \frac{\Delta x_k}{2} + dx_k$ and $x_k - \frac{\Delta x_k}{2} - dx_k$ in terms of the other components. Thus we approximate $s_T^{-k}|_{[--]k}$ to the first order using a first order Taylor series expansion such that $f(a+h) = f(a) + hf'(a)$ as

$$s_T^{-k}|_{[--]k} = s_T^{-k}|_{[-+]k} - 2dx_k\frac{(s_T^{-k}|_{[++]k} - s_T^{-k}|_{[-+]k})}{\Delta x_k} \tag{4.38}$$

and similarly approximate $s_T^k|_{[++]k}$ as

$$s_T^k|_{[++]k} = s_T^k|_{[+-]k} + 2dx_k\frac{(s_T^k|_{[+-]k} - s_T^k|_{[--]k})}{\Delta x_k} \tag{4.39}$$

Move the left side terms of equation 4.38 and 4.39 to the right hand side such that the equations are set to zero. Then add them to equation 4.37 such that the exterior terms become

$$\begin{aligned}s_T^k|_{[--]k} - s_T^{-k}|_{[++]k} = s_T^k|_{[--]k} - s_T^{-k}|_{[--]k} + s_T^{-k}|_{[-+]k} - \frac{2dx_k}{\Delta x_k}(s_T^{-k}|_{[++]k} - s_T^{-k}|_{[-+]k}) \\ - \big(s_T^{-k}|_{[++]k} - s_T^k|_{[++]k} + s_T^k|_{[+-]k} + \frac{2dx_k}{\Delta x_k}(s_T^k|_{[+-]k} - s_T^k|_{[--]k}\big)\end{aligned} \tag{4.40}$$

These terms can be rearranged as

$$\begin{aligned}s_T^k|_{[--]k} - s_T^{-k}|_{[++]k} = \left[s_T^k|_{[--]k} - s_T^{-k}|_{[--]k}\right] + \left(1 + \frac{2dx_k}{\Delta x_k}\right)s_T^{-k}|_{[-+]k} - \frac{2dx_k}{\Delta x_k}s_T^{-k}|_{[++]k} \\ + \left[s_T^k|_{[++]k} - s_T^{-k}|_{[++]k}\right] + \left(1 + \frac{2dx_k}{\Delta x_k}\right)(-s_T^k|_{[+-]k}) + \frac{2dx_k}{\Delta x_k}s_T^k|_{[--]k}\end{aligned} \tag{4.41}$$

These terms may then be further grouped together as follows

$$s_T^k|_{[--]k} - s_T^{-k}|_{[++]k} = \beta - \frac{2dx_k}{\Delta x_k} s_T^{-k}[++]k + \frac{2dx_k}{\Delta x_k} s_T^k[--]k \tag{4.42}$$

where

$$\beta = (s_T^k - s_T^{-k})|_{[++]k} - (1 + \frac{2dx_k}{\Delta x_k})(s_T^k|_{[+-]k} - s_T^{-k}|_{[-+]k}) + (s_T^k - s_T^{-k})|_{[--]k} \tag{4.43}$$

Substituting these results back into 4.37 we obtain

$$\psi = \Delta x_i \Delta x_j (2dx_k)\rho^2 \omega \left[\beta + s_T^{-k}|_{[-+]k} - s_T^k|_{[+-]k} + \frac{2dx_k}{\Delta x_k} \left(- s_T^{-k}|_{[++]k} + s_T^k|_{[--]k} \right) \right] \tag{4.44}$$

We now work with the remaining four terms. Take the actions from 4.44 and double them while dividing by two such that

$$- s_T^{-k}|_{[++]k} + s_T^k|_{[--]k} = \frac{-s_T^{-k}|_{[++]k} + s_T^k|_{[--]k} - s_T^{-k}|_{[++]k} + s_T^k|_{[--]k}}{2} \tag{4.45}$$

we then take by definition that $\vec{s} = s_T^k - s_T^{-k}$. In order to avoid using index notation at the same time as vector notation let the sum of s, $\vec{s}$ be given explicitly in indext notation as s_k such that $s_k = s_T^k - s_T^{-k}$. Then using the definition of momentum

$$s_T^{-k}|_{[++]k} = s_T^k|_{[++]k} - s_k|_{[++]k} \tag{4.46}$$

and in a similar way

$$s_T^k|_{[--]k} = s_k|_{[--]k} + s_T^{-k}|_{[--]k} \tag{4.47}$$

Combining 4.46 and 4.47 into 4.45

$$- s_T^{-k}|_{[++]k} + s_T^k|_{[--]k} = \frac{-(s_T^k + s_T^{-k})|_{[++]k} + (s_T^k + s_T^{-k})|_{[--]k}}{2} + \frac{s_k|_{[--]k} + s_k|_{[++]k}}{2} \tag{4.48}$$

The same manipulations can be carried out on the first two terms after β in equation 4.44 such that

$$s_T^{-k}|_{[-+]k} - s_T^k|_{[+-]k} = \frac{-(s_T^k + s_T^k)|_{[+-]k} + (s_T^k + s_T^{-k})|_{[-+]k}}{2} - \frac{s_k|_{[+-]k} + s_k|_{[-+]k}}{2} \tag{4.49}$$

We can now aggregate all of the terms of the flux on all the boundaries and take the limit that as $\Delta x \to 2dx$. In this limit it follows that $dx_i = \frac{\Delta x_i}{2}$ and the boundaries of the element Ω become

$$\begin{aligned} x_i + \frac{\Delta x_i}{2} - dx &= x_i \\ x_i - \frac{\Delta x_i}{2} + dx &= x_i \\ x_i + \frac{\Delta x_i}{2} + dx &= x_i + \Delta x_i \\ x_i - \frac{\Delta x_i}{2} - dx &= x_i - \Delta x_i \end{aligned} \tag{4.50}$$

Thus for the fluxes on opposing surfaces parallel to x_k we apply the limits of 4.50 to 4.29 and 4.30 add them together

$$\begin{aligned} (J^k - J^{-k})|_{[+]i} + (J^k - J^{-k})|_{[-]i} &= \Delta x_j \Delta x_k \Delta x_i \rho^2 \omega \lceil s \rceil \left[v_k|_{[++]i} - v_k|_{[+-]i} + v_k|_{[--]i} - v_k|_{[-+]i} \right] \\ &= \Delta x_j \Delta x_k \Delta x_i \rho^2 \omega \lceil s \rceil \left[v_k|_{x_i + \Delta x_i} - 2v_k|_{x_i} + v_k|_{x_i - \Delta x_i} \right] \end{aligned} \tag{4.51}$$

and the same is true when each x_i becomes x_j and each x_j becomes x_i. In a similar way the β given in equation 4.43 when taken in the limit reduces to an identical form as $\frac{2dx_k}{\Delta x_k} \to 1$ such that

$$\begin{aligned} \Delta x_j \Delta x_k \Delta x_i \rho^2 \omega \beta &= \Delta x_j \Delta x_k \Delta x_i \rho^2 \omega \Big[(s_T^k - s_T^{-k})|_{[++]k} \\ &\quad - (1 + \frac{2dx_k}{\Delta x_k})(s_T^k|_{[+-]k} - s_T^{-k}|_{[-+]k}) + (s_T^k - s_T^{-k})|_{[--]k} \Big] \\ &= \Delta x_j \Delta x_k \Delta x_i \rho^2 \Big[(s_T^k - s_T^{-k})|_{x_k + \Delta x} - 2(s_T^k - s_T^{-k})|_{x_k} + (s_T^k - s_T^{-k})|_{x_k - \Delta x_k} \Big] \\ &= \Delta x_j \Delta x_k \Delta x_i \rho^2 \lceil s \rceil \left[v_k|_{x_k + \Delta x_k} - 2v_k|_{x_k} + v_k|_{x_k - \Delta x_k} \right] \end{aligned} \tag{4.52}$$

Where the definition of velocity was used in the final step. This expression along with the other expressions of identical form in 4.51 can be expressed compactly as

$$\Delta x_j \Delta x_k \Delta x_i \sum_{l=i,j,k} \rho^2 \omega \lceil s \rceil \left[v_k|_{x_l + \Delta x_l} - 2v_k|_{x_l} + v_k|_{x_l - \Delta x_l} \right] \tag{4.53}$$

The remaining terms are those in 4.44, i.e. $\psi - \Delta x_j \Delta x_k \Delta x_i \rho^2 \omega \beta$, which were re-expressed in 4.48 and 4.49. Now in the limit imposed

$$\begin{aligned}
\psi - \Delta x_j \Delta x_k \Delta x_i \rho^2 \omega \beta &= \Delta x_j \Delta x_k \Delta x_i \rho^2 \omega \left[s_T^{-k}|_{[-+]k} - s_T^k|_{[+-]k} + \frac{2dx_k}{\Delta x_k} \left(s_T^k|_{[--]k} - s_T^{-k}|_{[++]k} \right) \right] \\
&= \Delta x_j \Delta x_k \Delta x_i \rho^2 \omega \left[s_T^{-k}|_{[-+]k} - s_T^k|_{[+-]k} + \left(s_T^k|_{[--]k} - s_T^{-k}[++]k \right) \right] \\
&= \Delta x_j \Delta x_k \Delta x_i \rho^2 \omega \Bigg[\frac{-(s_T^k + s_T^{-k})|_{[+-]k} + (s_T^k + s_T^{-k})|_{[-+]k}}{2} \\
&- \frac{s_k|_{[+-]k} + s_k|_{[-+]k}}{2} \\
&+ \frac{-(s_T^k + s_T^{-k})|_{[++]k} + (s_T^k + s_T^{-k})|_{[--]k}}{2} \\
&+ \frac{s_k|_{[--]k} + s_k|_{[++]k}}{2} \Bigg]
\end{aligned} \tag{4.54}$$

As the two terms in the fourth and sixth lines of 4.54 are an average at the same point x_k they approximate one another

$$\frac{s_k|_{[+-]k} + s_k|_{[-+]k}}{2} \approx \frac{s_k|_{[--]k} + s_k|_{[++]k}}{2} \tag{4.55}$$

and can be cancelled out of the final expression of 4.54. Each of the remaining terms may be paired with the components on the same side and act as an average in a similar way. Rearranging the final expression of 4.54.

$$\begin{aligned}
\psi - \Delta x_j \Delta x_k \Delta x_i \rho^2 \omega \beta = \Delta x_j \Delta x_k \Delta x_i \rho^2 \omega \Bigg[& \frac{-\left((s_T^k + s_T^{-k})|_{[+-]k} + (s_T^k + s_T^{-k})|_{[++]k} \right)}{2} \\
& + \frac{(s_k^+ + s_k^-)|_{[-+]k} + (s_k^+ + s_k^-)|_{[--]k}}{2} \Bigg]
\end{aligned} \tag{4.56}$$

Making use of the limit the terms in equation 4.56 can be re-expressed as

$$\begin{aligned}
\frac{(s_T^k + s_T^{-k})|_{[+-]k} + (s_T^k + s_T^{-k})|_{[++]k}}{2} &= \frac{(s_T^k + s_T^{-k})|_{x_k} + (s_T^k + s_T^{-k})|_{x_k + \Delta x_k}}{2} \\
\frac{(s_T^k + s_T^{-k})|_{[-+]k} + (s_T^k + s_T^{-k})|_{[--]k}}{2} &= \frac{(s_T^k + s_T^{-k})|_{x_k} + (s_T^k + s_T^{-k})|_{x_k - \Delta x_k}}{2}
\end{aligned} \tag{4.57}$$

and then treating them as averages over an intermediary point yields

$$\begin{aligned}\frac{(s_T^k + s_T^{-k})|_{x_k} + (s_T^k + s_T^{-k})|_{x_k+\Delta x_k}}{2} &= (s_T^k + s_T^{-k})|_{x_k+\Delta x_k/2} \\ \frac{(s_T^k + s_T^{-k})|_{x_k} + (s_T^k + s_T^{-k})|_{x_k-\Delta x_k}}{2} &= (s_T^k + s_T^{-k})|_{x_k-\Delta x_k/2}\end{aligned} \tag{4.58}$$

Applying the results of 4.58 to 4.56 we obtain

$$\psi - \Delta x_j \Delta x_k \Delta x_i \rho^2 \omega\beta = \Delta x_j \Delta x_k \Delta x_i \rho^2 \omega \Big[- \big[(s_T^k + s_T^{-k})|_{x_k+\Delta x_k/2} - (s_T^k + s_T^{-k})|_{x_k-\Delta x_k/2}\big]\Big] \tag{4.59}$$

All flux terms can now be collected from 4.53 and 4.59 to be expressed as

$$\begin{aligned}\frac{dp_k^\Omega}{dt} = &\left(\Delta x_j \Delta x_k \Delta x_i \sum_{l=i,j,k} \omega \lceil s \rceil \left[v_k|_{x_l+\Delta x_l} - 2v_k|_{x_l} + v_k|_{x_l-\Delta x_l}\right]\right) \\ &- \big[(s_T^k + s_T^{-k})|_{x_k+\Delta x_k/2} - (s_T^k + s_T^{-k})|_{x_k-\Delta x_k/2}\big]\end{aligned} \tag{4.60}$$

Since $\Delta x_i = 2dx_i$ and $2dx_i$ is the smallest extension between in the event lattice Δx_i may be taken as unity. In this case the element refers to a single cell of unit volume. We may express the element as a collection of particles of size $\rho\Delta x_i \Delta x_j \Delta x_k$ and allow a characteristic particle momentum s_k^Ω such that

$$\begin{aligned}\rho\Delta x_i \Delta x_j \Delta x_k \frac{ds_k^\Omega}{dt} = &\left(\Delta x_j \Delta x_k \Delta x_i \sum_{l=i,j,k} \rho^2 \omega \lceil s \rceil \left[v_k|_{x_l+\Delta x_l} - 2v_k|_{x_l} + v_k|_{x_l-\Delta x_l}\right]\right) \\ &- \Delta x_j \Delta x_k \Delta x_i \rho^2 \omega \big[((s_T^k + s_T^{-k})|_{x_k+\Delta x_k/2}) - (s_T^k + s_T^{-k})|_{x_k-\Delta x_k/2}\big]\end{aligned} \tag{4.61}$$

Cancelling the common terms on both sides

$$\begin{aligned}\frac{ds_k^\Omega}{dt} = &\rho\omega \lceil s \rceil \left(\sum_{l=i,j,k} \left[v_k|_{x_l+\Delta x_l} - 2v_k|_{x_l} + v_k|_{x_l-\Delta x_l}\right]\right) \\ &- \rho\omega\left(((s_T^k + s_T^{-k})|_{x_k+\Delta x_k/2}) - (s_T^k + s_T^{-k})|_{x_k-\Delta x_k/2}\right)\end{aligned} \tag{4.62}$$

As this is a discrete space we do not take the limit as $\Delta x \to 0$. However the first term has the clear structure of a symmetric discrete second derivative, the second the form of a first order discrete derivative. The missing denominators are Δx_i^2 and Δx_i respectively which both equal unity and so have no effect on the assertion of these terms as proper discrete derivatives. For demonstration

we re-write 4.62 as

$$\frac{ds_k^{\Omega}}{dt} = \rho\omega\Big(\lceil s \rceil \, \tilde{\nabla}^2 v_k - \tilde{\nabla}((s_T^k + s_T^{-k}) \Big) \tag{4.63}$$

where the discrete derivatives are rewritten as their continuous counterparts with a tilde to indicate that they are improper. In making the identification of the transmittable action for a single dimension akin to pressure $P_k = s_T^k + s_T^{-k}$ we obtain

$$\frac{ds_k^{\Omega}}{dt} = \rho\omega\Big(\lceil s \rceil \, \tilde{\nabla}^2 v_k - \tilde{\nabla} P_k \Big) \tag{4.64}$$

Where the k subscript is an index and so the above represents three equations, one for each dimension. This analysis reveals in a very plain way that we should expect a collection of these point particles to behave like a classical fluid. This analysis is only preliminary in the fact that it heavily rests on making all the interactions equally probable, assuming constant density, and use of first order approximations. However these assumptions are not unreasonable and this general behaviour should be realizable in a suitable algorithm which utilizes the generalized interactions.

4.4 Vector Formulation of Generalized Interactions

In the sequence formulation of point particles mass containing objects moving at velocities much smaller than the speed of light are primarily composed of non-transmitting actions. That is inverse actions pairs where a particular action is followed by its inverse thereby causing the object to move back and forth between two cells. These action pairs are critical for the object to maintain mass or bounded action. Accordingly over a duration smaller than the time for the object to execute all its actions it would consistently return to the same cell. This cell would then change periodically with an action which is transmittable, i.e. not followed by an inverse. Accordingly there is a cell which the object could be said to reside within as it executes a long series of non-transmitting actions, and this resident cell would change periodically in accordance with the net momentum given by the transmitting actions. Since the great majority of actions would be non-transmitting, simulating the algorithm devised in full detail would be highly unproductive. Not to say that sequence detail algorithms would not be productive for other objects. For example an object which moves very fast and appears well extended in space such as an electron may very well require a sequence detail

algorithm. However to continue the analysis of the point particle envisioned here another approach is desirable. Preferably one which allows us to use computational tools already available.

This behaviour can be achieved by allowing objects to have definite positions in a real space and allow that definite position to evolve according to the velocity of the object as given by its action composition. The space which this position is within can be partitioned into cells, such that each real position can be mapped to a specific cell. All interactions can then be carried out through the cellular structure as given by the action set of the event-lattice, but the real space underneath it is used to periodically change the resident cell of the object in accordance with its velocity, i.e. its composition of transmittable actions. In the following such an approach is presupposed and a computational framework is obtained which is very similar to the Lattice Boltzmann Method, but differs fundamentally in that each object is a discrete and separate entity independent of the cells.

Consider a set of objects N enumerated such that

$$N = \{i : i = 1, 2, 3, ..., n\} \tag{4.65}$$

where n is the number of objects. In preparation for simulation consider the particles to be in a d dimensional space with periodic boundaries such that the total width of the box is l_b for each dimension. Each particle i has a position $r_i \in \mathbb{R}^d$. Let this box undergo cellular decomposition into the the set of cells Γ which make up the cells of the event-Lattice Γ. We require that the length of the sides of any given cell be the same length l_c and for any given domain and cells it is required that

$$\frac{l_b}{l_c} \in \mathbb{N} \tag{4.66}$$

In order to organize the interaction of the particles their location must be known. There is a map $L : R \to \Gamma$ called the indexing function. A particle $i \in N$ with position $r_k^i \in R$ is said to occupy, or be an occupant of, or reside in, a given cell $\gamma \in \Gamma$ if

$$L(r_i) = \gamma \tag{4.67}$$

Similarly if one were to check cell $\gamma \in \Gamma$ there is a check function $C : \Gamma \to N \cup \{0\}$ such that

$$C(\gamma) = \begin{cases} i, & \text{if } L(r_k^i) = \gamma \\ 0, & \text{otherwise} \end{cases} \tag{4.68}$$

where $r_i \in R^d$.

To facilitate the generalized interaction over the cellular domain the set Γ is endowed with an extended action set S^x of actions with an external binary operation $\sigma : S^x \times \Gamma \to \Gamma$. This is a different action set then the one outlined in the event-lattice in that it accounts for relations between particles that may act on the same cell. Thus it is extended beyond those cells which may participate in direct actions of a single object. The extended action set defines the neighborhood of γ as the subset of Γ which if an object is present in γ, the object can transmit action to other particles in or acting on cells in the neighborhood of γ. The neighborhood of the cell $\gamma \in \Gamma$ is then the set

$$\Gamma = \{\nu : \forall s \in S^x \, (\nu = \sigma^s(\gamma))\} \tag{4.69}$$

Hereafter $j = \sigma^s(i)$ refers to $j \in \Gamma$ as a neighbor of i obtained through the member $s \in S^x$. Furthermore let i and j denote the particles in those cells called i and j. For convenience we define the occupancy of a neighboring cell j of i to be given by the function ϕ_{ij} such that

$$\phi_{ij} = \begin{cases} 1, & \text{if } S(L(\sigma^s(i)) = j \in N \\ 0, & \text{otherwise} \end{cases} \tag{4.70}$$

Accordingly $\phi_{ij} = \phi_{ji}$. This function is defined for convenience and will not be used after this discussion. This cellular structure constitutes the framework which can be used to exchange actions between objects. Accordingly the action set of an object can be described by a vector with as many

components as the action set S (not extended). Each object i is endowed with an action-state

$$|s_T\rangle_i = \begin{bmatrix} s_T^1 \\ s_T^2 \\ \vdots \\ s_T^{|S|} \end{bmatrix} \tag{4.71}$$

In order to make use of this action-state, we must be able to extract the resulting particle momentum from $|s\rangle_i$ to compute the velocity of i. This is obtained by taking the inner product with a vector which describes the orientation of each action relative to its inverse

$$|\hat{\kappa}\rangle \tag{4.72}$$

The notation indicates this to be a vector of vectors. For example $|\hat{\kappa}\rangle$ for a three dimensional system is

$$|\hat{\kappa}\rangle = \begin{bmatrix} (1,0,0) \\ (0,1,0) \\ (0,0,1) \\ (-1,0,0) \\ (0,-1,0) \\ (0,0,-1) \end{bmatrix} \tag{4.73}$$

Notice that there are three inverse action pairs and so each vector of $|\hat{\kappa}\rangle$ has three components. Since each dimension has an inverse action pair there are six vectors for $|\hat{\kappa}\rangle$ in total. Ultimately the net momentum will have one definite direction. The total momentum of a point particle object is given by the inner product

$$\vec{s}_i = \langle\hat{\kappa}|s_T\rangle_i \tag{4.74}$$

An interaction of one particle with another entails a transmission of action. In order for an action to be transmitted the action must have been executed. Accordingly actions can only be transmitted in the direction of which it acts. Let W_k be a diagonal matrix which specifies the actions particle i transmits to particle j when related by a member of the extended action set

$k \in S^x$. At the same time j transmits action to i thus there is another transmission matrix $W_{k^{-1}}$. The total change in action state of particle i is then the action it transmits to other particles in its neighborhood and the action it receives from those particles.

$$|\Delta s_T\rangle_i = \sum_{\forall k \in S^x} \phi_{ij}\big(W_{k^{-1}}|s_T\rangle_j - W_k|s_T\rangle_i\big) \tag{4.75}$$

and

$$j = C(\sigma^k(L(i))) \tag{4.76}$$

If $|\Delta s_T\rangle_{ij}$ denotes the change of the action state of i due to j we readily see that for a pairwise interaction

$$|\Delta s_T\rangle_{ij} = \phi_{ij}(W_{k^{-1}}|s_T\rangle_j - W_k|s_T\rangle_i) \tag{4.77}$$

and additionally

$$|\Delta s_T\rangle_{ji} = \phi_{ij}(W_{k^{-1}}|s_T\rangle_i - W_k|s_T\rangle_j) \tag{4.78}$$

which clearly indicates

$$|\Delta s_T\rangle_{ij} = -|\Delta s_T\rangle_{ji} \tag{4.79}$$

In making the identification between a change in momentum with a force as given by Newtons equations of motion equation 4.79 is the equivalent of $F_{ij} = -F_{ji}$ and the net momentum will always be conserved. Each action at a given instant may give rise to classical kinetic energy or it may not depending on the quantity of inverse actions in the same particle. It is essential that a particle does not transmit more action than it possesses such that

$$\sum_{\forall k \in S^x} W_k \leq \delta_{mn} \tag{4.80}$$

where δ_{mn} is the Kronecker delta

$$\delta_{mn} = \begin{cases} 1, & \text{if } n = m \\ 0, & \text{if } n \neq m \end{cases} \tag{4.81}$$

it is then that the result of a collision yields a new action state for particle i. If an interaction were

to occur over a time step Δt it would follow that

$$|s_T\rangle_i(t+\Delta t) = |s_T\rangle_i(t) + |\Delta s_T\rangle_i \tag{4.82}$$

which requires $|\Delta s_T\rangle_i = f(\Delta t)$. Let us parametrize W_k with $\bar{W}_k$ such that

$$\sum_{\forall k \in S^x} \bar{W}_k = \delta_{mn} \tag{4.83}$$

and then

$$\omega \bar{W}_k = W_k \tag{4.84}$$

Allowing particles to interact over a time step Δt in equation 4.82 suppose there is a characteristic time τ such that all the transmittable action of a particle i is transmitted to its neighbors. If in a given time step all transmittable action is transmitted in accordance with 4.82 then ω of 4.83 equals unity. In a time step of $\Delta t < \tau$ not all action will be transmitted. Accordingly $\omega < 1$. If no time passes such that $\Delta t = 0$ then every element in W_s equals zero then it must be that $\omega = 0$. Substituting 4.84 into 4.75 we obtain

$$|\Delta s_T\rangle_i = \omega \sum_{\forall k \in S^x} \phi_{ij} \left(\bar{W}_{k^{-1}} |s_T\rangle_j - \bar{W}_k |s_T\rangle_i \right) \tag{4.85}$$

identifying $|\Delta \bar{s}_T\rangle_i$ with the summation portion of 4.85 such that

$$|\Delta \bar{s}_i\rangle = \sum_{\forall k \in S^x} \phi_{ij} (\bar{W}_{k^{-1}} |s_T\rangle_j - \bar{W}_k |s_T\rangle_i) \tag{4.86}$$

the compact form

$$|\Delta s_T\rangle_i = \omega |\bar{s}_T\rangle_i \tag{4.87}$$

is obtained which is the change in momentum of particle i during a time step Δt. The momentum of particle i at time t is $\vec{s}_i(t) = \langle \hat{\kappa} | s_T \rangle_i$ and the momentum at $t + \Delta t$ is then

$$\vec{s}_i(t+\Delta t) = \langle \hat{\kappa} | s_T + \Delta s_T \rangle_i \tag{4.88}$$

or by distributing $\langle\hat{\kappa}|$ and substituting in equation 4.87 for $|\Delta s_T\rangle_i = \omega|\bar{s}_T\rangle_i$ it follows

$$\vec{s}_i(t+\Delta t) = \langle\hat{\kappa}|s_T\rangle_i + \omega\langle\hat{\kappa}|\Delta\bar{s}_T\rangle_i \tag{4.89}$$

using the inner product defined in 4.74

$$\vec{s}_i(t+\Delta t) = \vec{s}_i(t) + \omega\Delta\vec{s}_i \tag{4.90}$$

If the time step occurs such that $\Delta t = \tau$ then $\omega = 1$ and we have

$$\vec{s}_i(t+\tau) = \vec{s}_i(t) + \Delta\vec{s}_i \tag{4.91}$$

multiplying equation 4.91 by ω and subtracting it from 4.90 and rearranging we obtain

$$\vec{s}_i(t+\Delta t) = \vec{s}_i(t)(1-\omega) + \omega\vec{s}_i(t+\tau) \tag{4.92}$$

Since $\vec{s}_i(t+\Delta t) = \vec{s}_i(t)$ when $\Delta t = 0$ and $\vec{s}_i(t+\Delta t) = \vec{s}_i(t+\tau)$ when $\Delta t = \tau$ it follows that

$$\omega = \frac{\Delta t}{\tau} \tag{4.93}$$

substituting equation 4.93 into 4.92

$$\vec{s}_i(t+\Delta t) = \left(1 - \frac{\Delta t}{\tau}\right)\vec{s}_i(t) + \left(\frac{\Delta t}{\tau}\right)\vec{s}_i(t+\tau) \tag{4.94}$$

which has identical form to the Lattice Boltzmann Collision step 2.2. Accordingly we should be able to use a framework like the Lattice Boltzmann Method to create a point particle algorithm in order to exhibit their general character. We are then free to select the elements of W_k so long as they only transmit action in the direction of the action. This framework can be used for either discrete amounts of action or continuous actions.

The translation of a given particle i can then be achieved by incrementing the particle position

with its momentum through first order integration

$$r_k^i(t + \Delta t) = r_k^i(t) + \Delta t \frac{\vec{s}_i}{m_i} \tag{4.95}$$

where Δt is the time step and m_i is the mass of particle i. As it is more convenient the framework will be used with a continuous action spectrum and a unit mass.

Chapter 5

Algorithmic Implementation of the Point Particle Model

This chapter describes how to implement the vector formulation of the point particle model developed in the previous chapter. It is given due weight as it is effectively the apparatus which allows us to experiment with the model. Figure 5.1 is a flow diagram for a generic simulation and serves to guide the following discussion. The flow diagram is endowed with an entry point on the left and an exit point on the right. Two gray regions partition the flow diagram into a setup component and a main simulation loop. The white boxes are categories of operations that are carried out in succession as indicated by the arrows which join them. In the programming side we shall frequently be using arrays, many variables stored together in succession in memory. The general form of an array shall be $A[:]$ for a one dimensional array, $A[:][:]$ for a two dimensional array and so forth. For a given array $r[:][:]$, $r[i][j]$ refers to the element in the i^{th} row and j^{th} column. Each time an array is first introduced the size of the array dimensions will be directly stated with the array such that the position array would be introduced as $r[n][d]$ which is a two-dimensional array with size $n \times d$. When referring to arrays in general discussion $r[n][d]$ will be preferred to $r[:][:]$ as it reminds the reader of the details of the array. It does not mean the value in the last element. When referencing specific elements in arrays as in formulas, effort will be made to use i, j, and k. However k will generally be used for components related to spatial dimensions such as in positions and velocities. When referring to action types in vector form they will sometimes be accessed with

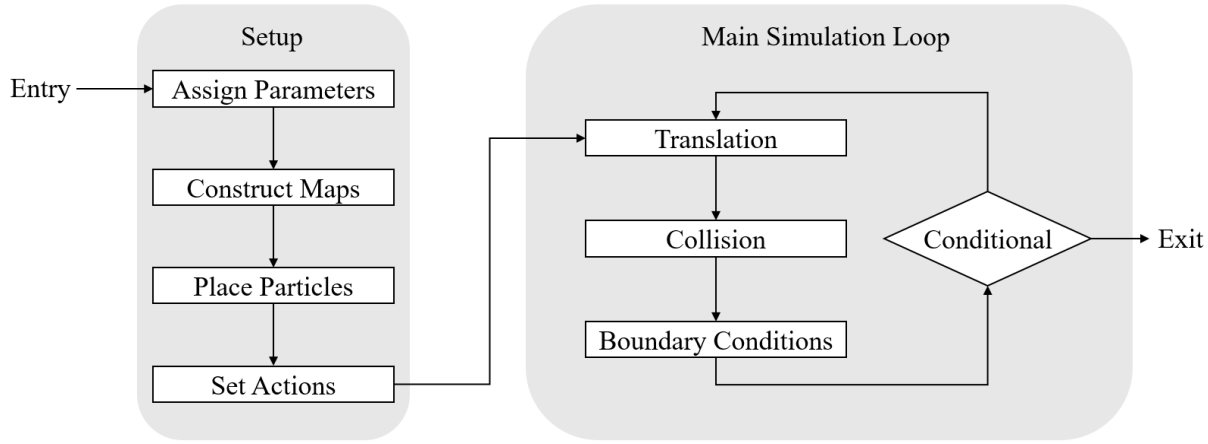

Figure 5.1: A general flow diagram for the simulations

k and sometimes with κ depending on how it is being used. Use of i and j will occur for counters, particular cells, and objects in general. Use of n_x is for counts of things x such as the number of cells as n_c where c indicates cells. The context for its use, or its relevance, is indicated by the subscript. When conducting calculations about a given particle i it is imperative that i be used in the referencing of the array for that particle however, intermediate calculations do not need specific reference to i as the intermediate variables are used for all particles so the i will often be omitted from intermediate steps.

5.1 Setup Procedure

5.1.1 Assign Parameters

Beginning the simulation requires a great many parameters be assigned. The single most important parameter is the dimensionality of the system. It is often useful to be able to run simulations in both two and three dimensions. Although it can be a little more difficult it is possible to leave the dimensionality of the system as an input parameter. If one is to have dimensionality as an input it is better to decide sooner than later as it has significant consequences. Even if one were to only use a certain dimensionality it is still better to specify the dimensionality as a variable and pass it as an argument to subsequent functions. The reason is that computational expense greatly increases with an increase in dimension. This is especially the case in simulations which discretize

the domain into cells. When debugging such a program some errors will only become apparent after long times. Accordingly to debug with a full scale model can take a very long time. Thus the dimensionality should always be an assigned parameter when possible. Here d refers to the dimensionality of the system.

Following the dimensionality the number of cells is assigned albeit indirectly. Instead of the total number of cells the number of cells per side of the simulation box is assigned as an integral number n_w which indicates the number of cells along a specific wall of the simulation box. The total number of cells is also the cardinality of the set Γ as defined as the cells of the event lattice. Accordingly

$$|\Gamma| = n_c = {n_w}^d \tag{5.1}$$

It is most convenient to set the box length equal to the number of cells along a wall such that

$$l_b = n_w \tag{5.2}$$

resulting in l_c to take a value of unity, and since $n_w \in \mathbb{N}$ equation 4.66 is immediately satisfied.

In order to construct the external binary operation σ the extended action set S^x must be assigned in some way so as to generate a list of neighboring cells which an object will interact with. The assigned parameter which is used to generate σ is termed a shift vector set. Each shift vector specifies a relation from a given cell to a specific neighbor cell. The general form of a shift vector is

$$c_k = (c_1, c_2, ..., c_d) \tag{5.3}$$

where the components of c_k are elements from the set D where

$$D = \{x : x = \pm\lambda l_c,\ \lambda = 0, 1, 2, ..., r,\ r \in \mathbb{N},\ 0 < r < n_w\} \tag{5.4}$$

For example if $r = 2$ and $l_c = 1$ then

$$D = \{-2, -1, 0, 1, 2\} \tag{5.5}$$

Some example shift vectors are $(0, 1, 0)$, $(1, -1, 0)$, $(-2, 0, -1)$ and so forth. No two shift vectors

should reference the same cell with respect to a given cell as that would be redundant. As one would expect the shift vector of $(1, 0, 0)$ applied to a given cell in a three dimensional model refers to the cell directly adjacent to the given cell in the positive x-direction. The actual construction of the map which gives the relation of cells by shift vectors and thus σ is the subject of the following section. Let n_σ denote the number of cells indicated by the extended action set. The shift vector set can be conveniently packaged in an array $c[n_\sigma][d]$ where each row corresponds to a shift vector. The set of all cells given by the shift vectors in relation to a given cell define the neighborhood of that cell. It is convenient to enumerate these neighbors in accordance with the order in which the corresponding shift vectors appear in $c[n_\sigma][d]$.

In addition to the assignments already mentioned the number of particles, velocity of the particles, transmittable actions, time step, and transmission coefficients must all be assigned. The effects of these parameters vary according to the investigation and will be discussed when relevant.

5.1.2 Construction of the σ Mapping

Although $\sigma : S \times \Gamma \to \Gamma$ is useful for clear mathematical formulation the implementation in a program is quite different and takes the form of a 1-dimensional array $\sigma[n_\sigma n_c]$ and a function which generates an index for this array. This map is constructed from the shift vector set $c[n_\sigma][d]$.

The first step is to enumerate the cells which compose the simulation box. The case of three dimensions will be discussed as the case of two dimensions is a simplification. Figure 5.2 shows the resulting enumeration of the cells from the following process when $n_w = 3$. The function consists of three nested loops, one for each dimension, in opposite order of a standard vector i.e z then y then x such that x is the inner most loop. Each loop is a for-loop with a counter that increments each counter from 1 to n_w. Call these counters i_x, i_y, and i_z. Since i_x is the innermost counter when iterated we move along a given z-plane i.e. at a fixed i_z value, and a given y-plane i.e. a fixed i_y value. Thus in incrementing i_x we are incrementing along the intersect of these two planes. When the $i_x = n_w$ the y-plane shifts such that $i_y = i_y + 1$ and we again increment through the intersect of the i_z and i_y planes. This continues until $i_y = n_w$ at which point $i_z = i_z + 1$ and the process repeats on the new i_z plane. In this way we loop through all the cells in the domain sequentially. The two dimensional case is obtained by dropping the z component.

As each cell is sequentially incremented through they are assigned names in accordance with

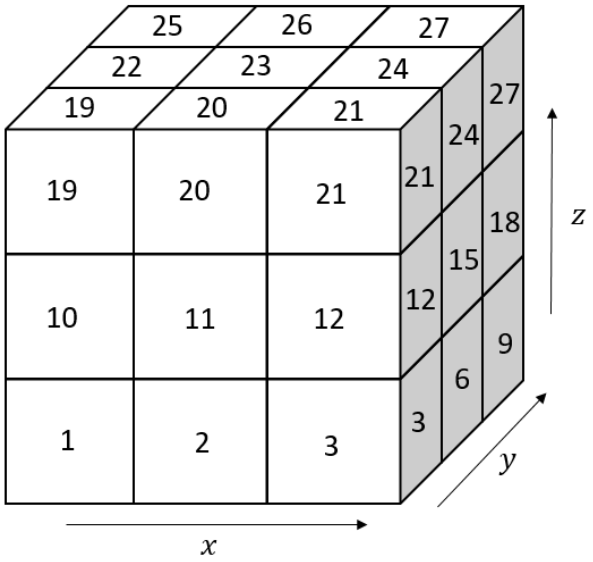

Figure 5.2: Enumeration of the cells as given by the algorithm in the text for $n_w = 3$.

the counters which correspond to that cell's position. A simple equation to assign a name γ to each cell given by i_x, i_y, and i_z is just like one used to flatten a three dimensional array

$$\gamma = 1 + (i_x - 1) + (i_y - 1)n_w + (i_z - 1)n_w^2 \tag{5.6}$$

which corresponds exactly to the naming scheme of 5.2. Now the cells have been enumerated. We now want to create a map such that by using a given cell name $\gamma \in \Gamma$ and the j^{th} shift vector $c[j][d] = (c_1, ..., c_d)$ the name of the j^{th} neighbor cell $\beta \in \Gamma$ relative to γ is obtained.

We create an array $\sigma[n_\sigma n_c]$ such that the first n_σ entries of the array contain the n_σ neighbors of cell 1, the following n_σ entries of the array contain the neighbors of cell 2, and so forth. In this way the j^{th} neighbor cell of γ is obtained by giving the index $(\gamma - 1)n_\sigma + j$ to σ such that

$$\beta = \sigma[(\gamma - 1)n_\sigma + j] \tag{5.7}$$

Where β is the j^{th} neighbor of γ. A very smooth method to populate $\sigma[n_\sigma n_c]$ for periodic boundary conditions has been presented by Allen and Tildesly. [92] Let i_c designate the name of a

cell given by its indexes such that

$$i_c = 1 + (i_x - 1)\%n_w + [(i_y - 1)\%n_w]n_w + [(i_z - 1)\%n_w]n_w^2 \tag{5.8}$$

where % is the modulo operator. To obtain the j^{th} neighbor of i_c add the j^{th} shift vector $c[j][d] = c_k = (c_x, c_y, c_z)$ to the i_k values of i_c i.e. if β is the j^{th} neighbor of γ and the indexes which yield i_c given equation 5.8 are i_x, i_y, and i_z then β is obtained as

$$\beta = 1 + (i_x + c_x - 1)\%n_w + [(i_y + c_y - 1)\%n_w]n_w + [(i_z + c_z - 1)\%n_w]n_w^2 \tag{5.9}$$

Thus σ may be populated while enumerating the cells such that for every unique i_x, i_y, and i_z we loop over all j neighbors and populate $\sigma[n_\sigma n_c]$ as

$$\sigma[(\gamma-1)n_\sigma+j] = 1+(i_x+c[j][1]-1)\%n_w+[(i_y+c[j][1]-1)\%n_w]n_w+[(i_z+c[j][3]-1)\%n_w]n_w^2 \tag{5.10}$$

In this way the map may be constructed for any neighborhood defined by a shift vector set. Be sure to remove the initial 1 of both equations if the array counts from zero in the programming language being used and keep it if otherwise.

5.1.3 Place Particles

The following describes how to place particles in a domain such that they are spaced from one another in a Cartesian lattice with a small perturbation so that they are not perfectly spaced. The positions of these particles are stored in a two dimensional array $r[n][d]$ where n is the number of particles in the system. First calculate the expected number of particles to align along a wall of the domain as an integral number for example the number of particles along a side of the box can be computed as

$$n_s = \left\lceil n^{1/d} \right\rceil \tag{5.11}$$

Where $\lceil x \rceil$ is a ceiling function which rounds $x \in \mathbb{R}$ to the next highest integer. The spacing between the particles, r_s, in the Cartesian lattice is then

$$r_s = \frac{l_b}{n_s} \tag{5.12}$$

Initialize a counter j which will be used as a reference for the particles. Loop over each dimension with $i_k = 1$ to n_s nesting each subsequent dimension inside of the previous as in section 5.1.2 except here the order of the dimension is unimportant. The index k refers to each dimension. Inside the innermost loop evaluate the counter j with the conditional $j > n$. If the conditional returns true all particles have been assigned a position, else particle j and potentially subsequent particle positions are yet to be assigned according to the following

$$r_k = (i_k - \frac{1}{2})r_s + \tilde{h}\, k = 1, ..., d \tag{5.13}$$

where r_k is the k component position of particle j, and $\tilde{h}$ is a small random number selected at each instance of assignment as desired. Each r_k is assigned to the position array for each dimension k

$$r[j][k] = r_k \tag{5.14}$$

After assigning the position to a particle increment the counter $j = j + 1$ and continue looping. Once the conditional in the loop is true i.e. $j > n$ the loops are all terminated, as all particles have been assigned a position. This technique is best suited when the total amount of particles is an integral number to the power d but will work otherwise. This method is a bit excessive for these objects as they have no interaction potential and will not give a catastrophic failure if the particles are placed randomly but in doing so this routine can be used for other simulations.

5.1.4 Set Actions

For a d dimensional system there are $2d$ members in the action set S (not extended). In order to start the simulation these actions need to be assigned. This is achieved in three parts. First, choosing an initial velocity $|v|$ for the particles. Second, setting the transmittable action for each action type designated $s_{T_0}^{\pm k}$ where

$$\lceil s_T \rceil = \sum_{(k,-k)\,\in\, S} s_T^k + s_T^{-k} = 2d s_{T_0}^{\pm k} \tag{5.15}$$

Third, modifying the initial transmittable actions $s^k_{T_0}$ and $s^{-k}_{T_0}$ to reflect the desired velocity as s^k_T and s^{-k}_T for each dimension k.

In order to conduct equilibrium simulations for measuring transport coefficients it must be ensured that the system has no net momentum. It is also desirable that there are no correlations in the velocity distribution. An array is created to store velocity of each particle $u[n][d]$. An array $A[n][2]$ is created. In the first column of $A[n][2]$ all rows are assigned an integral value equivalent to their row number

$$A[i][1] = i,\ \forall i\ \in\ N \tag{5.16}$$

These values are to be used to represent the particle indexes. In the second row random numbers are assigned from a random number generator.

$$A[i][2] = \tilde{h}_i,\ \forall i\ \in\ N \tag{5.17}$$

The subscript of $\tilde{h}_i$ indicates that each entry i is receiving its own random number $\tilde{h}$. Next the rows of array $A[n][2]$ are sorted so as to order the second column in some way. Thus the particle indexes in the first column have been shuffled. Next the first column of $A[n][2]$ is looped through beginning with the second entry, skipping every other entry, and finishing on the second last entry. Define this with an index $j = 2, 4, 6, ..., n-1$. For each iteration d random numbers are drawn from the set $(0, 1)$ and 0.5 is subtracted from these numbers to create a random vector $\tilde{v}_k$ where each component k is in the range $(-0.5, 0.5)$. Then a scaling parameter is obtained

$$\alpha = \sqrt{\frac{\tilde{v}_k \cdot \tilde{v}_k}{|\bar{v}|^2}} \tag{5.18}$$

and a velocity is obtained

$$v_k = \alpha \tilde{v}_k \tag{5.19}$$

this velocity is assigned to the particle given by $A[j][1]$

$$u[\,A[j][1]\,][k] = v_k \tag{5.20}$$

the equal and opposite velocity is assigned to the next particle of the shuffled list

$$u[\, A[j][1]+1\,][k] = -v_k \tag{5.21}$$

After all these are set two particles remain, namely the particles of $j = 1$ and $j = n$. The velocity for these particles is set the same way as above by letting $u[\, A[1][1]\,][k] = v_k$ and $u[\, A[n][1]\,][k] = -v_k$. In this way the net momentum is zero and the particle velocities are uncorrelated. A net momentum or velocity can be set later as desired.

With velocities available the transmittable action $s_{T_0}^{\pm k}$ is used to to construct the action vector $|s_T\rangle_i$. Construct the array $s[n][2d]$. Looping through the set of all particles $j = 1, 2, 3, ..., n$.

$$s_T^k = s_{T_0}^{\pm k} + \frac{v_k}{2} \tag{5.22}$$

$$s_T^{-k} = s_{T_0}^{\pm k} - \frac{v_k}{2} \tag{5.23}$$

These actions are then assigned to the action array

$$s[j][k] = s_T^k = s_{T_0}^{\pm k} + \frac{1}{2}u[j][k] \tag{5.24}$$

$$s[j][k+d] = s_T^{-k} = s_{T_0}^{\pm k} - \frac{1}{2}u[j][k] \tag{5.25}$$

for $k = 1, ..., d$. Note that as the loop continues s_T^k and s_T^{-k} are reassigned for each j. The velocity of a given particle i in direction k is readily recovered from the action vector as

$$u[i][k] = s[i][k] - s[i][k+d] \tag{5.26}$$

with a unit mass assumed. Note that if a unit mass was not assumed the above equations would need to be modified.

5.2 Main Simulation Loop

5.2.1 Translation Routine

The translation step in the simulation has three components, first the particle's positions must be incremented in accordance with their velocities, second the proper cell must be determined, third this particle-cell relation must be later stored for the collision routine. An array is created to store the cell indexes of the particles $z[n]$. Another array $q[n_c]$ is created to store the contents of each cell. This process is carried out in a loop. There is first a counter i for $i = 1, 2, 3, ..., n$ looping through all the particles. The translation is carried out via equation 4.95 but instead in terms of the arrays

$$r[j][k] = r[j][k] + \Delta t u[j][k] \tag{5.27}$$

At this instant the positions are already nearby in terms of the computer memory so it is best to immediately obtain the cell index of the particle. First normalize the particle position then scale it by the box length. This can be done in one operation

$$r'_k = r[j][k]\frac{n_w}{l_b} \tag{5.28}$$

The values r'_k now represent the position in lattice units. This process is already achieved when $l_b = n_w$. Next floor r'_k to round it to the next lowest integer where $\lfloor x \rfloor$ is the floor of x. The cell index must then be determined in terms of how the domain was discretized. Identifying $\lfloor r'_k \rfloor = i_k$ for all k equation 5.6 can then be used to obtain the cell index. Equation 5.6 can be implemented in a dimension agnostic way. Initialize $i_c = 1$ then loop over $k = 1, .., d$ such that

$$i_c = i_c + r'_k \cdot {n_w}^{k-1} \tag{5.29}$$

then store this index

$$z[j] = i_c \tag{5.30}$$

finally use the cell index i_c to reference that particular cell's entry in $q[n_c]$ and store the particles identity in $q[n_c]$ such that

$$q[i_c] = j \tag{5.31}$$

The array $q[n_c]$ can now play the role of the check function of equation 4.68. Once all of the particles have been incremented, indexed, and surveyed, the translation process is complete.

5.2.2 Collision Routine

The collision routine is the true work horse of the algorithm as it handles all particle-particle interactions. The general functioning of the collision routine is to save the current action states of all the particles, then compute the amount of action each particle will transmit to its neighbors. Since the initial action state of all particles defines the amount of action a particle can transmit, this data must not be tampered with. Accordingly the final action state of the particles is a separate array, which is initialized as an identical copy of the initial action state. As each interaction is computed this second array is modified leaving the initial action state unaltered. Once all the interactions have been computed the final state becomes the new initial state. The translation process ensues, boundary conditions are enforced, and then the collision process begins once again.

In detail, an array $s2[n][2d]$ is made as an exact copy $s[n][2d]$. Thus $s[n][2d]$ is the initial action state of all the particles and must not be changed as the interactions are computed. Array $s2[n][2d]$ is altered by each interaction to obtain the final state.

After creating $s2[n][2d]$ the interactions are computed by looping through all of the particles $i = 1, 2, 3, ..., n$. For each particle i the cell index is identified using the cell index array

$$i_c = z[i] \tag{5.32}$$

This index is used to generate a reference point for the map $\sigma[n_\sigma n_c]$. Recall that $\sigma[n_\sigma n_c]$ stores all of the neighbors of a cell in an ordered fashion. The precise entry where the neighbors of cell i begins is $1 + n_\sigma(i - 1)$. Given particle i and the list of its neighbors in $\sigma[n_\sigma n_c]$ loop through all the neighbors for each i and compute the interactions. Thus for particle i

$$i_0 = n_\sigma(i_c - 1) \tag{5.33}$$

is taken as the reference point for $\sigma[n_\sigma n_c]$. Looping through $i_\sigma = 1, 2, 3, ...n_\sigma$ the neighbor cells are

obtained as

$$\beta = s[i_0 + i_\sigma] \tag{5.34}$$

That is, β is the i_σ^{th} neighbor of cell i_c which may contain a particle for interaction. The cell β may then be queried such that

$$q[\beta] = \begin{cases} j, & \text{if } \exists j \text{ such that } z[j] = \beta \\ 0, & \text{otherwise} \end{cases} \tag{5.35}$$

If the query yields a particle j an interaction is carried out. This conditional just expressed is equivalent to the occupant function ϕ_{ij} of equation 4.70. This is done for all neighbor particles j given by σ, and done for all particles i. One will of course notice that when the relationship between a given i and j is found, and the interaction is carried out, it is an ideal time to carry out the inverse interaction where particle j transmits action to i. Indeed it would be a waste to wait until j is in the place of i and i in the place of j to carry out $W_{k^{-1}}$. For this reason only half of the shift vectors need to be specified for all interactions in the neighborhood to be accounted for. The nature of how W_k is effected is specific to the model and will be deferred for now. Ultimately the effect of each interaction is to create a change of the final action state of the form

$$|\Delta s_T\rangle_i = (W_{k^{-1}}|s_T\rangle_j - W_k|s_T\rangle_i) \tag{5.36}$$

granted i and j are neighboring. The change represented by 5.36 is achieved by looping through each action $\kappa = 1, 2, ..., 2d$. Since W_k are diagonal and of size $2d \times 2d$ each κ can refer to a specific element along the diagonal of W_k the content W_k may be represented as a one dimensional array of form $w[2d]$. It follows that the change in action due to interaction is then

$$s2[i][\kappa] = s2[i][\kappa] + w[k]s[j][\kappa] - w[\kappa]s[j][\kappa] \tag{5.37}$$

and

$$s2[j][\kappa] = s2[j][\kappa] + w[\kappa]s[i][\kappa] - w[\kappa]s[i][\kappa] \tag{5.38}$$

Note that the $w[\kappa]$ are applied to the actions antecedent to any interaction namely the initial action state $s[n][2d]$ otherwise the nature of the interaction between i and neighbors j will be order

specific which should not be the case. This is done for all particles.

In the final step of the collision routine the final action state array $s2[n][2d]$ is redefined as $s[n][2d]$ which is essentially an update of the actions. If we implement the parametrization of W_k such that $W_k = \omega \bar{W}_k$ then $\bar{W}_k$ may be applied as $w[2d]$ in equations 5.37 and 5.39 but the final step of replacing $s[n][2d]$ with $s2[n][2d]$ can be replaced with

$$s[j][\kappa] = s[j][\kappa](1-\omega) + (\omega)s2[j][\kappa] \tag{5.39}$$

In this way ω and thus the transmission coefficients of W_k can be altered in magnitude but their relative values remain unchanged.

The exact implementation details of the collisions for point particle objects which interact over a neighborhood restricted to those cells which are in direct contact with a given cell are now discussed as this case was heavily used. The approach here is specific to this case. For different neighborhoods other approaches may be more effective. Direct contact refers to the case where D is limited to the set $D = \{1, 0, -1\}$ in 5.4 designating the Moore neighborhood in cellular automata. As point particles lack shape the interactions should be spatially isotropic. Thus in three dimensions there is only three unique relations which two cells may have when within each others Moore neighborhood. They may share a face, share an edge, or share a corner. Examples of the first kind are shift vectors like $(0, -1, 0)$ and $(0, -1, 0)$, examples of the second kind are $(1, -1, 0)$ and $(1, 0, 1)$, and examples of the third kind are $(1, 1, -1)$ and $(-1, -1, -1)$. Thus there are only three principle relations and each of these relations is the same for every action due to isotropy of the point particle. Select the transmission coefficients that each of these principle relations will have and place them in a one dimensional array with the number of entries proportional to the number of principle relations n_o as $w^*[n_o]$. We may then construct another array which organizes these transmission coefficients as $w[n_\sigma/2][n_o]$. Each shift vector must then be associated to one of these principle relations. For example in the case of a neighborhood defined by direct contact this can be achieved by taking the dot product of the shift vector with itself. The array $w[n_\sigma/2][n_o]$ can then be populated by looping through each neighbor i_σ such that

$$w[i_\sigma][k] = w^*[c[i_\sigma][k] \cdot c[i_\sigma][k]] \times |c[i_\sigma][k]| \tag{5.40}$$

For each dimension k. The last term $|c[i_\sigma][k]|$ is multiplied to the transmission value so that $w[n_\sigma/2][n_o]$ only has non-zero values for those neighbors which the actions should be transmitted to. This method can only be used here because the number of principal relations is equivalent to the dimensionality of the system.

The array $w[n_\sigma/2][d]$ is then readily implemented in the collision routine. Looping through the neighbors $i_\sigma = 1, 2, ..., n_\sigma/2$. For each neighbor i_σ loop over dimensions $k = 1, ..., d$. At neighbor i_σ for dimension k of particle i

$$\Delta s[i][k] = \begin{cases} w[\sigma][k]s[j][k], & \text{if } c[i_\sigma][k] < 0 \\ 0, & \text{if } c[\sigma][k] = 0 \\ -w[\sigma][k]s[i][k], & \text{if } c[i_\sigma][k] > 0 \end{cases} \tag{5.41}$$

and

$$\Delta s[i][k+d] = \begin{cases} -w[\sigma][k]s[i][k+d], & \text{if } c[i_\sigma][k] < 0 \\ 0, & \text{if } c[i_\sigma][k] = 0 \\ w[\sigma][k]s[j][k+d], & \text{if } c[i_\sigma][k] > 0 \end{cases} \tag{5.42}$$

Accordingly for particle j which particle i interacts with,

$$\Delta s[j][k] = \begin{cases} -w[\sigma][k]s[j][k], & \text{if } c[i_\sigma][k] < 0 \\ 0, & \text{if } c[\sigma][k] = 0 \\ w[\sigma][k]s[i][k], & \text{if } c[i_\sigma][k] > 0 \end{cases} \tag{5.43}$$

$$\Delta s[j][k+d] = \begin{cases} w[\sigma][k]s[i][k+k], & \text{if } c[i_\sigma][k] < 0 \\ 0, & \text{if } c[i_\sigma][k] = 0 \\ -w[\sigma][k]s[j][k+k], & \text{if } c[i_\sigma][k] > 0 \end{cases} \tag{5.44}$$

Equations 5.41 to 5.44 look horrid but only because they are forced into this format. Each equation has three cases which are determined with the same conditional, $c[\sigma][k]$ is $>, =$, or < 0. This conditional enforces that the transmission of the action of type κ only takes place if it is positive and non-zero with respect to the direction of the neighbor. It would be redundant to

check each action for the condition when it is known that if one action does not meet the condition then the inverse action does. Thus only half the actions need to be computed. Consequently this condition can be checked once and the results implicated for both j and i where j is the i_σ^{th} neighbor of i. If i is passing action k to j it follows that j cannot be passing the same action to i but j is definitely transmitting the inverse action k^{-1} to i. Thus the total change of action in j for action k of i is the negative of the change of action k of i. Thus each action being exchanged is only computed once for the pair. They are not computationally burdensome equations even though they may look it. Once $\Delta s[i][2d]$ and $\Delta s[j][2d]$ are obtained the new action in equation 5.37 is

$$s2[i][k] = s2[i][k] + \Delta s[i][2d] \tag{5.45}$$

and equation 5.46 as

$$s2[j][k] = s2[j][k] + \Delta s[j][2d] \tag{5.46}$$

all else being the same. These final states can then be implemented as described earlier. It is possible to make an entirely generalized process for any number of principle relations however it was not sought here. The Moore neighborhood was sufficient to provide interesting behaviour.

5.3 Boundary Conditions

In order to investigate the continuum like properties of the model the point particle model will be implemented to solve a couple conventional flow problems. What characterizes these problems is that the particles undergo exchange with the surfaces in order to enforce certain boundary conditions by altering the velocity of the particle adjacent to the surface. This section is concerned with how to carry out this process. During the simulation a boundary causes a distinct change in the velocity of the particle adjacent to it. Prior to carrying out this change there must be first a decision to make the change. As there is already a cellular structure available which designates the absolute resolution of the system in terms of particle-particle interaction it is appropriate to use this same structure for enforcing the boundary conditions. To do this create an array $B[n_c]$. Each element in this array is associated with a cell in the domain and is used to enforce a boundary condition. The elements of the array are to be such that the cell index of the particle as given

by $i_c = z[i]$ for particle i can be used to check the boundary condition array to produce a value $b = B[i_c]$. The value b may be an instruction in which case it will usually be a small integer value or it may be a real number such that it is used in a subsequent computation for enforcing the boundary condition or it may be either depending on the problem at hand. However it must at least have a value that designates that there is no boundary condition to be enforced on that particle. The ideal time to enforce a boundary condition is immediately after the cell index of the particle is identified in the translation step. At this point the cell index i_c is readily available such that $B[n_c]$ can be checked and the boundary condition enforced.

The walls of the simulation box may be either solid or periodic but any internal boundaries are always considered solid. For the flow geometries which are to be analyzed the boundary surface will always be parallel to the z axis. Thus the orientation of the surface will be characterized by an angle θ where $0 \leq \theta \leq 2\pi$. Figure 5.3 displays four surfaces and the corresponding θ which begins at the x axis and is measured counter clockwise from it.

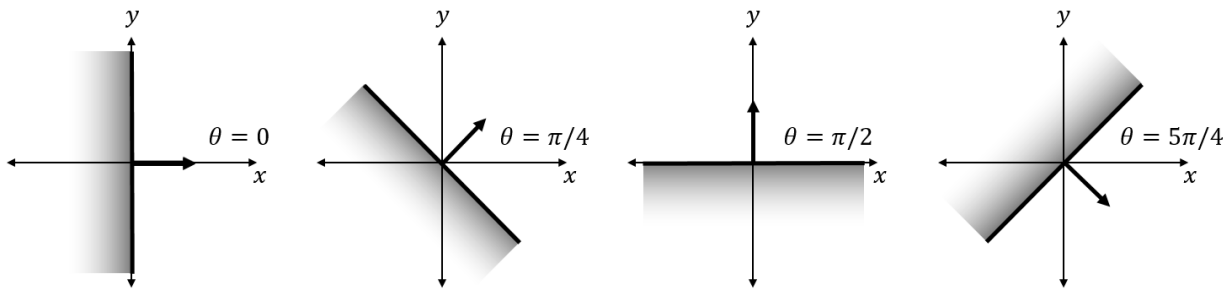

Figure 5.3: Images displaying the meaning of θ as regards the orientation of a solid surface.

When a particle is adjacent to a surface which is not parallel to one of the axes of the system it is most convenient to change the basis of the velocity vector such that there is strictly tangent and normal components. Given the coordinate system displayed in 5.3 the vector normal to the surface is obtained with the rotation matrix $\boldsymbol{R}$

$$\boldsymbol{R} = \begin{bmatrix} \cos\theta & -\sin\theta \\ \sin\theta & \cos\theta \end{bmatrix} \tag{5.47}$$

However this rotation itself is composed of the x and y unit vectors upon rotation in the first and second columns of $\boldsymbol{R}$ respectively. Thus the inverse of the rotation matrix can be used to

change the basis of any velocity vector into the basis of the rotated vectors.

$$\hat{v}_k = \boldsymbol{R}^{-1} v_k \tag{5.48}$$

The transformed velocity $\hat{v}_k$ is now in terms of a component normal to the surface and parallel to it in the x and y components respectively. The parallel component is then assigned the desired velocity as given by the boundary condition. With the new velocity $\hat{v}'_k$ obtained use the rotation matrix to convert it back into the original basis.

$$v_k = \boldsymbol{R}^{-1} \hat{v}'_k \tag{5.49}$$

These new velocities are to be implemented by changing the actions of the particles. This process can be demonstrated by considering the flow past an infinite cylinder in a periodic channel with solid walls. Figure 5.4 displays the system just mentioned. A cross section of the domain is shown with the x and y dimensions as indicated while the z dimension is perpendicular to the page. Since the z boundary is periodic the $B[n_c]$ for those cells which lie along the z walls have the default condition of no boundaries. Cells shaded in light gray are cells which in the array $B[n_c]$ should contain an instruction for a boundary condition to be implemented. Cells along the left most wall at $x = 0$ have a flow condition to maintain the inlet velocity but the conditions are still periodic for the x walls. As the system is not periodic in the y boundaries there should be specific instructions for the cells at $y = l_b$ and different instructions for $y = 0$. The cells near the cylinder also have their own instruction which handles the interaction of particles with the cylinder.

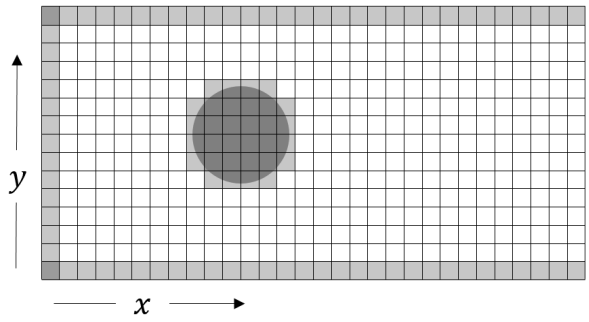

Figure 5.4: Cells overlaying a cylinder in a channel for boundary condition calculations.

As an example let the instructions for the left x wall boundary, bottom y wall boundary, top y wall boundary, and the cylinder boundaries be 1, 2, 3 and 4 respectively. These are the values of $B[n_c]$ which will be returned for particles in any of those cells. Let 0 denote the default case that no boundary conditions need to be applied. Once a particle's position has been incremented as usual and the new cell is obtained as i_c then the boundary condition for the cell of i_c is obtained as $b = B[i_c]$. A conditional is then used. If b does not equal zero a boundary condition function is called which takes b along with any other necessary parameters such as the position and action of the particle and implements the boundary condition indicated by b. This function will return the new positions and actions of the particle in accordance with the boundary condition. A simple way to implement this condition is through the use of a switch-case procedure. The basic idea of a switch-case procedure is that there is a switch-statement and a number of case-statements. If a given case-statement is equal to or matches the switch-statement then the code associated with the case-statement is executed. The switch-statement is set by the function calling the switch-case procedure.

5.4 Methods of Analysis

In order to characterize the behavior of the point particle model some techniques of analysis are required. The primary means of characterization will be the transport coefficients of self-diffusion and viscosity as well as the radial distribution function. The following sections explain the algorithmic techniques to measure these quantities for particles without interaction potentials.

5.4.1 Self-Diffusion Coefficients

The Einstein method will be used to obtain the self-diffusion coefficiet as implemented by Frenkel and Berend. [93] In the Einstein method the diffusion coefficient is given by

$$\frac{\partial \langle r^2(t) \rangle}{\partial t} = 2dD_s \tag{5.50}$$

On the left side $\langle r^2(t) \rangle$ is the mean-squared displacement of the particle in a time interval. On the right hand side D_s is the diffusion coefficient, and d is the dimensionality of the system. This

equation comes directly from Fick's Law and relates the width of the the concentration profile of a particle diffusing from a single point to the self-diffusion coefficient. To obtain this for the point particles we plot $\langle r^2(t)\rangle$ as a function of time intervals $t-t_0$ and obtain the self-diffusion coefficient from the slope. The squared distance a particle travels over an interval is given by

$$\Delta r^2(t-t_0) = [\boldsymbol{r}(t) - \boldsymbol{r}(t_0)]^2 \tag{5.51}$$

Obtaining this for all particles and a sufficiently long time interval the mean square displacement (MSD) of a particle as a function of time interval is obtained

$$\langle \Delta r^2(t-t_0)\rangle = \frac{1}{N_m}\sum_{i=1}^{N_m} \Delta r^2(t-t_0) \tag{5.52}$$

where N_m is the number of measurements for that particular time interval $t-t_0$. The slope of this plot at sufficiently long times is constant and can be taken to obtain the self-diffusion coefficient with 5.50. To calculate it in practice a time t_c is selected which represents the longest time interval for which $\langle \Delta r^2(t-t_0)\rangle$ will be computed. Note that if t_c is the length of the simulation then only one set of $|N|$ measurements will be available for that time interval i.e. one for each particle. The asymptotic behavior is acquired reasonably fast that t_c can be much less than the total simulation time. Also we must have stored positions and times throughout the simulation such that we have N_t sets of positions with associated times for those positions. For convenience do not iterate through the actual time steps but use integral time $\tau = 1, 2, ..., \tau_f$ which enumerates the actual time steps $t = 0, \Delta t, 2\Delta t, ..., t_f$ where Δt is the time step of the simulation and t_f is the final time of the simulation. Thus τ represents time but as an integral number can be used to reference arrays. Accordingly $\tau_c = \frac{t_c}{\Delta t}$.

Create arrays $m_r[\tau_c]$ and $\hat{n}[\tau_c]$ to store the mean square displacements and normalizing factors N_m respectively. Begin the outer loop using τ_0 as the counter for $\tau_0 = 1, 2, ..., \tau_f$. Extract the positions of all particles at time τ_0 as array $r(\tau_0)[n][d]$. Next loop through the times intervals beginning at the current τ_0 and ending at the smaller of either the final time τ_f or $\tau_c + \tau_0$. That is to say nest an inner loop which iterates with $\tau = \tau_0, \tau_0 + 1, \tau_0 + 2, ..., \min(\tau_f, \tau_c + \tau_0)$. For each τ of the inner loop obtain $r(\tau)[n][d]$. Compute the distance travelled over the time interval $\tau - \tau_0$,

by first subtracting each component k of $r(\tau_0)[n][k]$ from $r(\tau)[n][k]$, square the result and sum over all k. Then sum over all particles, divide by the total number of particles, and store the result i.e.

$$m_r[\tau - \tau_0 + 1] = m_r[\tau - \tau_0 + 1] + \frac{1}{|N|}\sum_{j=1}^{n}\sum_{k=1}^{d}\Big[r(\tau)[j][k] - r(\tau_0)[j][k]\Big]^2 \tag{5.53}$$

since there will be more short time intervals in a given $_c$ than long intervals the results have to be normalized. For each data point added to array $m_r[\tau_c]$ increment a normalizing array $\hat{n}[\tau_c]$ the same size as $m_[\tau_c]r$ such that

$$\hat{n}[\tau - \tau_0 + 1] = \hat{n}[\tau - \tau_0 + 1] + 1 \tag{5.54}$$

Once all loops are complete normalize the mean square distances obtained

$$m_r[\tau_i] = \frac{m_r[\tau_i]}{\hat{n}[\tau_i]},\ \tau_i = 1, 2, 3, ..., \tau_c \tag{5.55}$$

The entries of $m_r[\tau_i]$ are now the $\langle r^2(t)\rangle$ for times $t = 0, \Delta t, 2\Delta t, ..., t_c$. Plot and observe the region in which the $\langle r^2(t)\rangle$ is linear and use a linear regression to obtain the slope. This slope corresponds to the left hand side of 5.50 and the diffusion coefficient is readily obtained with the dimensionality d.

5.4.2 Obtaining Viscosity through Relaxation Measurements

Without interaction potentials Green-Kubo relations cannot be implemented to extract the viscosity as a stress correlation. Instead we will utilize relaxation measurements by perturbing the fluid with a wave and tracking its return to equilibrium as was done by McNamara and Zanetti in measuring the viscosity for the first implementation of the Lattice Boltzmann Equation. [67]

Beginning with the Navier-Stokes Equation in the absence of external forces

$$\rho\frac{\mathrm{D}\boldsymbol{u}}{\mathrm{D}t} = -\nabla p + \mu\nabla^2\boldsymbol{u}\ , \tag{5.56}$$

where μ is the viscosity, and ρ is the mass density. With no pressure gradient, consider a small

transverse momentum field as a velocity plane-wave at t_0

$$u_i(r_i, t_0) = (0, u_y(x, t_0), 0) \tag{5.57}$$

$$u_y(x, t) = u_y^{t_0} e^{ik_x x} \tag{5.58}$$

For this initial condition the Navier-Stokes equation may be reduced to the one dimensional diffusion equation

$$\frac{\partial u_y}{\partial t} = \frac{\mu}{\rho} \frac{\partial^2 u_y}{\partial x^2} \tag{5.59}$$

which yields the general solution [94]

$$u_y(x, t) = u_y^{t_0} e^{ik_x x} e^{-\frac{\mu k_x^2}{\rho} t} \tag{5.60}$$

That is to say the transverse momentum decays exponentially with a decay constant proportional to the viscosity. This method is generally not used because of the amount of time it takes for the wave to relax to equilibrium but this is not a concern here as the algorithm is sufficiently fast. Set-up and run a simulation to equilibrium. Next the system is perturbed with a shear wave. Pick a dimension for which the wave is to be defined on, $k_\parallel$, and another dimension $k_\perp$ in which the velocity of the particles are actually perturbed. Let $\frac{2\pi}{l_b} n_\parallel$ be the wave number in dimension $k_\parallel$ where $n_\parallel$ is an integral number and all other dimensions of the wave number are zero.

The perturbation can then be applied to the actions of the particles $i = 1, 2, ...N$

$$s[i][k_\perp] = s[i][k_\perp] + \frac{u_0}{2} \sin\left(\frac{2\pi}{l_b} n_\parallel r[i][k_\parallel]\right) \tag{5.61}$$

$$s[i][k_\perp + d] = s[i][k_\perp + d] - \frac{u_0}{2} \sin\left(\frac{2\pi}{l_b} n_\parallel r[i][k_\parallel]\right) \tag{5.62}$$

After perturbation continue the simulation collecting position and velocity data throughout the relaxation process. Next the decay of the amplitude must be obtained as a function of time. Select a spacing δr and partition the domain into layers perpendicular to $k_\parallel$. For clarification see Figure 5.5 where x is the dimension $k_\parallel$ and z is $k_\perp$. The perturbation is shown for 3 values of $n_\parallel$ and the layers are clearly defined as perpendicular to the dimension of $k_\parallel$.

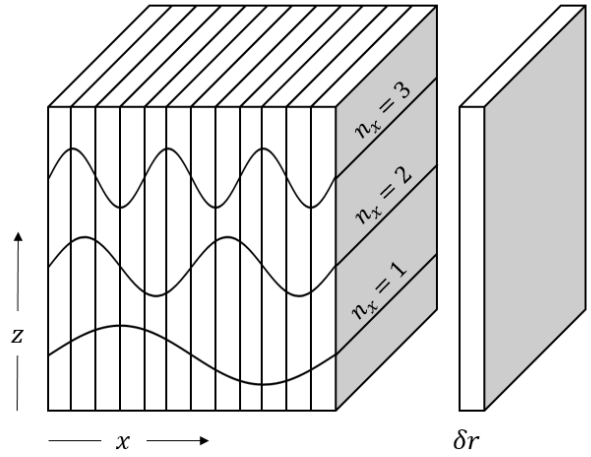

Figure 5.5: Depiction of three shear waves yielding different velocity profiles in a cubic element of fluid.

The particles are going to be partitioned in terms of these layers. There are

$$N_l = \frac{l_b}{\delta r} \tag{5.63}$$

layers in total. Since this process is computationally intensive enumerate the simulation times as $\tau = 1, 2, ..., \tau_f$ and introduce a $\Delta\tau \geq 1$, $\Delta\tau \in \mathbb{N}$ such that not all time steps need to be used. Begin the outer loop $\tau = \tau_p, \tau_p + \Delta\tau, \tau_p + 2\Delta\tau, ..., \tau_f$. The initial τ_p corresponds to the time of perturbation. The total τ's for which an analysis will be conducted is

$$N_\tau = \frac{\tau_f - \tau_p}{\Delta\tau} \tag{5.64}$$

Create an amplitude array $A[N_\tau]$ and begin looping through $\tau = \tau_p, \tau_p + \Delta\tau, \tau_p + 2\Delta\tau, ..., \tau_f$. At each new τ create a velocity distribution array $v_d[N_l]$ and a normalizing array $\hat{n}[N_l]$. Then loop through all particles $i = 1, 2, ...n$ to determine the average velocity of each layer. The appropriate layer l to which a particle contributes is obtained as

$$l = \left\lceil \frac{r[i][k_\parallel]}{\delta r} \right\rceil + 1 \tag{5.65}$$

then the velocity of particle i is added to the appropriate velocity distribution array element and

the addition is counted in the normalizing array

$$v_d[l] = v_d[l] + v[i][k_\perp] \tag{5.66}$$

$$\hat{n}[l] = \hat{n}[l] + 1 \tag{5.67}$$

after all particles are accounted for the velocity distribution for the given τ is obtained

$$v_d[i] = \frac{v_d[i]}{\hat{n}[i]}, \forall i \in N \tag{5.68}$$

This distribution should be the form of a sine wave. Fit $v_d[N_l]$ as a function of $r = 0, \delta r, 2\delta r, l_b$ as a sine wave with fitting parameters of amplitude α, and phase shift but fixed wave-number $\frac{2\pi}{l_b} n_\parallel$. Having the phase shift as a fitting parameter allows for variation via rounding when segregating the particles into the respective layers but is not used otherwise. The amplitude is then stored as

$$A\left[\frac{\tau + \Delta\tau + 1}{\Delta\tau}\right] = \alpha \tag{5.69}$$

and this is done for all τ such that the amplitude is then known as a function of time. This amplitude function can be fitted with an exponential decay function to obtain the viscosity. However, the fitting process to obtain the amplitude as a function of time was only valid near the time of perturbation. Once the particles have relaxed to equilibrium the amplitude obtained from fitting the sine wave is small but meaningless. Accordingly the exponential fit is conducted in two passes. A preliminary fitting is done to obtain a rough but sufficient estimate of the time constant and then used for a weighted fitting which removes the meaningless amplitudes. First the original time values are recovered by constructing an array $t[N_\tau]$. Using the simulation time step the times are determined which correspond to the amplitudes post perturbation stored in $A[N_\tau]$ thus

$$t[j] = j\Delta t\Delta\tau,\ j = 0, 1, 2...N_\tau \tag{5.70}$$

Then $A[N_\tau]$ is fit as a function of $t[N_\tau]$ with the form of an exponential decay

$$A[j] = u_0 \exp(-\eta t[j]),\ j = 0, 1, 2...N_\tau \tag{5.71}$$

Where u_0 is fixed and is the magnitude of perturbation while η is the fitting parameter. From this a rough η is obtained. Next an array of weights is constructed $w[N_\tau]$ where

$$w[j] = \exp(-\eta t[j]) \tag{5.72}$$

then normalize the weights

$$w[j] = \frac{w[j]}{\sum_{j=1}^{N_\tau} w[j]} \tag{5.73}$$

These weights can now be used for a weighted non-linear fitting of the same form as equation 5.71 where the meaningless amplitudes at equilibrium have no weight. The viscosity is then determined through relation 5.60 as

$$\frac{\mu}{\rho} = \left(\frac{\eta^{1/2} l_b}{2\pi n_\parallel} \right)^2 \tag{5.74}$$

5.4.3 Radial Distribution Function

The radial distribution function gives the probability of finding another particle a distance r from the given particle relative to the probability of finding the particle if they were non interacting as in an ideal gas. The method used here closely follows that of Allen and Tildesley. [92] Obtaining the radial distribution function is a computationally demanding task as it is in essence equivalent to the naive implementation of a molecular dynamics force routine. Accordingly for a set of positions as a function of time $t = 0, \Delta t, 2\Delta t, ...t_f$ it is appropriate to skip many of the instances. The calculated radial distribution function $G_r(r)$ for a fluid is the probability one will find a particle a distance between r and $r + \delta r$ from another particle relative to an ideal gas. To obtain $G_r(r)$ we record the number of particles in spherical shells with thickness δr around a given particle and divide this number by the volume of the shell. In doing so we obtain the average density of particles in the range r to δr around the given particle. By dividing this density by the average density of all particles in the volume we obtain the radial distribution function.

First we select a δr smaller than l_c and create a set of bins to partition the distances between particles into groups according to their size. Since the maximum distance obtainable with the minimum image convention is $l_b/2$

$$N_b = \left\lfloor \frac{l_b/2}{\delta r} \right\rfloor \tag{5.75}$$

bins will be required. Thus the bins take particle-particle distances 0 to δr, δr to $2\delta r$, ..., $N_b\delta r$ to $l_b/2$. Create an array $G_r[N_b]$ to store the radial distribution function. Enumerate every s^{th} time step $t = 0, s\Delta t, 2s\Delta t, ...t_f$ where s is a small integral number with $\tau = 0, 1, 2, ..\tau_f$ such that only every s^{th} time step is analyzed. Loop through τ and at each instance of τ use two more loops to loop through all pairs of particles. That is, at each τ loop through particles $i = 1, 2, ..., N-1$ and for each instance i loop through all particles $j = i+1, i+2, ..., N$. In this way all pairs are obtained. For each instance of i and j in the innermost loop calculate the distance between i and j

$$\Delta r_{ij}[k] = r[i][k] - r[j][k] - l_b \text{ round } \left(\frac{r[i][k] - r[j][k]}{l_b} \right) \tag{5.76}$$

The last term of equation 5.76 ensures the minimum image convention for periodic boundaries. The total distance is then

$$|r_{ij}| = \left[\sum_{k=1}^{d} (\Delta r_{ij}[k])^2 \right]^{1/2} \tag{5.77}$$

determine the appropriate bin as

$$b = N_b = \left\lfloor \frac{|r_{ij}|}{\delta r} \right\rfloor + 1 \tag{5.78}$$

Using the index b increment the the appropriate bin of array $G_r[N_b]$ to indicate a particle was found within the shell r to δr of another particle.

$$G_r[b] = G_r[b] + 1 \tag{5.79}$$

After all the loops have completed an array of values $G_r[N_b]$ is obtained. The the number of particles in the shell defined by the bin b is then normalized by the number of particles in the system and the number of instances used such that

$$G_r[b] = \frac{2G_r[b]}{\tau_f N}, \forall b \in N_b \tag{5.80}$$

Where a factor of 2 is needed since each distance from i to j is also a distance from j to i.

For the subsequent computation the ideal gas density is required and is obtained as

$$\rho = \frac{N}{l_b^d} \tag{5.81}$$

We obtain the density of particles in the shell by dividing the number of particles in the shell by the shell volume such that

$$V[b] = \frac{4\pi}{3}\left(\left[b\delta r\right]^3 - \left[(b-1)\delta r\right]^3\right) \tag{5.82}$$

The number density in the shell of bin b is the ratio of $G_r[b]$ to $V[b]$. The radial distribution function is then this density relative to the ideal density ρ such that

$$G_r[b] = \frac{G_r[b]}{\rho V[b]}, \forall b \in N_b \tag{5.83}$$

gives $G_r[N_n]$ as the radial distribution function for radii $r = 0, \delta r, 2\delta r, ..., l_b/2$.

Chapter 6

Point Particle Results and Discussion

As with the great multiplicity of sequences of objects that could be investigated there is also a large variety of parameters that could be explored when experimenting with the algorithm devised in the previous chapter. Ultimately we must be selective and explore those instances which will be productive and interesting. On the productive front it was decided that the set of interactions to be considered are those interactions between particles that are in cells which contact each other in some fashion, in cellular automata this neighborhood is known as the Moore neighborhood. [95] This case is productive by virtue of its convenience of formulation and computation. In the Moore neighborhood the cells which make up the neighborhood of a given cell are either in contact by sharing a face, sharing an edge, or sharing a corner.

In the sake of interest the exact ways in which sequence objects interact entirely depends on the rule set of the algorithm. This feature was abstracted from individual algorithms by considering generalized interactions later resulting in transmission coefficients which may be set freely. In doing so another feature arose which was related to but different from the transmission coefficients. This feature was parameterized as τ and it was the length of time that if a point-particle object is in direct relation with another object, it would exchange all of its transmittable action to that object in accordance with their spatial relation. This feature τ is interesting in that it relates to the subjective form of an object i.e. it expresses the character of an object in how it interacts with others. Thus it does not refer to a specific algorithm in the sense of resolving objects as per their sequence but instead expresses a subjective form in the object in its participation with other objects. Secondly when put into vector form this feature crops up in the exact same form as the

collision step of the Lattice Boltzmann Method in the place of the relaxation time. It is suggestive then that the parameter τ along with the time step Δt should exhibit time step invariance like the relaxation parameter of the Lattice Boltzmann Method. For these reasons an emphasis was put on this parameter τ in the simulations where it manifests as $\omega = \Delta t/\tau$.

A note on Figure Interpretation

The majority of the results are presented using the same figure format. This format was selected in order that the results are not clustered and easy to interpret. To avoid further repetition, the way to interpret the figures from their introduction will be discussed. For each figure there is an x-axis corresponding to the independent X variable, a y-axis corresponding to the responding Y variable, and a Z variable which is also independent and represents different cases in which the X variable was tested and Y data was obtained. Since the results of different cases are similar they can usually all be shown in one figure. Each case then corresponds to a set of Y data as a function of X data as a line or set of points. Cases are differentiated by being different shades of gray. Accordingly figures will be introduced as " Figure A shows Y as a function of X for the cases of $Z = z_1, z_2, \ldots, z_n$." Indicating that the variable referred to as X corresponds to the x-axis, Y corresponds to the y-axis and Z corresponds to the different cases represented as data sets. The color scheme to identify the cases is such that the lightness of the shade corresponds to the lowness of the case value z. That is to say if there are three cases $Z = z_1, z_2, z_3$ and $z_1 < z_2$ and $z_2 < z_3$ the lightest line is for the case of z_1 since it is numerically the lowest and the darkest line is for case z_3 since it is numerically the highest. Case z_2 will have a line darker than case z_1 and lighter than case z_3 because it has a numeric value greater than z_2 but less than z_3.

6.1 Parameter Selections

For a three dimensional system there are six unique actions and thus three inverse action pairs. In the Moore neighborhood described above each action may only be transmitted into a subset of the neighborhood. These subsets are indicated in Figure 6.1.

As point particle objects have no specific orientation beyond position there is only three unique types of neighbors which the action of an object can transmit into. This isotropy is depicted pictographically in Figure 6.2 where the number on each cell indicates the type of neighbor relations.

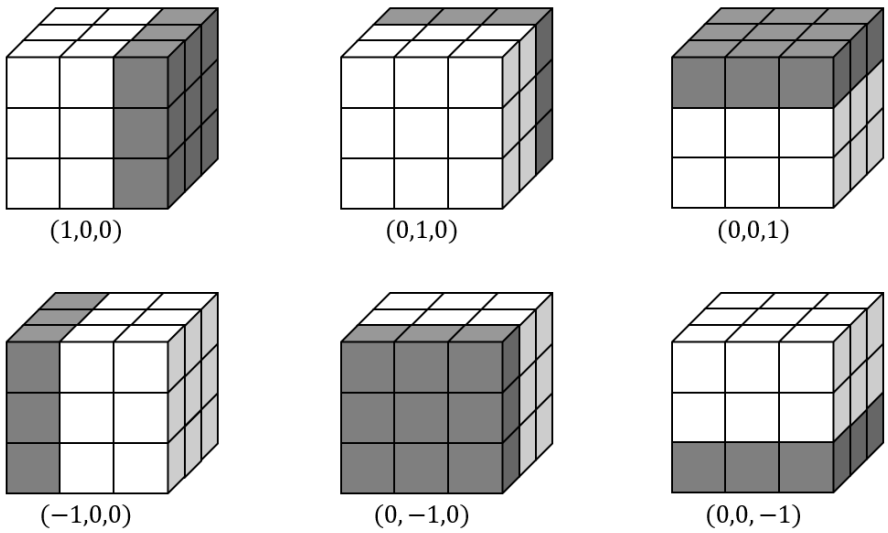

Figure 6.1: Depiction of the Moore neighborhood. Shaded regions of the neighbors indicate the subset of the neighborhood which an object can transmit action into given other objects reside in that subset.

Of the 9 neighbors in the three dimensional Moore neighborhood for a single action 1 has an adjacent face, 4 have a single adjacent edge, and 4 have a single adjacent corner. Suppose that during a given time step each of these neighbors has an object within it. The algorithm must not transmit more action than the object has available and at the same time neighbors of the same relation type should receive the same amount of transmittable action as the point particles have no specific orientation. Furthermore it is reasonable to suppose that the neighbor which has a contacting face would receive and transmit more action than the others, similarly those with a contacting edge should receive and transmit more than those of contacting corners. The transmission values $w* = [3/133/261/26]$ satisfy these ideals. They were selected arbitrarily but the consequences of this selection will be addressed.

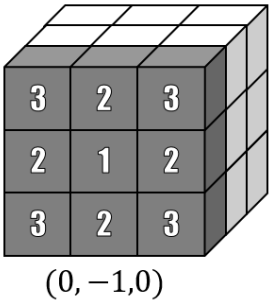

Figure 6.2: Exemplification of the three unique cells which an object can act on given a specific action.

A suitable shift vector set for defining the Moore neighborhood is

$$|c_k\rangle = \begin{bmatrix} (1, & 0, & 0) \\ (1, & 1, & 0) \\ (0, & 1, & 0) \\ (-1, & 1, & 0) \\ (1, & 0, & -1) \\ (1, & 1, & -1) \\ (0, & 1, & -1) \\ (-1, & 1, & -1) \\ (1, & 0, & 1) \\ (1, & 1, & 1) \\ (0, & 1, & 1) \\ (-1, & 1, & 1) \\ (0, & 0, & 1) \end{bmatrix} \tag{6.1}$$

Note that only half the neighboring cells need be specified as discussed in section 5.2.2.

In order to avoid wandering in the dark in search of functional parameter values the famous 1964 study of liquid argon by Rahman [96] was used for guidance. In that work 864 Lennard-Jones particles were studied in a domain of 10.299σ where σ is the particle radius. The non-dimensional velocity of the particles is approximately 1.5 with a time step of 0.005. The magnitudes of the time step and velocity were found to work well and were adhered to. Unless specified otherwise the

dimensions of the simulation box are such that $n_w = 20$ and $l_b = n_w l_c = 20$ to give a total of 8000 cells with periodic boundary conditions. A unit mass is used and the time step is $\dot{t} = 0.005\Delta t$.

6.2 Equilibrium Results

We begin by looking at the relaxation process of 1000 particles initiated with a point velocity distribution such that each particle has the same velocity of $|v_i| = 0.5\ l_c/\Delta t$ but with random direction. The transmittable action for each inverse action pair is set as $s_{T_0}^{\pm k} = 1$. The simulation was started and the particles were then left to relax to equilibrium. Every time step the velocity of the particles are computed from the actions and stored in a histogram of bin resolution $\delta v = 0.05\ l_c/\Delta t$ for $v = 0, \delta v, 2\delta v, ...10$. This relaxation-collection procedure was repeated 10000 times. The large magnitude of simulations gives smooth distributions. Figure 6.3 displays the scaled and normalized frequency as a function of velocity for many time steps. In order that each velocity distribution be visible in the figure the distribution of each time step was scaled by dividing it by the maximum value in the distribution at that instant and then scaling those distributions by their time divided by the time of the last distribution shown. At $|v| = 0.5\ l_c/\Delta t$ the initial point distribution is visible. Note that if this point was not scaled it would be much like a Dirac function such that $\delta(|v| - 0.5)$. The distribution quickly spreads and tends to a distribution of the Maxwell-Boltzmann family. The distribution does not appear to converge in the figure because of the scaling applied so as to make the distributions distinguishable from one another. The system undergoes a clear increase in mean velocity as the mean velocity for the starting value was $0.5\ l_c/\Delta t$ but converges to a finite value.

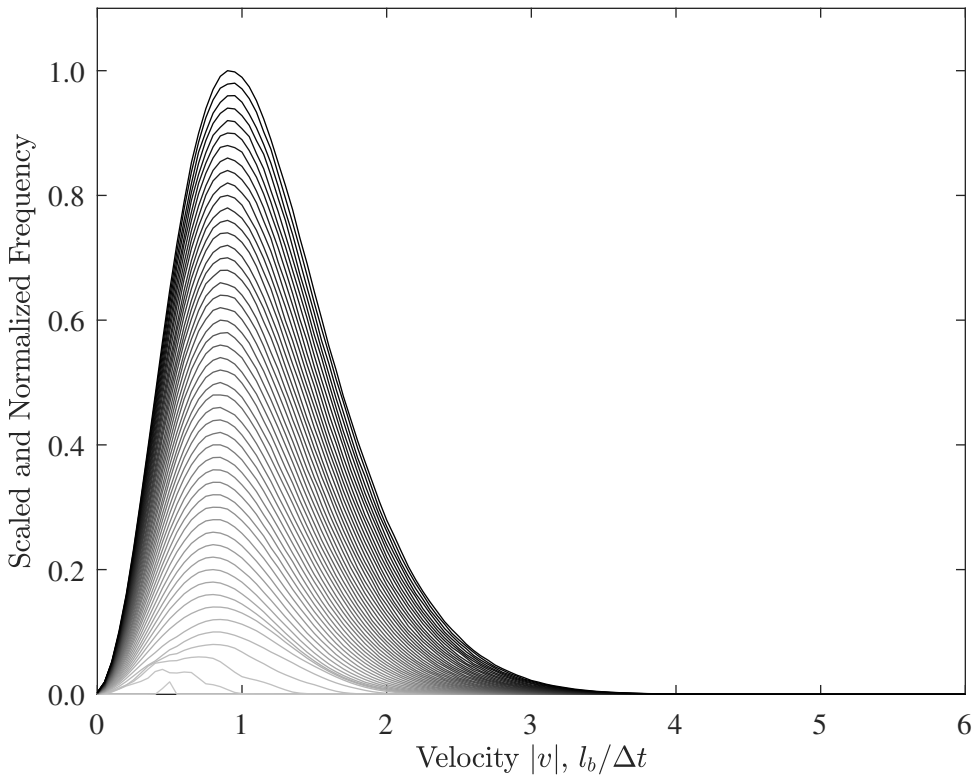

Figure 6.3: Relaxation of the point particle velocities from a initial Dirac distribution $\delta(|v| - 0.5)$ with random velocity orientations

Using the same simulation setup as above the mean velocity of all particles in the system, $|v|$, are obtained as a function of time for varying $s_{T_0}^{\pm k}$ and ω. Figure 6.4 displays the $|v|$ as a function of time for $s_{T_0}^{\pm k} = 0.5$, 1.0, 1.5, 2.0, 2.5, 3.0 and 6.5 displays the $|v|$ as a function of time for $\omega = 0.2$, 0.4, 0.6, 0.8, 1.0. It is clear that both $s_{T_0}^{\pm k}$ and ω effect the resultant mean velocity of the system. It is seen that $|v|$ converges to a finite value for all $s_{T_0}^{\pm k}$ tested. As $s_{T_0}^{\pm k}$ increases the variance of $|v|$ also increases. Figure 6.5 shows the mean velocity as a function of time for each ω factor. Each ω yields a different mean velocity. Figure 6.7 shows the equilibrium distribution function for the various ω factors.

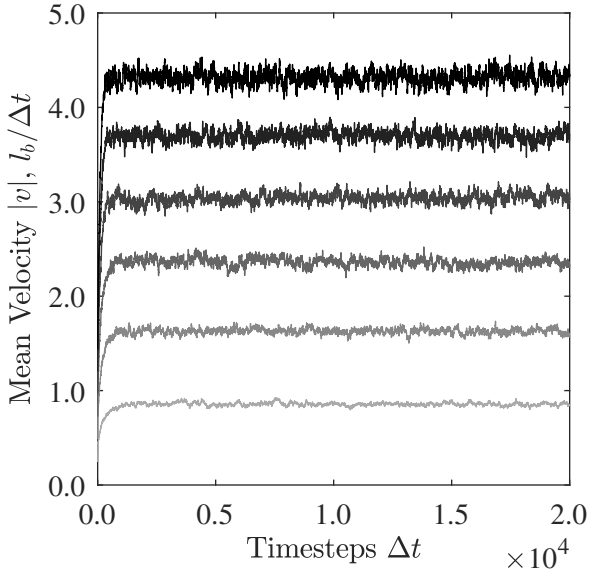

Figure 6.4: Mean velocity as a function of simulation time for various amounts of transmittable action.

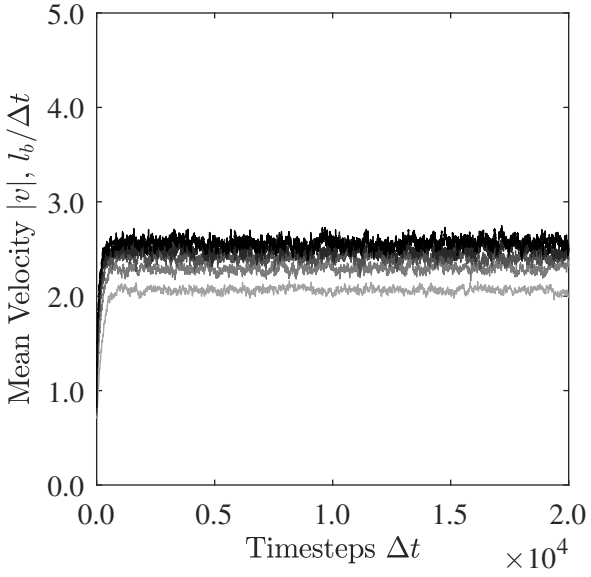

Figure 6.5: Mean velocity as a function of simulation time for different ω.

The corresponding velocity distributions for Figures 6.4 and 6.5 are shown in Figures 6.6 and 6.7 respectively, and reflect the increased velocity with transmittable action. The distributions follow a Maxwell-Boltzmann distribution regardless of the transmittable action. It was found by the same means that altering the initial magnitude of velocity has no effect on the resultant mean velocity i.e. the equilibrium mean velocity which the point particles exhibit depends directly on the amount of action, and the way that action is transmitted.

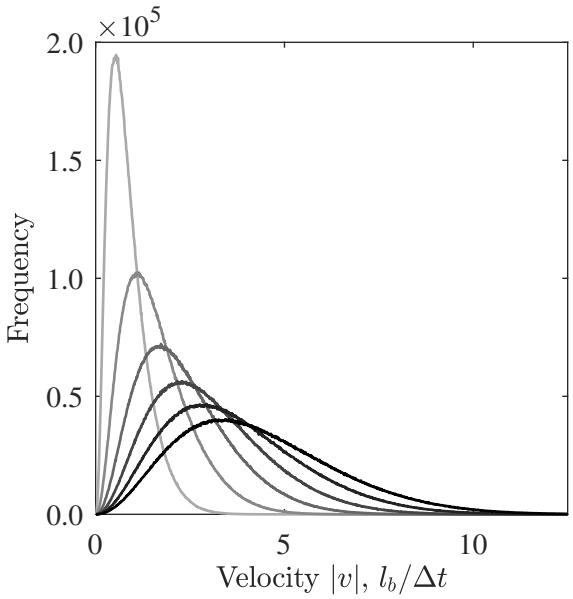

Figure 6.6: Velocity distributions for different amounts of transmittable action.

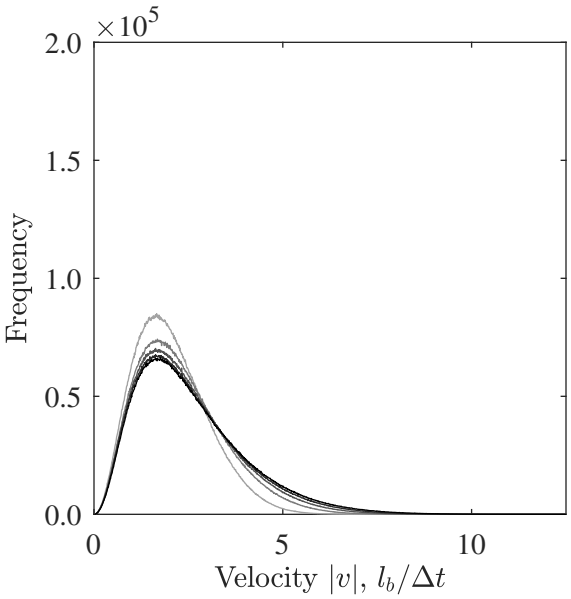

Figure 6.7: Velocity distributions for different ω.

The above results captured in Figures 6.3 to 6.7 indeed indicate that the particles have properties which would typically be associated with a classical fluid i.e. the relaxation of the system of particles to have a distribution of the Maxwell-Boltzmann form. With the above results in mind a more detailed data set was obtained relating the $s_{T_0}^{\pm k}$, ω and $|v|$. Figure 6.8 shows the equilibrium mean velocity as a function of $s_{T_0}^{\pm k}$ for values of $\omega = 0.05, 0.10, 0.15...1.00$. It is seen that for low $s_{T_0}^{\pm k}$ the change in ω has small effect on the overall mean velocity but its effect becomes significant at higher $s_{T_0}^{\pm k}$. Isotherms were obtained between $s_{T_0}^{\pm k}$ and ω in the range of $0.5 < |v| < 2.5\ l_c/\Delta t$ as shown in Figure 6.9.

Using the isotherms just developed in Figure 6.9 the velocity distribution and total transmittable action distributions are shown for the case of constant velocity of $|v| = 1.5\ l_c/\Delta t$ in figures 6.10 and 6.11 obtained over a period of 20000 time steps with a 5000 time step equilibriation period. The velocity distribution clearly maintains around $v = 1.5\ l_c/\Delta t$ showing slight deviations. The corresponding ω values range as 0.1, 0.2, 0.3, 0.4, ..., 1.0. The corresponding average $s_T^{\pm k}$ from the isotherms are 1.1907, 1.0264, 0.9658, 0.9342, 0.9134, 0.8963, 0.8830, 0.8704, 0.8562, and 0.8450. Since an increase in ω increases the mean velocity of the system the initial transmittable action has to decrease to keep the mean velocity constant. The distribution is practically symmetric for the case of $\omega = 0.1$ but becomes more more skewed as ω increases.

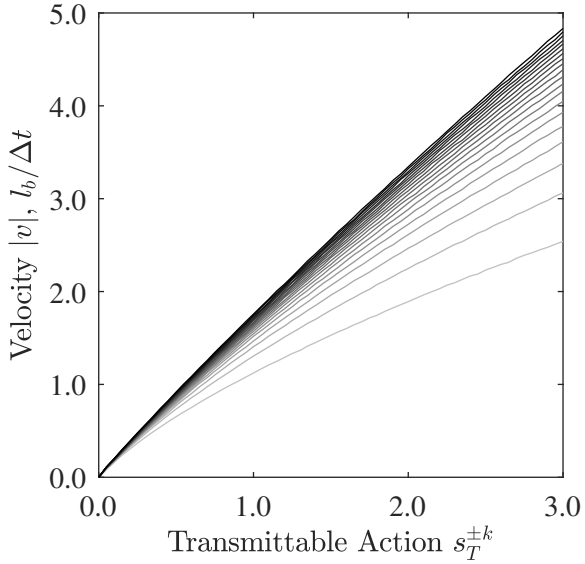

Figure 6.8: Mean velocity as a function of transmittable action for different ω values.

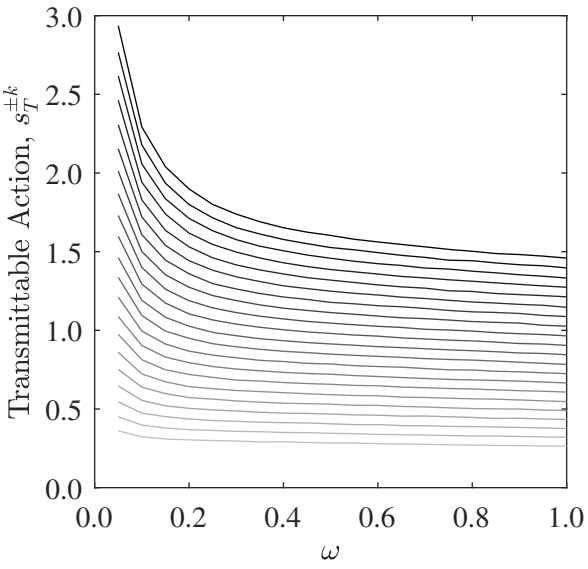

Figure 6.9: Lines of constant mean velocity for transmittable action as a function of ω.

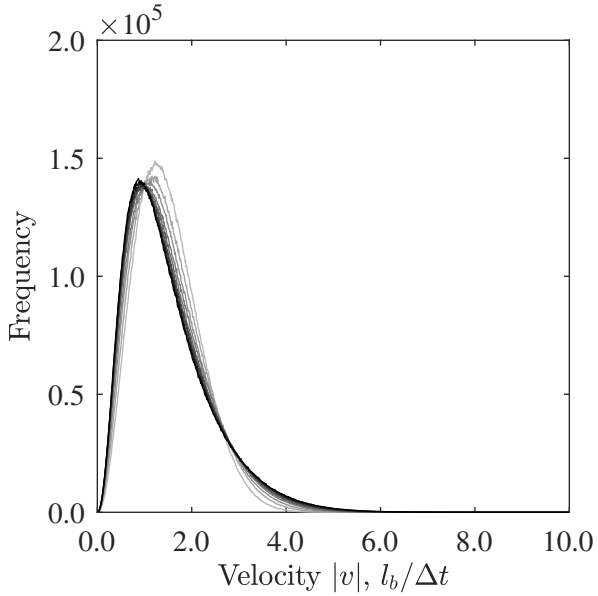

Figure 6.10: Velocity distribution functions for $\omega = 0.1, 0.2, ...\ 1.0$. Each result is for a constant mean velocity of $|v| = 1.5\ l_c/\Delta t$.

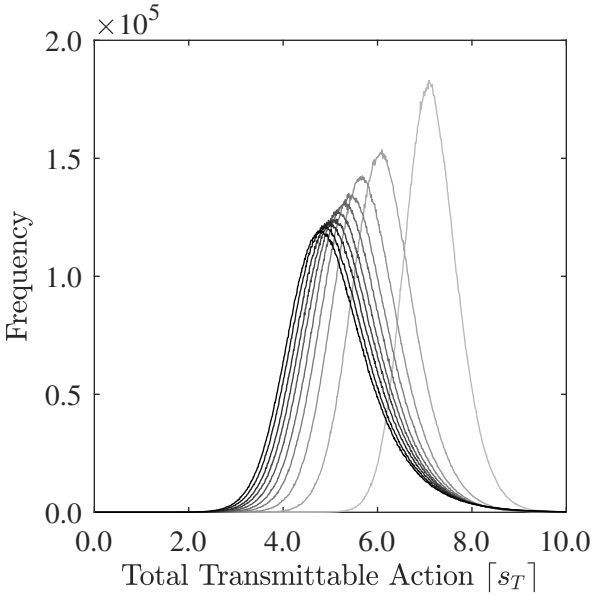

Figure 6.11: Distributions of total transmittable actions for $\omega = 0.1, 0.2, ...\ 1.0$. Each result is for a constant mean velocity of $|v| = 1.5\ l_c/\Delta t$.

Figure 6.12 shows distributions of transmittable action for $s_{T_0}^{\pm k} = 0.50, 0.75, 1.00, 1.25, 1.50$ over the course of 10000 time steps after a 5000 time step equilibriation period with $\omega = 0.5$. Figure 6.12 shows that for increasing initial transmittable action $s_{T_0}^{\pm k}$ there is an overall increase in resulting

transmittable action $s_T^{\pm k}$. Figure 6.13 shows the corresponding component velocity distributions for increasing transmittable action. The velocity is seen to be distributed around zero and increases in width with transmittable action.

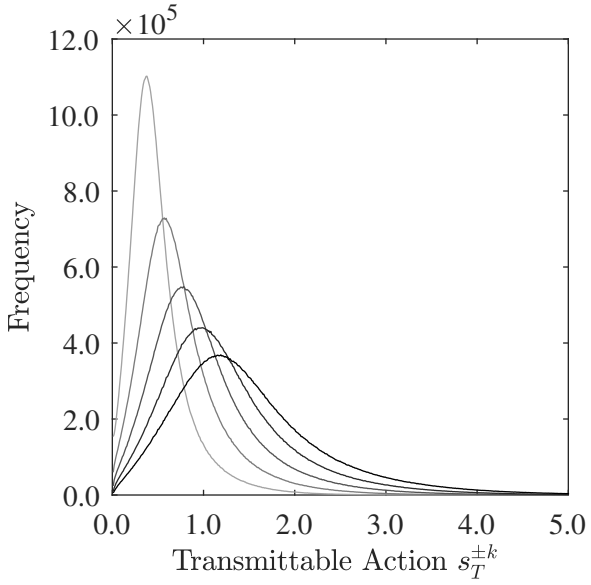

Figure 6.12: Distributions of transmittable actions for initial transmittable actions of 0.50, 0.75, 1.00, 1.25 and 1.50.

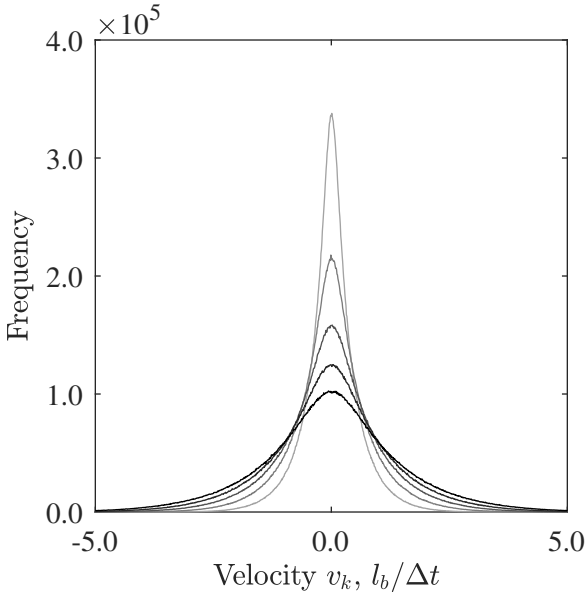

Figure 6.13: Corresponding component velocity distributions for the results of Figure 6.12.

How this distribution relates to ω can be determined by checking the transmittable action distributions for different ω at the same mean velocity. Figures 6.14 and 6.15 show the distributions of transmittable action and component velocity for $\omega = 0.1, 0.2, ..., 1.0$ at a mean velocity of $|v| = 1.5$ respectively. The initial transmittable actions were selected from the isotherms obtained earlier. Results were obtained over a period of 20000 time steps with a 5000 time step equilibriation period. It is seen that the lower the ω the greater the transmittable action, though the change is much smaller than the changes due to changes in initial transmittable action. These results mimic the general trends of the isotherms. For low ω the transmittable action distribution fades before reaching the origin at 0 transmittable action. With the change in transmittable action there is a corresponding change in the component velocity distributions. As ω increases the peak of the distribution at $v_k = 0$ also increases but widens at the tails.

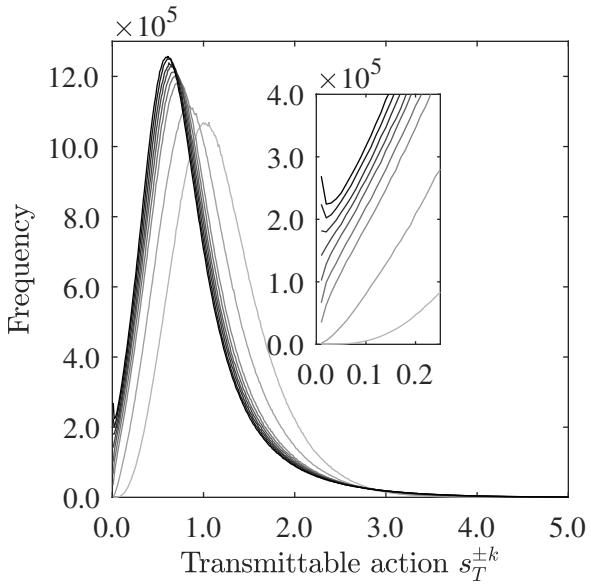

Figure 6.14: Distributions of transmittable action for $\omega = 0.1$,0.2,...,1.0.

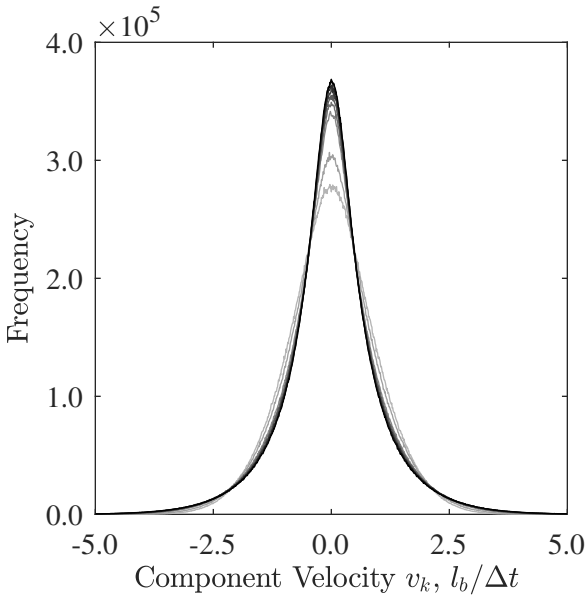

Figure 6.15: Corresponding velocity distributions for the results of Figure 6.14.

The ability for the model to maintain finite size of the particles can be ascertained using the radial distribution function. Figures 6.16, 6.17, and 6.17 show the radial distribution functions for $\omega = 0.1$, 0.5 and 1.0 respectively. Each figure displays the case of $|v| = 0.5$, 1.5, and 2.5 $l_c/\Delta t$. In each figure the G_r corresponding to $|v| = 0.5$ has the smoothest curve. The G_r becomes more pronounced and jagged for larger ω and $|v|$. Each distribution has peaks at $r = 2.3$ l_c. This is the average distance from particle position to particle position. Thus the effective radius of the particles is 1.15 l_c. Taking attention now to the origin it is seen that the higher ω is the finite size of the particles is better respected. At each ω the $|v| = 0.5$ case shows clear existence of particles in the same cells. The relative amount of this occurrence is very small nonetheless. From these observations it is clear that the impact of the cellular structure is less pronounced for smaller ω and $|v|$. It is clear that in this range the model is respecting the finite size of the particles and indeed shows a primitive liquid structure. With a particle radius of 1.15 l_c the total volume of the particles is

$$V_p = N\frac{4}{3}\pi r^3 \tag{6.2}$$

Thus the volume of the particles is 6370 l_c^3 whereas the volume of the box is 8000 l_c^3 cells corresponding to a very high particle fraction of approximately 80% as an upper bound. It is worth

noting that no means were taken to prohibit particles from entering the same cell.

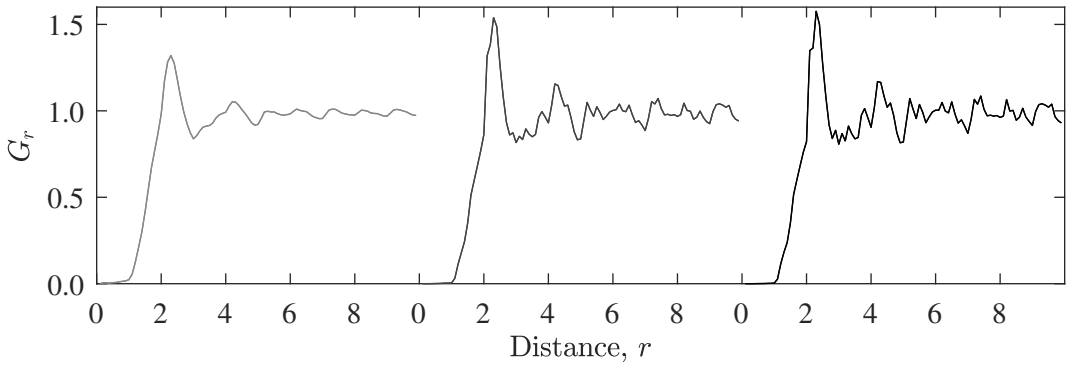

Figure 6.16: Radial distribution functions for $\omega = 0.1$ for velocities of $|v| = 0.5$, 1.5 and 2.5 $l_c/\Delta t$ shown from left to right respectively.

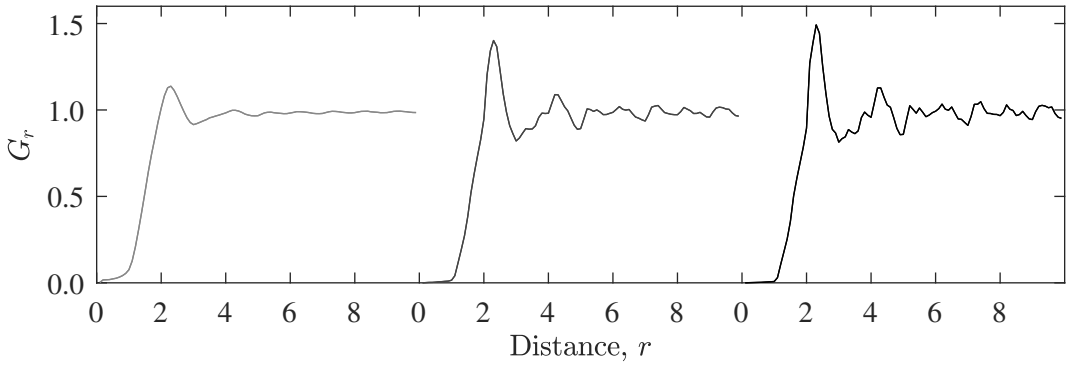

Figure 6.17: Radial distribution functions for $\omega = 0.5$ for velocities of $|v| = 0.5$, 1.5 and 2.5 $l_c/\Delta t$ shown from left to right respectively.

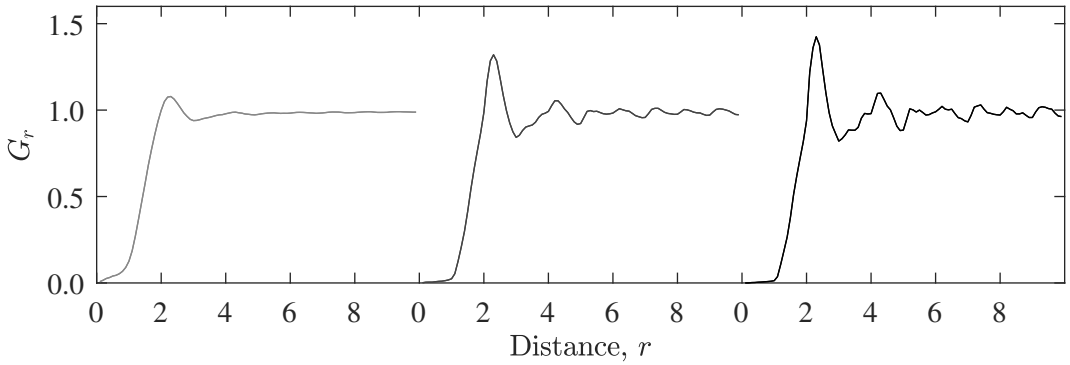

Figure 6.18: Radial distribution functions for $\omega = 1.0$ for velocities of $|v| = 0.5$, 1.5 and 2.5 $l_c/\Delta t$ shown from left to right respectively.

Whether or not the radius just obtained was dependent on the packing density is ascertained by looking at the radial distribution functions for particles at different densities with $\omega = 1$ and $s_{T_0}^{\pm k} = 0.9134$. With number of particles in the simulation of 400, 500, 800, 1000, 1333, 1600, and 2000. The corresponding radial distribution functions are shown in Figure 6.19. In each case the peak of the radial distribution function is at approximately 2.3 l_c such that this may be taken as the general radius of the particles granted this implementation. At high densities there is significant interpenetration of the particles and the radial distribution function is very jagged.

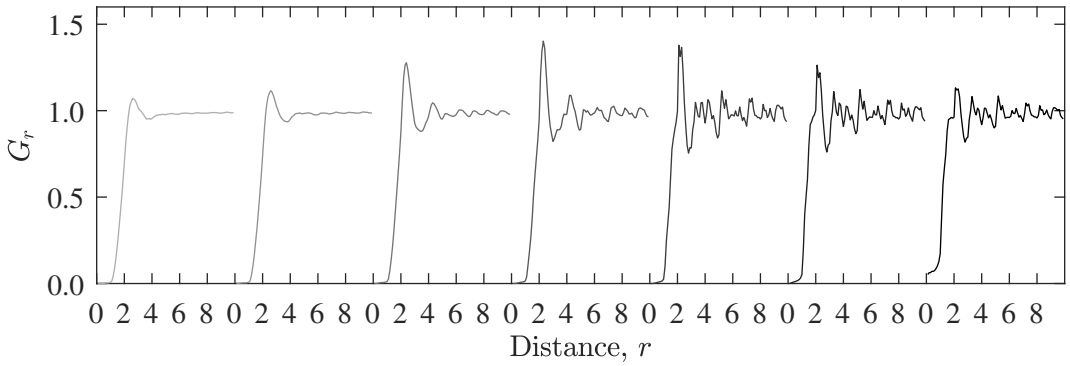

Figure 6.19: Radial distribution functions for varying particle density. Distributions are shown from left to right of 400, 500, 800, 1000, 1333, 1600, and 2000 particles in the a domain of $20 \times 20 \times 20$ cells.

Using the techniques outlined in section 5.4 the transport properties of self-diffusion and viscosity were investigated for varying mean velocity and ω. Specifically $\omega = 0.1, 0.2, ..., 1.0$ and $|v| = 0.5, 1.0, ...2.5\ l_c/\Delta t$. Each instance of an $(\omega, |v|)$ was repeated 10 times for a total of 500 simulations.

Selections of the mean square displacement (MSD) as a function of time interval for the cases of $\omega = 0.1$, 0.2, ..., 1.0 for the mean velocity of $|v| = 1.0\ l_c/\Delta t$ and $|v| = 2.0\ l_c/\Delta t$ are presented in Figures 6.20 and 6.21 respectively. The mean square displacement for for velocities $|v| = 0.5$, 1.0, ... 2.5 for $\omega = 0.3$ and $\omega = 0.7$ are shown in Figures 6.22 and 6.23 respectively. These MSD results are representative of the results for all combinations of ω and $|v|$. The maximum error of the MSD over ten runs was 1.1%.

The general trends among these results is presented in Figures 6.24 and 6.25 which display the self-diffusion coefficient, D_s as a function of ω for each $|v|$ and the D_s as a function of $|v|$ for each ω respectively. Rather surprising is the familiar form of the self-diffusion coefficient in Figure 6.24.

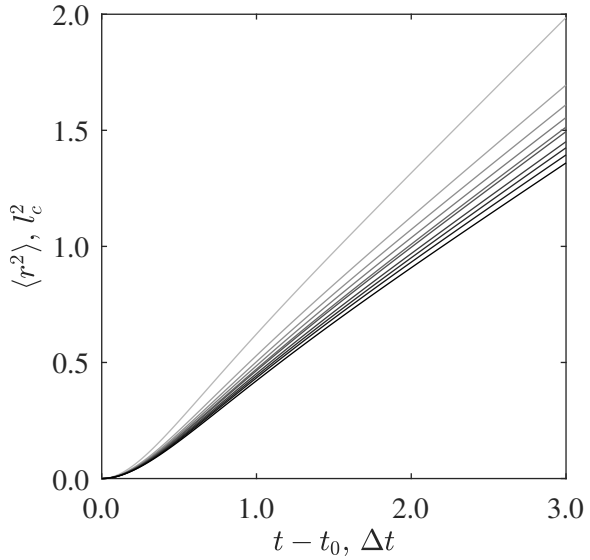

Figure 6.20: Mean square displacements for all ω for $|v| = 1.0\ l_c/\Delta t$.

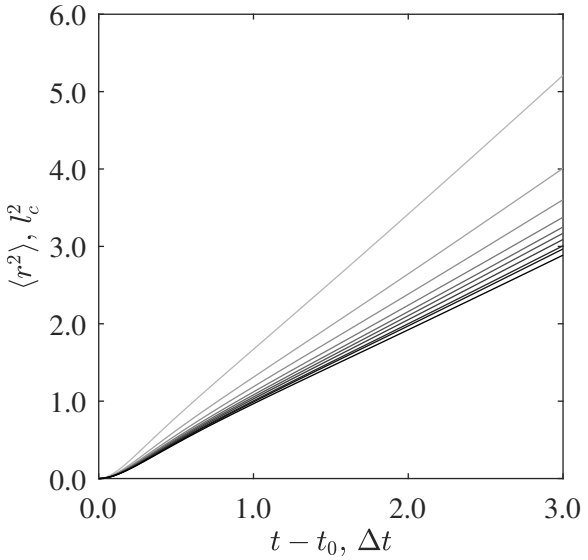

Figure 6.21: Mean square displacements for all ω for $|v| = 2.0\ l_c/\Delta t$.

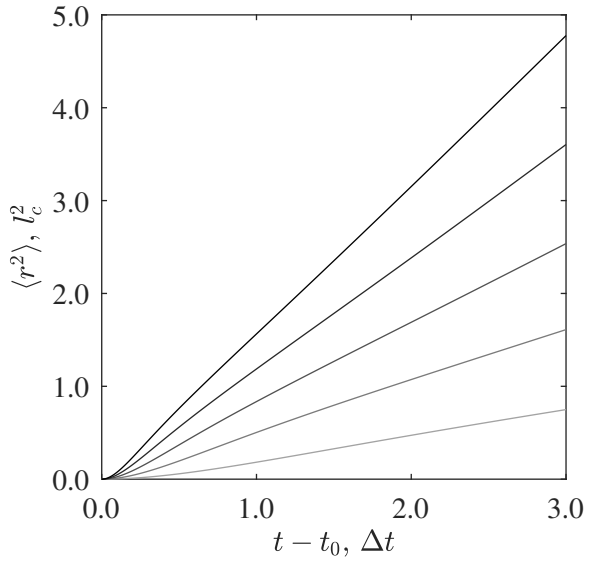

Figure 6.22: Mean square displacements for all $|v|$ for $\omega = 0.3$.

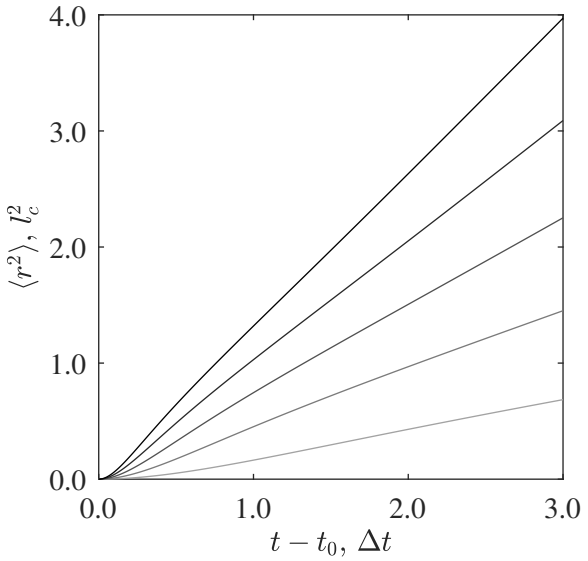

Figure 6.23: Mean square displacements for all $|v|$ for $\omega = 0.7$.

Applying the multi-scale technique, also called the Chapman-Enskog expansion, to the Lattice Boltzmann Equation recovers the kinematic shear viscosity as [77]

$$\nu = \frac{k_B T}{m}\left(\frac{1}{\omega} - \frac{1}{2}\right) \tag{6.3}$$

The lines of 6.24 were fitted using

$$D_s = a\left(\frac{1}{\omega} - b\right) \tag{6.4}$$

Clearly this is not 6.3 but the similarity is worth noting. It is clearly seen that as ω increases D_s decreases for each $|v|$. This makes sense since ω is the rate at which particles can exchange their momentum. The faster the particles can exchange momentum the less they can use momentum for translation and thus have a smaller diffusivity. Secondly D_s exhibits a quadratic relation with the mean velocity. Although diffusivity would increase with mean velocity the quadratic form of this result is in direct disagreement with experiment. The closest system to having such basic properties would be that of spherically symmetric molecules in liquid form. Naghizadeh and Rice measured the self diffusion coefficients of Argon, Krypton, Xenon, and Methane. [97] The characteristic relation which fit all data in their experiments is of the form

$$D_s = A\exp(-B/T) \tag{6.5}$$

where A and B are fitting parameters and T is the temperature. For the spectrum of temperatures equation 6.5 states that the diffusivity is practically zero for small temperatures, as T increases $\exp(-B/T)$ approaches unity implying a maximum value for the D_s which is given by A. That the point particle model does not follow equation 6.5 is not surprising. All particle interaction is carried out through ω and which has not been programmed to change under any conditions. In a real fluid as temperature increases the interaction of the molecules change thus changing the transport properties.

The same set of data is displayed for the viscosity in Figures 6.26 and 6.27 which display the kinematic viscosity, μ/ρ as a function of ω for each $|v|$ and the μ/ρ as a function of $|v|$ for each ω respectively. Viscosity shows a clear non-linear increase with ω. This is actually the near opposite behaviour to the Lattice Boltzmann Method. In the LBM the viscosity is related to ω through 6.3.

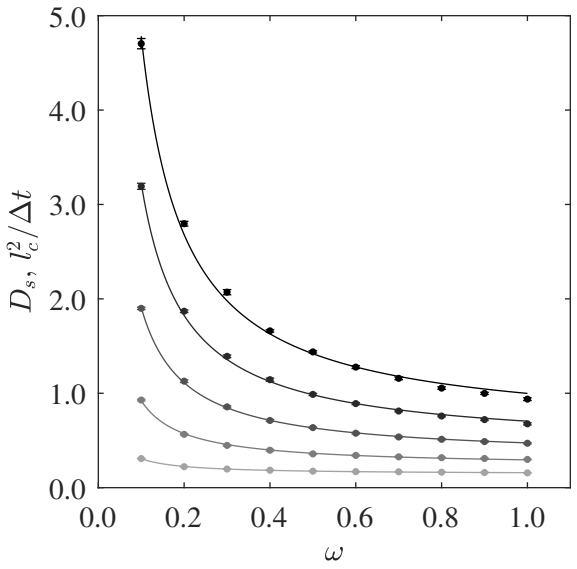

Figure 6.24: Self-diffusion coefficient as a function of ω for varying velocity.

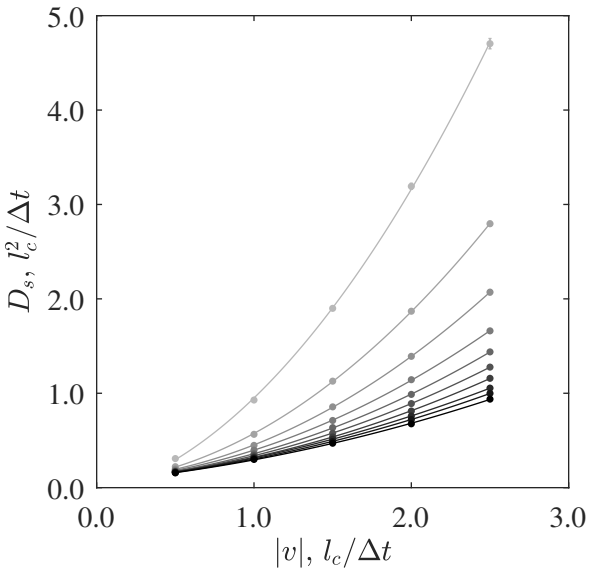

Figure 6.25: Self-diffusion coefficient as a function of velocity for varying ω.

It is important to note that the collision process of the LBM does not cause a change in the velocity or momentum of a node in the LBM. It re-distributes the momentum among the components of the discrete distribution function. The value of ω determines how quickly this proceeds in accordance with the time step, still in the form $\omega = \Delta t/\tau$. If ω is unity the equilibrium distribution function is obtained in a single time step. In the particle model however, ω determines how much of the action a particle has is transferred to another particle within its neighborhood. Thus ω is directly proportional to the rate at which the point particles change momentum. The increase in viscosity with an increase in ω was predicted by the momentum balance since an increase in ω corresponds to an overall increase in transmission probability which was the main ingredient in the generalized interactions. The increase in viscosity with mean velocity is characteristic of gases and reflects the fact that the faster the particles are moving the faster momentum can be transversely transported.

In the above results the transmission coefficients were selected arbitrarily. The consequence of this selection can be determined by changing the relative values of the transmission coefficients. First the neighborhood is reduced by removing the neighboring cells which are contacting by virtue of sharing a corner. Thus a single action type may project into five members of the neighborhood as shown in Figure 6.28.

Four of these neighbors have identical relations to the base cell as shown in Figure 6.29. With

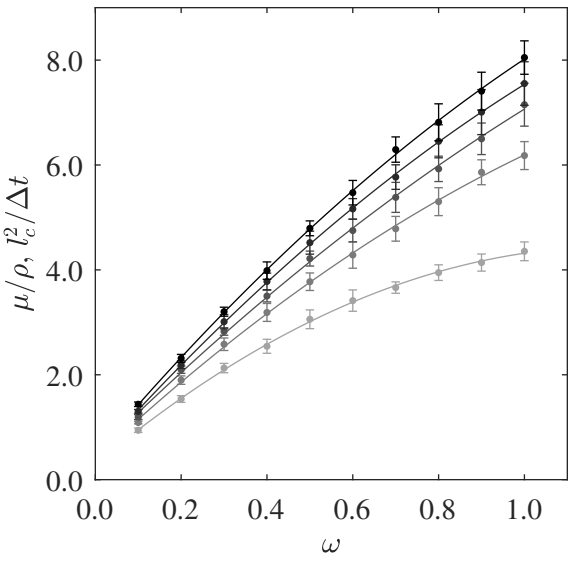

Figure 6.26: Kinematic viscosity as a function of ω for varying mean velocity.

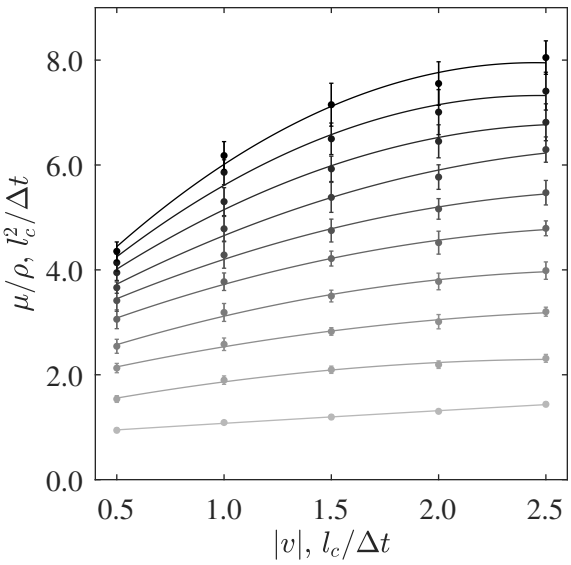

Figure 6.27: Kinematic viscosity as a function of velocity for varying ω.

only the two types of neighbors and the isotropy of the particles the relative value of transmission coefficients can be reduced to a single parameter.

Over a single time step the object must not transmit more action than it has, accordingly the total transmission values may be written as $w^* = [w_f \quad (1 - w_f)/4]$. Where the first element of w^* is the action transmitted to the single neighbor which shares a face and the second element of w^* is the action transmitted to the remaining four neighbors. In the limit as w_f approaches unity the model becomes insufficiently symmetric such that we would not be able to derive all the components of the stress tensor in the Navier-Stokes equation in considering momentum exchange through action transmission alone. [77] However there is still a transverse flux of momentum as the particles are still free to move in any direction. Properties were collected as a function of w_f = 0, 0.1, 0.2, ..., 1.0 for three ω values of 0.2, 0.5, 0.8 in the same way the properties were collected previously. The mean velocity as a function of w_f for the three ω values are shown in Figure 6.30. The mean velocity decreases abruptly from $w_f = 0$ to $w_f = 0.1$ and then decreases steadily from $w_f = 0.1$ to $w_f = 0.7$. For all three ω the mean velocity spikes as w_f approaches unity as particles can no longer exchange action to the majority of the neighboring particles around them.

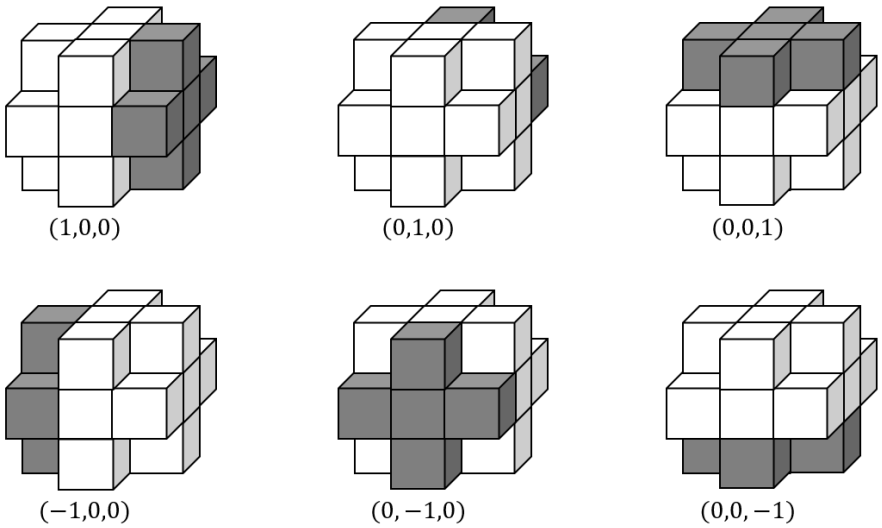

Figure 6.28: Shaded regions of the neighbors indicate the subset of the Moore neighborhood which an object can transmit action into other objects in that subset.

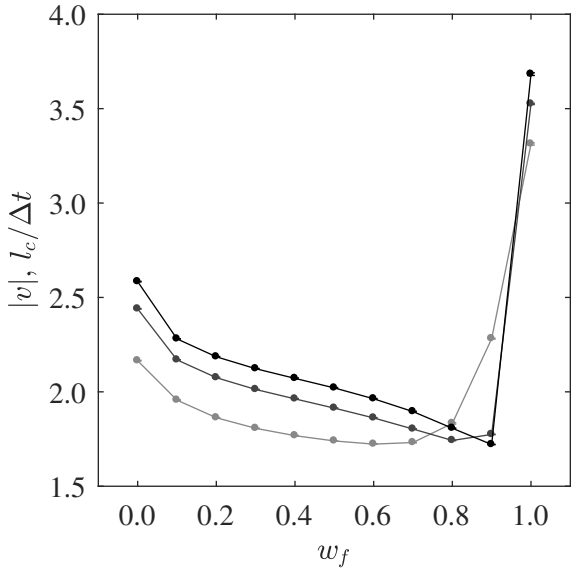

Figure 6.30: Mean velocity as a function of w_f for $\omega = 0.2$, 0.5, and 1.0.

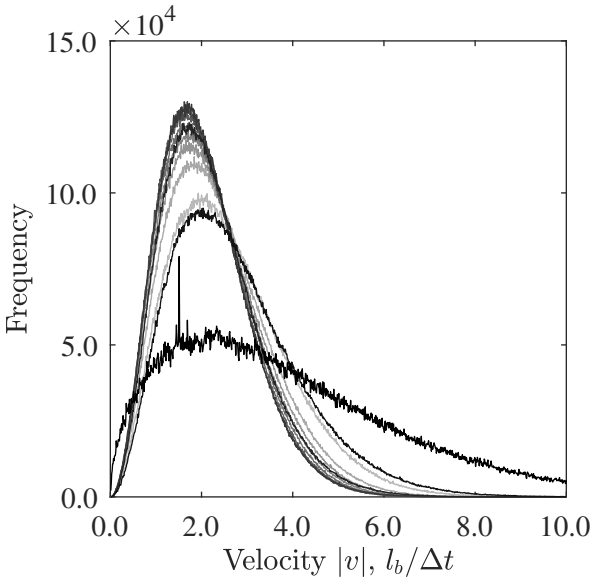

Figure 6.31: Velocity distributions corresponding to the w_f values of Figure 6.30 for $\omega = 0.2$.

Figures 6.31, 6.32,and 6.33 are the velocity distributions of the particles for $\omega = 0.2$, 0.5, and 0.8 respectively. In each case the distributions are typical for the range of $w_f = 0.0$ to $w_f = 0.9$. When $w_f = 1$ the distribution becomes atypical. The atypical distribution of $\omega = 0.2$ differ from those of $\omega = 0.5$ and $\omega = 0.8$. Whereas the atypical distribution of $\omega = 0.2$ maintains that most

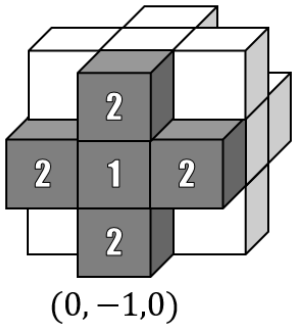

Figure 6.29: Exemplification of the different relations which the subset of neighbors relative to a given action can have.

particles have some velocity, the other distributions exhibit a maximum at $|v| = 0$. Each of the atypical distributions also exhibit increasing maximum velocity beyond the typical distributions. The non-isotropic behaviour characteristic of $w_f = 1$ clearly destroys the capability of these point particles to exhibit primitive fluid behaviour.

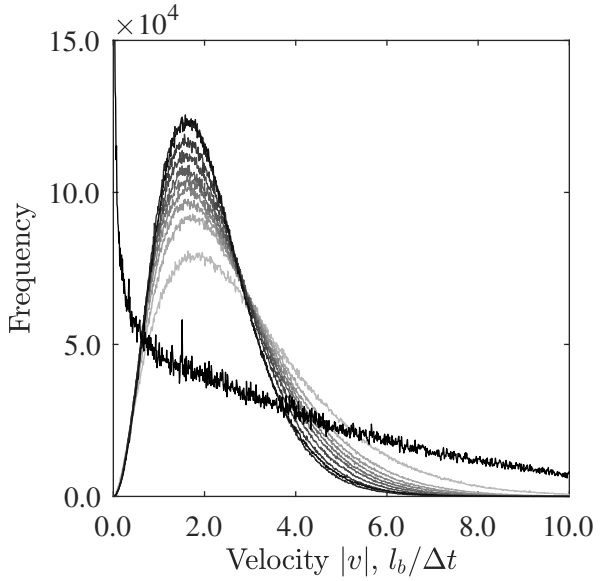

Figure 6.32: Velocity distributions corresponding to the w_f values of Figure 6.30 for $\omega = 0.5$.

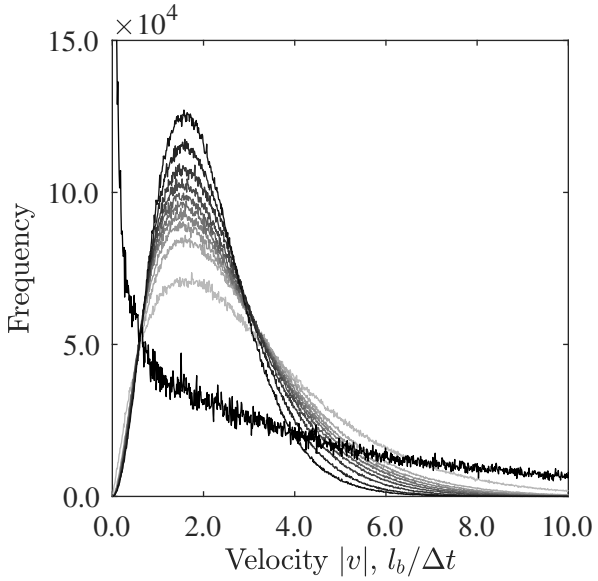

Figure 6.33: Velocity distributions corresponding to the w_f values of Figure 6.30 for $\omega = 1.0$.

Figures 6.34 and 6.35 show the diffusivity and viscosity as a function of w_f respectively. As the w_f progresses from zero to unity the diffusivity slightly decreases and then rises again. As w_f approaches unity there is an increase in D_s and once $w_f = 1$ the D_s spikes to approximately three

times the D_s compared to the D_s in the range of $w_f < 1$ for all ω tested. Throughout the range of $0 < w_f < 1$ the same trend is observed that the higher the ω the lower the diffusivity which was found earlier. The viscosity was found to decrease for $\omega = 0.2$ from $w_f = 0$ to 0.8 afterwards it slightly increases but with significant error. For $\omega = 0.5$ and 0.8 the viscosity first increases in the change from $w_f = 0$ to $w_f = 0.1$ then decreases until $w_f = 0.9$. The error then becomes large for $w_f = 1$ but the three ω cases converge to the same viscosity within error. Importantly this value is not zero and is representative of the transverse momentum flux due to particle translation.

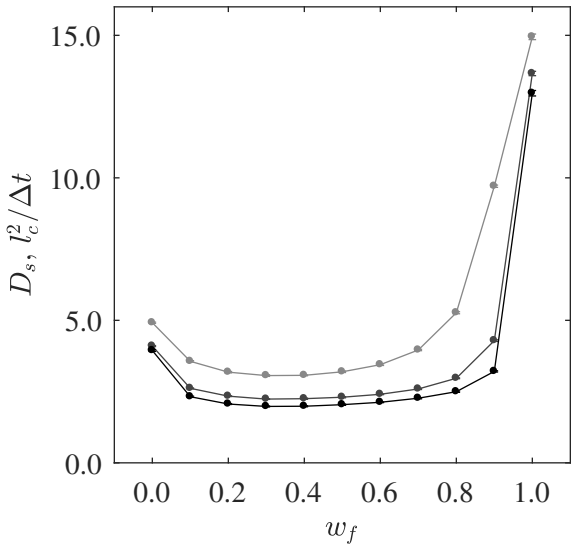

Figure 6.34: Self-diffusion coefficient as a function of w_f for $\omega = 0.2$, 0.5, and 0.8.

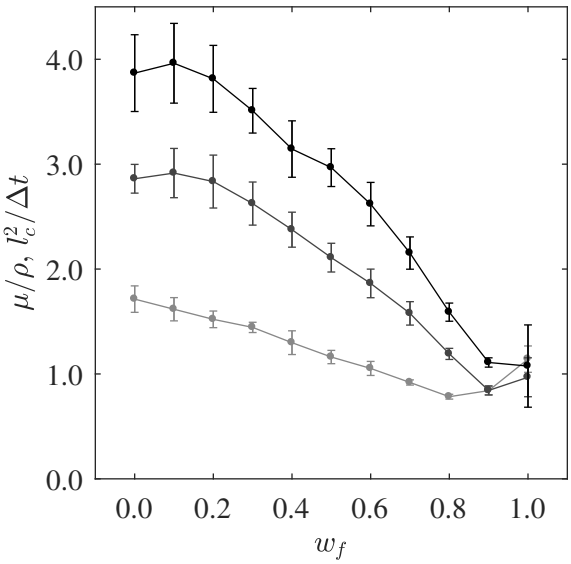

Figure 6.35: Kinematic viscosity as a function of w_f for $\omega = 0.2$, 0.5, and 0.8.

Due to the similarity of ω with the relaxation time of the LBM it should exhibit time-step invariance such that there is a characteristic time τ which is a property of the particles and not of the simulation time step. Taking twice the time step i.e. $dt = 0.010\Delta t$ the viscosity is computed for $\omega = 0.2$, 0.4, 0.6, 0.8 1.0 and compared with the viscosities found in the results section for the same ω. The results are depicted in a calibration curve in Figure 6.36. It is clear that this viscosity does not agree with the same ω at alternate time steps. Computing the equivalent τ for each case and plotting the calibration curve again in Figure 6.37 the viscosities show agreement.

Figures 6.38 and 6.39 show the MSD as a function of time interval for both the original and doubled time time steps from the smallest mean velocity $|v| = 0.5\ l_c/\Delta t$, to the largest mean velocity $|v| = 2.5\ l_c/\Delta t$. The smaller time step is plotted as lines while the larger time step is

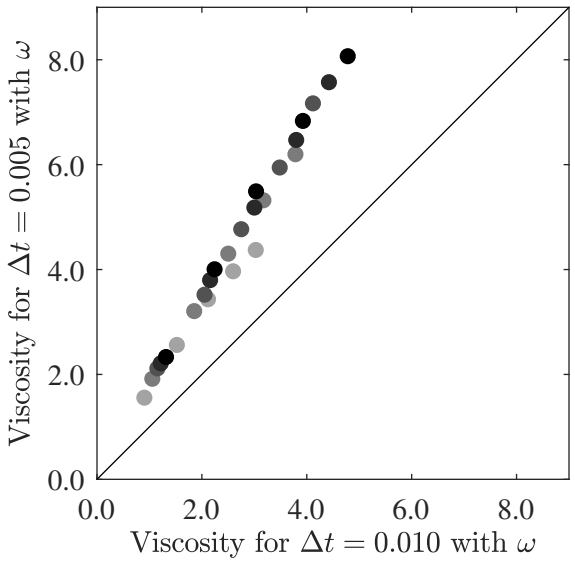

Figure 6.36: Calibration curve of kinematic viscosity for two different time steps parameterized with ω.

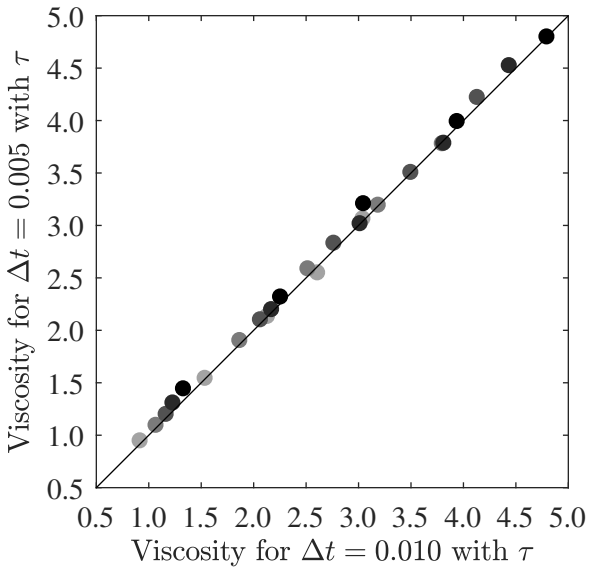

Figure 6.37: Calibration curve of kinematic viscosity for two different time steps parameterized with τ.

plotted as points. The ω factor was calculated so that the particles in both cases had the same characteristic time τ. Agreement was found. No agreement was found if the time step was changed and ω was left unchanged.

6.3 Flows In Conventional Geometries

In conducting the momentum balance on a volume element of particles it was found that the particles should exhibit flow behaviour similar to the Navier-Stokes equation. In addition the pressure was found to be a function of the sum of the inverse action pairs, an interesting result. This section evaluates the reasonableness of those results by using the point particle model in classical flow geometries. Two conventional geometries were used to study the point particles. The first geometry is shearing of the fluid between two plates with a non-zero relative velocity. The second is forced flow through an array of circular cylinders. The first case was conducted in a thorough manner and used to study the effects of different boundary conditions on the fluid. The second case was conducted in a qualitative manner and was used to see if the particles would exhibit a pressure drop when flowing through a confined geometry.

In consideration of the spectrum of surface interactions two types of interaction will be inves-

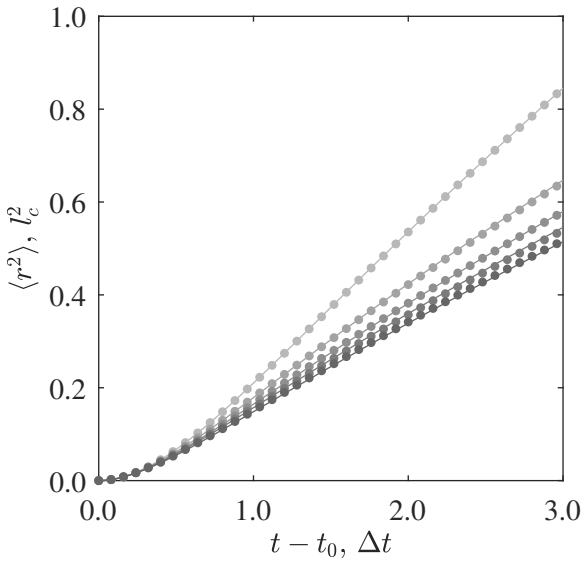

Figure 6.38: Mean square displacement for both time steps, for all ω when $|v| = 0.5$ $l_c/\Delta t$.

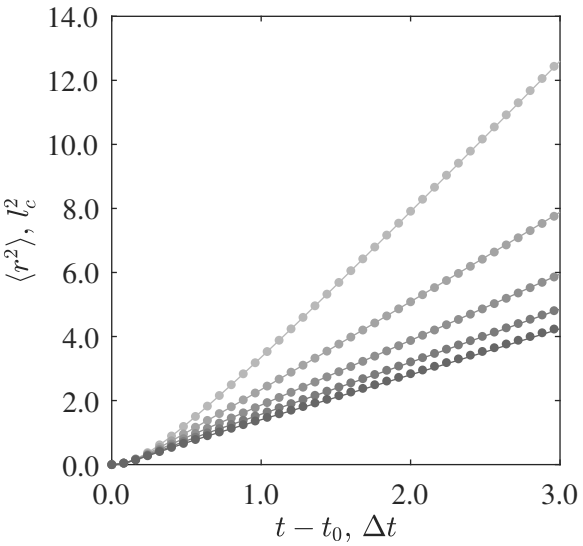

Figure 6.39: Mean square displacement for both time steps, for all ω when $|v| = 2.5$ $l_c/\Delta t$.

tigated, that of a total adsorption condition and that of a bounce back condition. These types represent polar ends of the adsorption spectrum, namely indefinite adsorption and infinitesimal adsorption. In the indefinite adsorption case the fluid layer is adsorbed to the surface and that layer of particles will work to dissipate action from the bulk fluid into the surface. Essentially the adsorbed particles become the means by which the surface interacts with the bulk fluid. The second arrangement is related to the conventional Lattice Boltzmann Method bounce back condition. When a particle collides with a surface the velocity component of the particle perpendicular to the surface is reversed causing the particle to bounce back off the surface.

6.3.1 Enforcing Boundary Conditions

The only way to change the velocity of a particle is to change the transmittable actions of the particle. Three methods of altering the action, called the conservative, maximally conservative, and non-conservative methods were investigated. Let $(s_T^k + s_T^{-k})_0$ denote the transmittable action of an inverse action pair for dimension k prior to enforcing the boundary condition and let v_k be the desired k component of the velocity for the boundary condition.

In the conservative method only the transmittable action from an inverse action pair may be used to set the velocity of the particle. The new actions when enforcing the boundary conditions

in the conservative method is then

$$s_T^k = \begin{cases} \frac{(s_T^k + s_T^{-k})_0 + v_k}{2}, & \text{if } |v_k| \leq (s_T^k + s_T^{-k})_0 \\ (s_T^k + s_T^{-k})_0, & \text{if } v_k > (s_T^k + s_T^{-k})_0 \\ 0, & \text{if } v_k < -(s_T^k + s_T^{-k})_0 \end{cases} \tag{6.6}$$

and for the inverse component

$$s_T^{-k} = \begin{cases} \frac{(s_T^k + s_T^{-k})_0 - v_k}{2}, & \text{if } |v_k| \leq (s_T^k + s_T^{-k})_0 \\ 0, & \text{if } v_k > (s_T^k + s_T^{-k})_0 \\ (s_T^k + s_T^{-k})_0, & \text{if } v_k < -(s_T^k + s_T^{-k})_0 \end{cases} \tag{6.7}$$

In the conservative cases of 6.6 and 6.7 the assigned velocity will not be obtained if it is beyond the range of the transmittable action available.

In the maximally conservative case action is permitted to be added to the particles to obtain the velocity but only in the direction in which the surface is moving relative to the fluid such that

$$s_T^k = \begin{cases} \frac{(s_T^k + s_T^{-k})_0 + v_k}{2}, & \text{if } |v_k| \leq (s_T^k + s_T^{-k})_0 \\ v_k, & \text{if } v_k > (s_T^k + s_T^{-k})_0 \\ 0, & \text{if } v_k < -(s_T^k + s_T^{-k})_0 \end{cases} \tag{6.8}$$

and for the inverse component

$$s_T^{-k} = \begin{cases} \frac{(s_T^k + s_T^{-k})_0 - v_k}{2}, & \text{if } |v_k| \leq (s_T^k + s_T^{-k})_0 \\ 0, & \text{if } v_k > (s_T^k + s_T^{-k})_0 \\ v_k, & \text{if } v_k < -(s_T^k + s_T^{-k})_0 \end{cases} \tag{6.9}$$

In the non-conservative case the action of the particles is set for the boundary condition in the same way that the actions of the particles are initialized in the simulation. It requires that the action assigned to the particle be greater than or equal to the velocity. The non-conservative

method is enforced by the following equations.

$$s_T^k = s_{T_0}^{\pm k} + \frac{v_k}{2} \tag{6.10}$$

$$s_T^{-k} = s_{T_0}^{\pm k} - \frac{v_k}{2} \tag{6.11}$$

6.3.2 Shearing Between Plates

Consider the classical case of a fluid in between two plates with non-zero velocities relative to each other. The Navier-Stokes equation when solved under these conditions with a constant pressure field yields a linear velocity profile where the fluid velocity at the plate boundaries is equal to the plate velocities. This system is recreated here. Boundary conditions are placed on the lattice such that if the particles are in the top layer of cells or bottom layer of cells the actions are changed to enforce the boundary conditions. The parameters of the system were set at $s_{T_0}^{\pm k} = 0.9134$, $\omega = 0.5$, and $\Delta t = 0.005$. The system box is $200 \times 20 \times 20$ and contains 10000 particles. The z-axis is perpendicular to the plates and denotes the height of the particle within the system. The plate velocities at are $v_k^{z=0} = (0, -1.5, 0)\ l_c/\Delta t$ and $v_k^{z=l_c} = (0, 1.5, 0)\ l_c/\Delta t$ for the bottom and top plates respectively.

We begin by implementing the total adsorption case where the velocity to be enforced is the plate velocities. First the completely conservative method of equations 6.6 and 6.7 are analyzed. Figures 6.40 and 6.41 display the evolution of the velocity and relative density as a function of height over multiple time steps respectively. The velocity and density profile are obtained precisely as described in section 5.4.2 except that the layers are cut along the z-axis and are the width of the cells. The reported density is relative to the ideal gas density as in the radial distribution function. The evolution in time is indicated by the shade of the line. The lightest line corresponds to the earliest time step and the darkest line is the latest. The solution to the Navier-Stokes equation is also plotted in the velocity profile as a black line diagonally across the figure. The velocity profile does not tend to the solution of the Navier-Stokes equation. The particles appear to have insufficient transmittable action to meet the velocity of the boundary conditions. Extreme structuring is seen in the density profile. The relative density is highest at the boundaries where adsorption is occurring. The density oscillates throughout the height of the channel and is minimal

only at the middle of the channel.

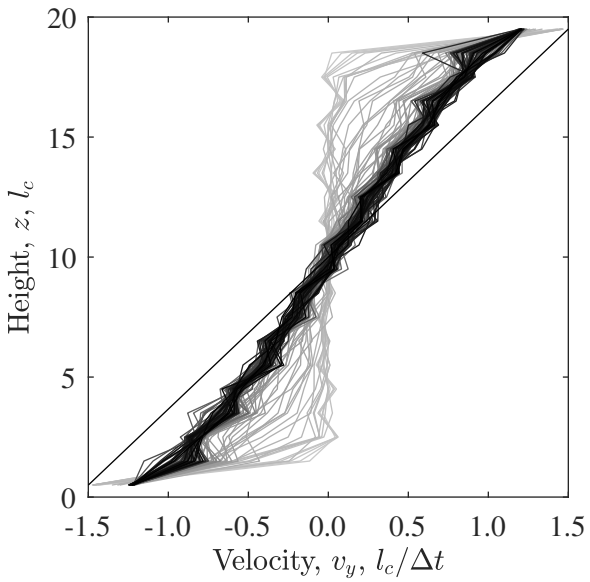

Figure 6.40: Velocity profile evolution for point particles between two shearing plates with adsorption boundary conditions enforced using the conservative method.

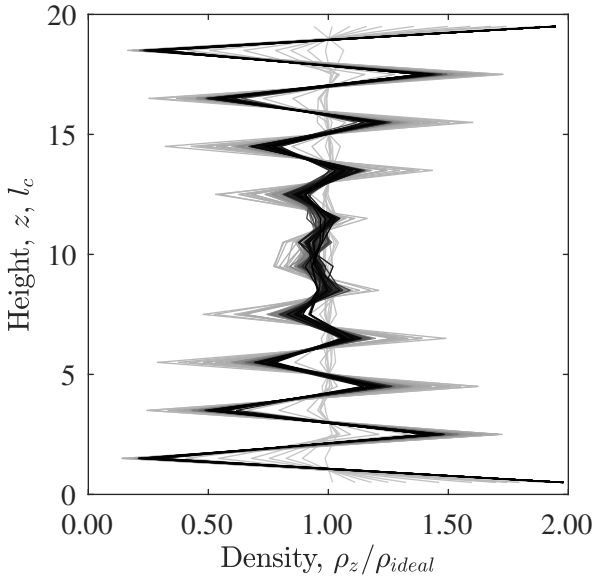

Figure 6.41: Relative density profile evolution for point particles between two shearing plates with adsorption boundary conditions enforced using the conservative method.

Next the maximally conservative method is tested which implements equations 6.8 and 6.9. The velocity profile evolution is shown in Figure 6.42. The velocity of the particles meets the bounds but the entire profile does not tend to the Navier-Stokes solution. The relative density, not shown, is identical to the result of Figure 6.41 displaying significant liquid structuring. Lastly the non-conservative method is tested which implements equations 6.10 and 6.11. The transmittable action for which the simulation was started is implemented as the transmittable action of the boundary conditions. The velocity profile evolution is shown in Figure 6.43 and the relative density profile is not shown because it is the same as the others. The results of the total adsorption case are abysmal in the context of the Navier-stokes solution. None of the three methods return the Navier-Stokes solution. In general, the less conservative the approach the closer the velocity profile comes to the Navier-Stokes equation.

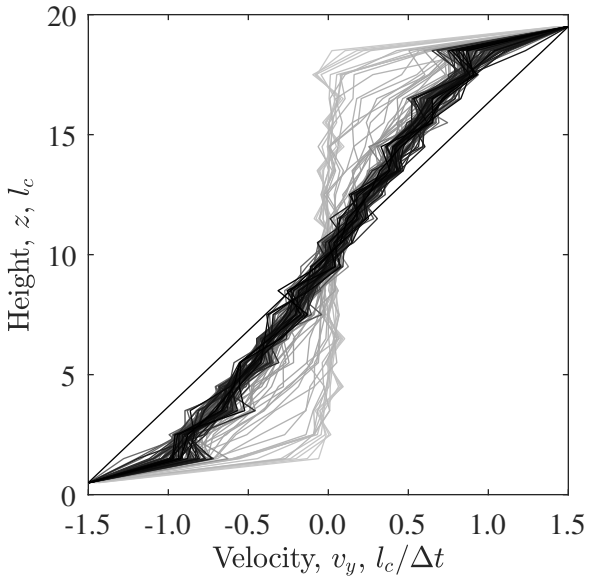

Figure 6.42: Velocity profile evolution for point particles between two shearing plates with adsorption boundary conditions enforced using the maximally conservative method.

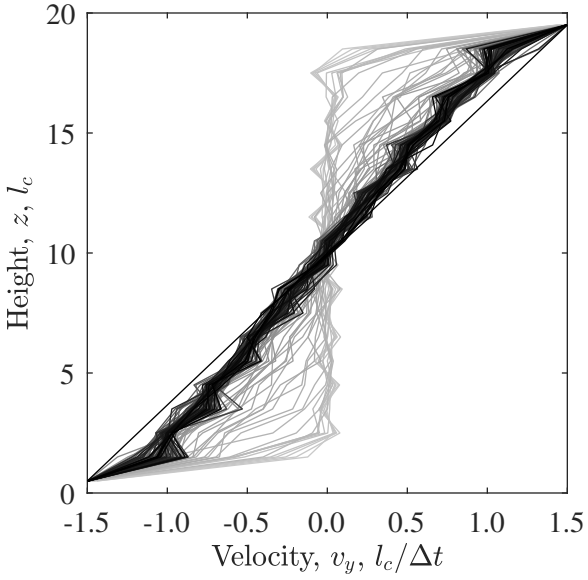

Figure 6.43: Velocity profile evolution for point particles between two shearing plates with adsorption boundary conditions enforced using the non-conservative method.

We now turn to the condition of infinitesimal adsorption i.e. bounce back conditions. In the previous adsorption condition once the particle was within a l_c of a moving plate the boundary condition was imposed for all velocity components. In the bounce back condition if the particle comes into contact with a boundary plate the velocity of the particle perpendicular to the plate is reversed by interchanging the inverse action pairs. Since z is perpendicular to the plates the bounce back condition enforces that

$$s_T^z = \begin{cases} s_T^{-z}, & \text{if } 0 \leq r_z \leq l_b \\ s_T^z, & \text{otherwise} \end{cases} \tag{6.12}$$

$$s_T^{-z} = \begin{cases} s_T^z, & \text{if } 0 \leq r_z \leq l_b \\ s_T^{-z}, & \text{otherwise} \end{cases} \tag{6.13}$$

For the dimensions parallel to the surface the x component of the action will not undergo any changes when in contact with the plate because the plate has no net velocity in the x direction. Only changes to the action will be imposed on the y component with the conservative, maximally

conservative and non conservative methods. Figure 6.44 and 6.45 show the velocity and relative density as a function of height for multiple time steps with the conservative method used to enforce the bounce back condition. As before, if the action is insufficient the velocity cannot tend to the Navier-Stokes solution. However the profile is more linear than any of the total adsorption results. The density profile indicates that the structuring of the particles was not due to the adsorption condition but rather the presence of solid boundaries.

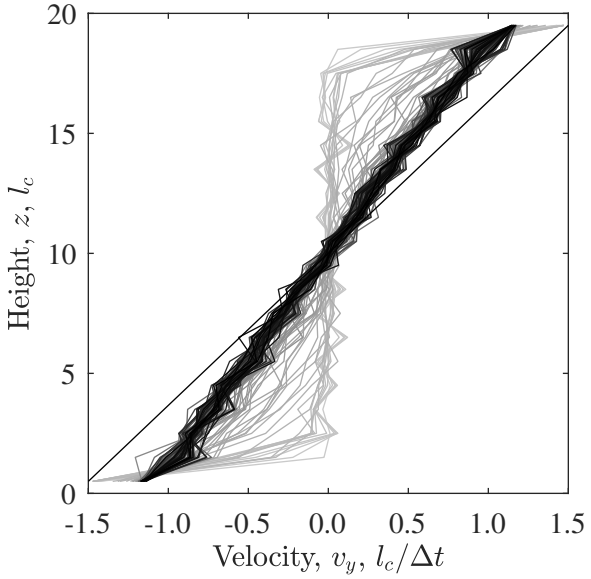

Figure 6.44: Velocity profile evolution for point particles between two shearing plates with bounce back boundary conditions enforced using the conservative method.

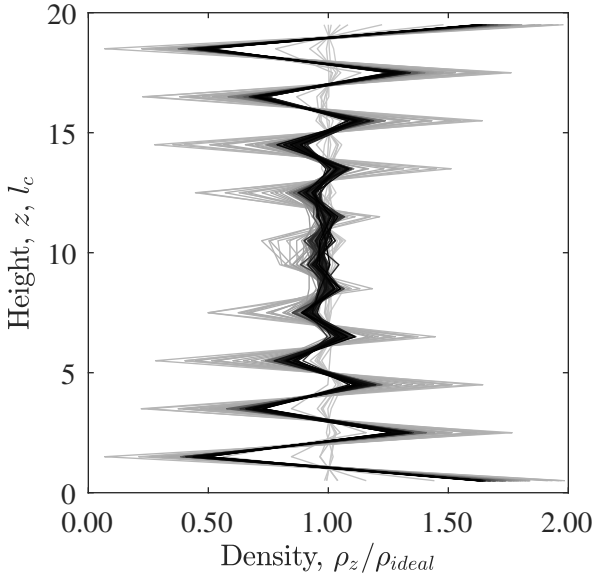

Figure 6.45: Relative density profile evolution for point particles between two shearing plates with bounce back boundary conditions enforced using the conservative method.

Results of the maximally conservative method and the non-conservative method for the bounce back condition are shown in Figures 6.46 and 6.47. In the maximally conservative method the solution approaches the Navier-Stokes better than the rest so far. In the non-conservative case the Navier-Stokes equation is nearly obtained and is the best result.

It is difficult to ascertain from the velocity profile evolutions whether or not the simulation has converged to a final solution. This information can be indirectly obtained by evaluating the mean velocity of particles as a function of time. Figure 6.48 displays the mean velocity as a function of time for each of the methods with the adsorption boundary condition along with a simulation with no plates under free evolution acting as a control. The mean velocity of the conservative method

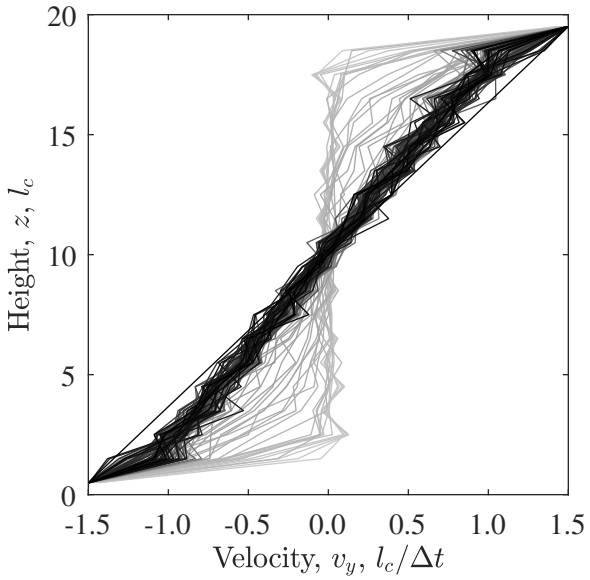

Figure 6.46: Velocity profile evolution for point particles between two shearing plates with bounce back boundary conditions enforced using the maximally conservative method.

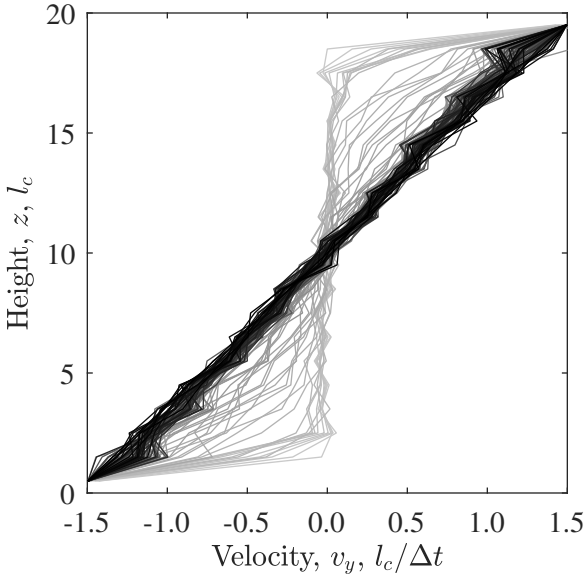

Figure 6.47: Velocity profile evolution for point particles between two shearing plates with bounce back boundary conditions enforced using the non-conservative method.

tends to a finite value slightly higher than the mean velocity of 1.5 $l_c/\Delta t$ of the free evolution case. The maximally conservative method shows a consistent increase in mean velocity for the time range tested. This result is not surprising in that if the total action is insufficient, then more is added. If the action is in excess nothing is removed. In the non-conservative method the mean velocity converges to a finite value slightly above the control case and greater than the conservative method. The mean velocity of the non-conservative method converges to a finite value as it has the capacity to add action and remove action but acts independently of the action of the particle at the boundary. Figure 6.49 shows the mean velocity as a function of time for the bounce back conditions enforced with the three methods and instead of the control as a free evolution with no plates the control consists of a case where there are plates but with zero velocities. The mean velocity of the control case with bounce back conditions is a little higher than the free evolution control case of Figure 6.48 which suggests that the boundaries themselves may be the reason for the increase in mean velocity observed in the completely conservative methods. The general trend remains the same between the total adsorption and bounce back conditions. The mean velocity of the non-conservative method converges to a finite value but is greater than the conservative

method. The mean velocity of the maximally conservative method continues to increase steadily over the period tested.

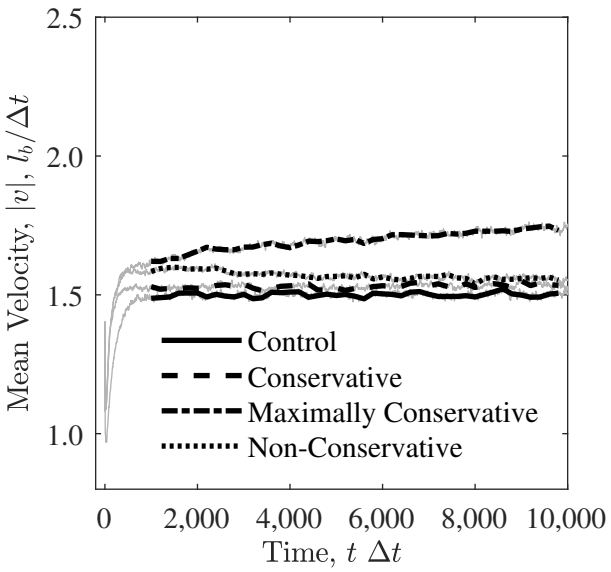

Figure 6.48: Mean velocity as a function of time for adsorption boundary conditions enforced using the conservative, maximally conservative, and non-conservative methods along with a control case of no periodic boundary conditions with no plates.

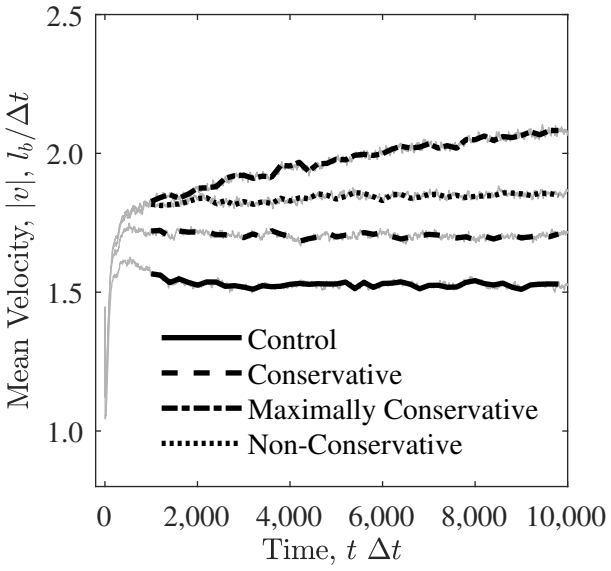

Figure 6.49: Mean velocity as a function of time for bounce back boundary conditions enforced using the conservative, maximally conservative, and non-conservative methods along with a control case of plates with zero velocity.

A more direct method of analyzing the convergence of the simulation can be achieved by defining an error function $E(t)$ such that

$$E(t) = \int_{z=0}^{z=l_b} \left[v_{NS}(z,t) - \bar{v}(z,t)\right]^2 dz \tag{6.14}$$

which defines the square deviation of the point particle velocity profile from the Navier-Stokes (NS) solution at each time step. The error function does not need to be rigorously integrated over ever point in z but can be done by subtracting the array of the velocity profile from an array of Navier-Stokes solutions, squaring the elements of the resultant array, and summing the resulting elements together. Figures 6.50 and 6.51 show the results for the adsorption and bounce back conditions. None of the adsorption condition results tend to the Navier-Stokes equation within the time the simulation was carried out. In the bounce back condition the non-conservative method displayed the closest approach to the Navier-Stokes solution.

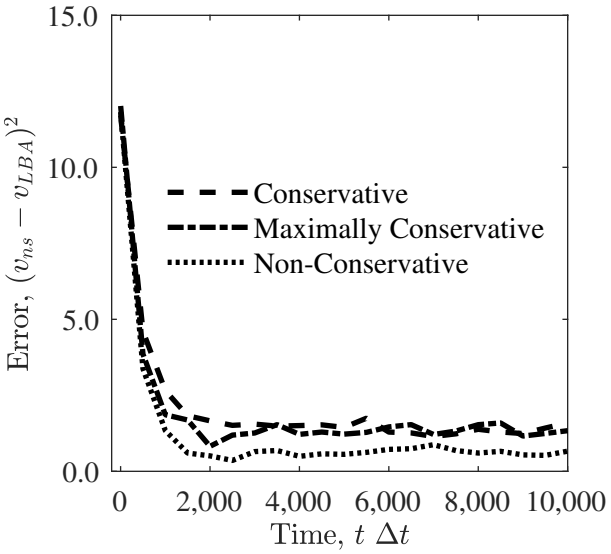

Figure 6.50: Square deviation from the Navier-Stokes solution as a function of time for the adsorption boundary condition enforced using the conservative, maximally conservative, and non-conservative methods.

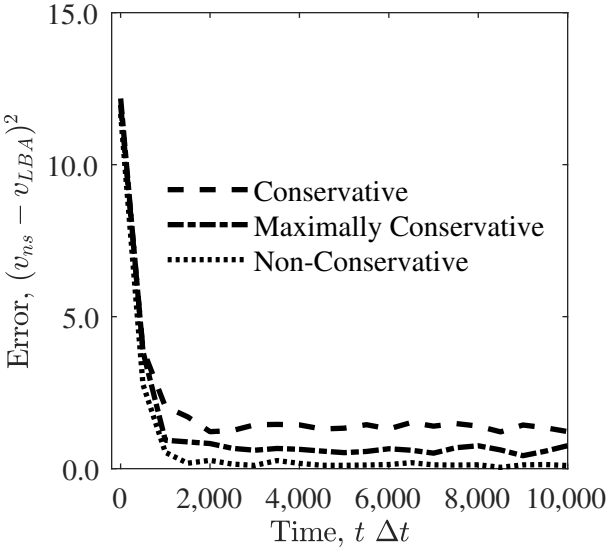

Figure 6.51: Square deviation from the Navier-Stokes solution as a function of time for the adsorption boundary condition enforced with the conservative, maximally conservative, and non-conservative methods.

It is interesting to compare the density profile of particles in periodic boundary conditions and the bounce back control density profiles which are shown in Figures 6.52 and 6.53 respectively. The periodic boundary shows virtually no density profile whereas the bounce back certainly does. The structuring is highest right at the plates and diminishes in the middle between the plates. The lack of structuring at the height farthest from the plates suggests that if there is a larger spacing between the plates there will be regions which do not exhibit significant structuring.

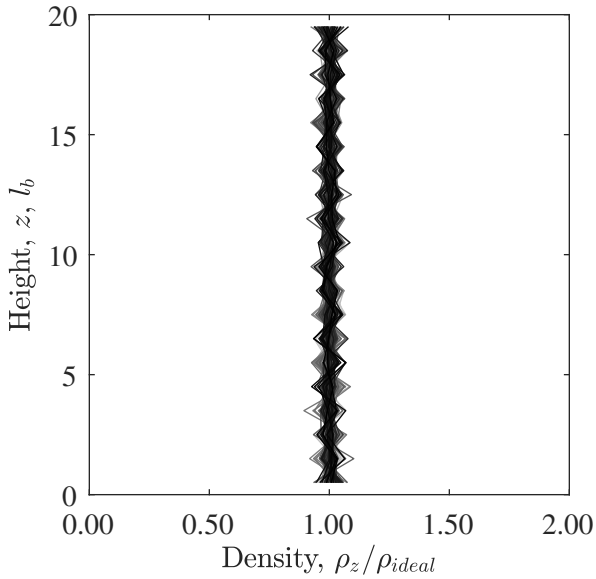

Figure 6.52: Density profile of particles in periodic boundary conditions exhibiting no significant structuring.

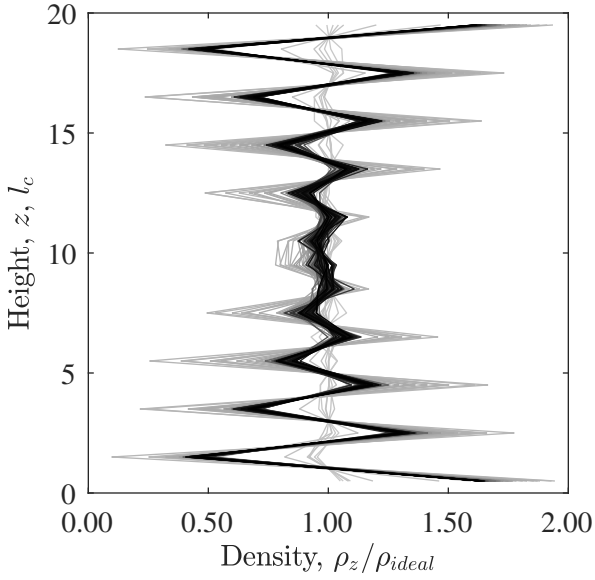

Figure 6.53: Density profile of particles in between stationary plates with bounce back conditions.

Lastly we investigate a domain with greater spacing between the plates. The domain was defined as $20 \times 20 \times 80$ cells in the x, y, and z directions. Shearing was implemented via plates with the bounce back non-conservative condition where $v_k^{S,z=0} = (0, -1.5, 0)\ l_c/\Delta t$ and $v_k^{S,z=l_b} = (0, 1.5, 0)\ l_c/\Delta t$. The simulation was ran for 40000 time steps, all else the same as the previously tested cases. The mean velocity of the layers of the cells were collected for the last 10000 time steps every 1000^{th} time step to yield ten data points per layer of cells. Figure 6.54 shows the average of these ten data points along with their standard deviations as error bars as a function of height. Figure 6.55 shows the relative density as a function of height using the same data collection scheme. The line connects the points in order that the profile may be traced. Significant structuring is seen at the box edges and persists approximately 10 l_c into the fluid. Beyond that region the fluid does not show significant structuring behaviour.

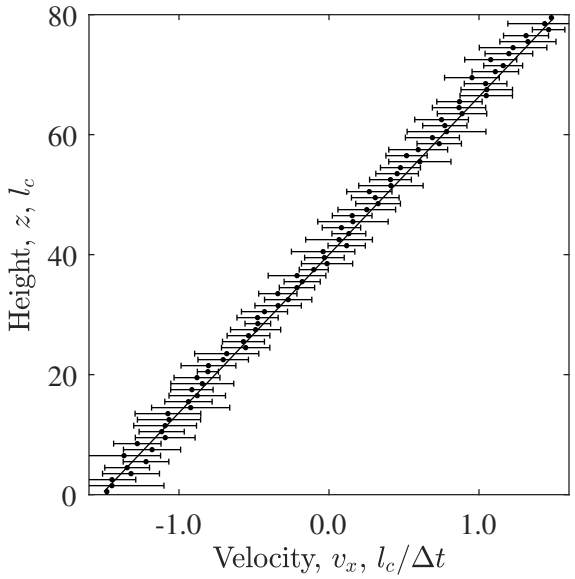

Figure 6.54: Mean velocity as a function of height with standard deviations in a larger domain with bounce back conditions enforced using the non-conservative method.

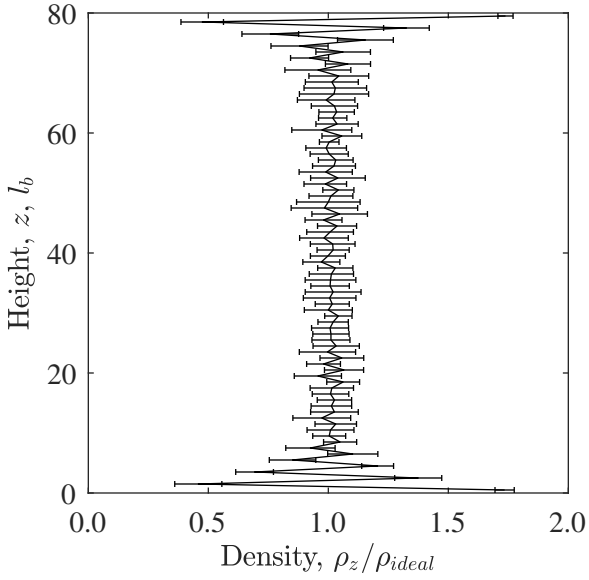

Figure 6.55: Relative density as a function of height with standard deviations in a larger domain with bounce back conditions enforced using the non-conservative method.

6.3.3 Flow Through an Array of Circular Cylinders

The shearing studies provide good reason to suspect that the point particle model can be used in the context of more complex flow domains. Four simulations were conducted for flow through an array of circular cylinders.

It was not clear how best to implement the inlet velocity of the particles in a flowing arrangement. As success was found with the non-conservative method of section 6.3.2 it was decided that the same method could be used for the first slab of cells at the inlet of of the domain thereby setting the velocity with the corresponding transmittable action that tends to that velocity at equilibrium. This approach was first tested using the simpler case of flow between stationary parallel plates which should exhibit a parabolic flow profile with zero velocities at the boundaries. The domain consisted of $88 \times 22 \times 22$ cells with periodic boundary conditions on the x and z sides and the bounce back boundary condition at $y = 0$ and $y = l_b$ enforced with the non-conservative method. A total of 5324 particles were flown through the channel with an inlet velocity of $v_{x=0} = 1.5\ l_c/\Delta t$ and $s_{T_0}^{\pm k} = 0.9134$. Figure 6.56 shows the evolution of the flow profile at four equally distributed points along the channel. The left-most profile is closest to the inlet while the rightmost is farthest

from the inlet. At each point a parabolic profile is obtained but is shaped differently depending on the distance from the inlet which has a uniform distribution. Nonetheless this inlet condition works satisfactorily.

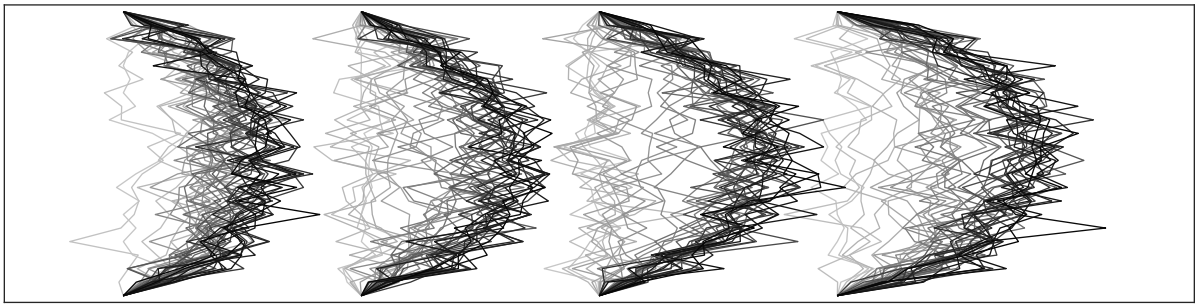

Figure 6.56: Evolution of velocity profiles for forced flow between two stationary plates.

The domain for the cylinder array was rectangular with $168 \times 42 \times 42$ cells in the x, y, and z dimensions respectively. A cylinder was placed with its center at $x = 63\,l_c$ and $y = 21\,l_c$. This gives $3/8$ of the domain in the x dimension before the cylinder and $5/8$ of the domain in the x dimension after the cylinder. All boundaries are periodic making the system an infinite array of cylinders.

Four cases were simulated. Cases (i) and (iii) entail a fluid with $\omega = 0.5$ and an inlet velocity of $v = 1.5\ l_c/\Delta t$ with $s_{T_0}^{\pm k} = 0.9134$. These cases represent high viscosity at low flows thus creating low Reynolds numbers. Cases (ii) and (iv) entail a fluid with $\omega = 0.1$ and an inlet velocity of $v = 2.5\ l_c/\Delta t$ with $s_{T_0}^{\pm k} = 2.2920$. These cases entail low viscosity in high flows and thus obtain higher Reynolds numbers. The transmittable actions were set to maintain an equilibrium velocity equivalent to the inlet so that the inlet boundary condition does not create a gradient in transmittable action on its own. Cases (i) and (ii) are for a cylinder with a radius of five cells and cases (iii) and (iv) are for a cylinder with a radius of 10 cells. The approximate Reynolds numbers for the cases are 4, 18, 7 and 36 where the Reynolds number is defined as $\mathrm{Re} = \frac{2|v|r_c\rho}{\mu}$ and r_c is the cylinder radius. [98] The details of the simulation cases are summarized in Figure 6.57.

	$r_c = 5$	$r_c = 10$
$\omega = 0.5$ $v = 1.5$	$Case\ (i)$ $Re = 4$	$Case\ (iii)$ $Re = 7$
$\omega = 0.1$ $v = 2.5$	$Case\ (ii)$ $Re = 18$	$Case\ (iv)$ $Re = 36$

Figure 6.57: Summary of the cases tested for flow through an array of cylinders.

The particle density was the same as the majority of the simulation results with one eighth of the cells occupied by particles. Thus the simulation consisted of 37044 particles in 296352 cells. The simulation was ran for 5000 time steps as an equilibrium period and then data was collected for 20000 time steps. As the geometry of the domain is invariant with respect to the z dimension all data was stored for each time step after the equilibration period with respect to the location of cells in the x-y plane. Thus although the simulation is three dimensional the results may be represented in two dimensions. The data that was collected includes the x and y velocities of the particles with respect to x-y position, the sum of the transmittable action of the particles, $\lceil s_T \rceil$ with respect to x-y position, and a count of all the particles that are used for the previous data sets in order to normalize them. As these are particles interacting with a cylinder of a radius their own magnitude or one magnitude larger we do not expect to see anything beyond Stokes flow.

The flow results are shown in Figures 6.58, 6.59, 6.60, 6.61. Each figure has three sections. The top section is a stream-line plot which shows the path a small object would trace if carried by the flow. The middle section is a skewed quiver plot. Each line of the quiver plot is a vector indicating the velocity at the root of the vector. It is skewed in order to making the velocity profile along the boundary easier to discern. The quiver plot also supplements the stream plot in the regions where the streamlines are absent. The bottom section is a contour plot of the relative pressure of the fluid with a scale bar indicating the relative pressure. The flow enters from the left and exits on the right.

While the velocity is the average velocity of a particle if it belongs in given cell the pressure

is a measure of the transmittable action within a given cell regardless of direction. For example if there were two particles in the same cell the velocity would refer to the most likely velocity of each of those particles while the pressure would refer to the sum of the action of both those particles. Thus for an ideal gas, i.e. uniformly distributed particles, the pressure for a cell is proportional to the average transmittable action $s_T^{\pm k}$ multiplied by the average particle density. This pressure is not used in the figures below. Instead the relative density of the cell is used to normalize the total transmittable action. The total transmittable $\lceil s \rceil$ is also divided by the cardinality of the action set, and then divided by the average transmittable action of an ideal gas i.e $s_{T_0}^{\pm k}$. This way the contour plot shows a value of unity if the pressure is equivalent to an ideal gas of the same density at equilibrium.

In each case the stream lines are well formed passing around the cylinder. They do return to each other in the same way which they split in approaching the cylinder differing from the potential flow solution of a single cylinder. The boundary layer around the cylinder surface exhibits a parabolic profile. No evidence of re-circulation is seen around the cylinder which would be characteristic for higher Reynolds numbers. The pressure is higher at the inlet and drops when passing the cylinder array. The pressure is also seen to be higher in the middle of the channel on the approach to the cylinder obtaining peaks at the cylinder surface. The lowest pressure is found behind the cylinder extending for a while afterwards. Various lattice artifacts can be seen around the cylinder in the pressure contour plots of all cases and in the stream plots of cases (i) and (ii). These are characterized by irregular straight lines and corners. There is evidence of liquid structuring at the inlet as given by the vertical lines of higher pressure in the contour plot.

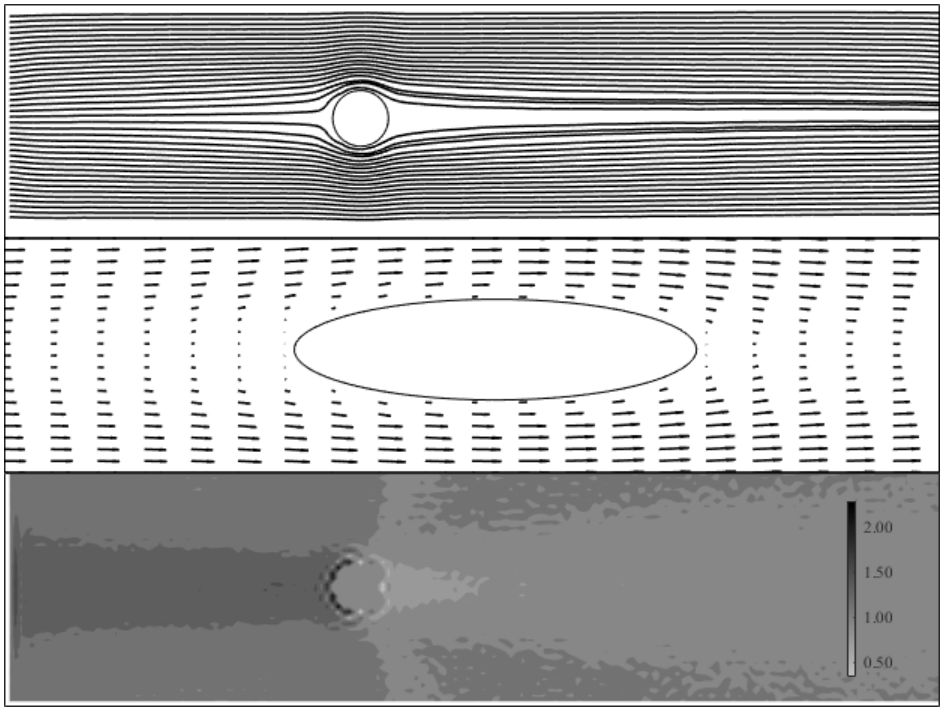

Figure 6.58: Velocity stream line plot, skewed velocity quiver plot, and relative pressure contour plot for case (i) of flow through an array of cylinders.

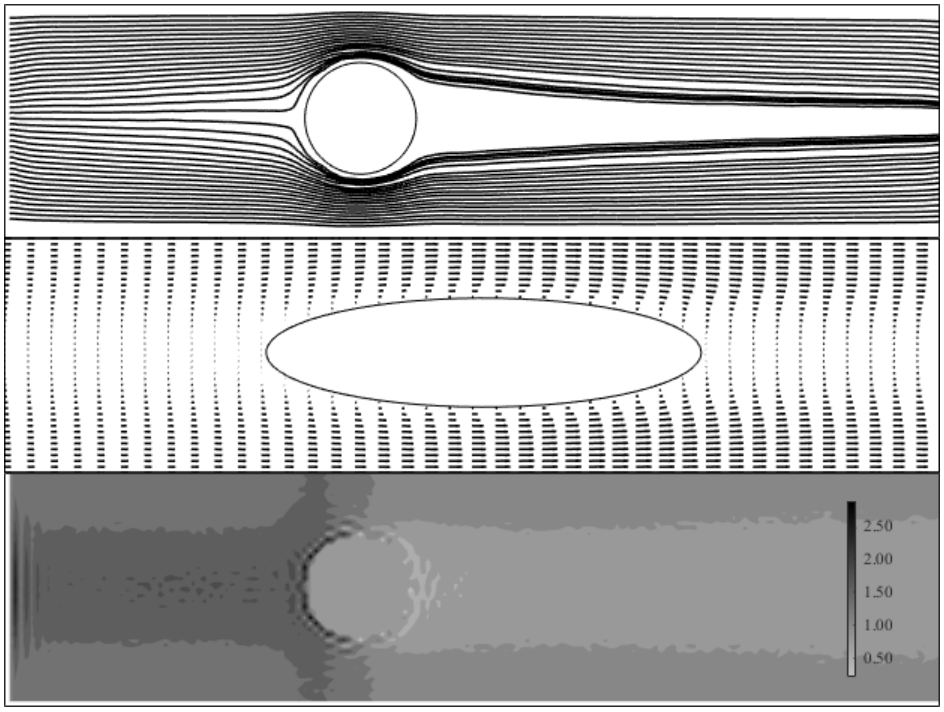

Figure 6.59: Velocity stream line plot, skewed velocity quiver plot, and relative pressure contour plot for case (ii) of flow through an array of cylinders.

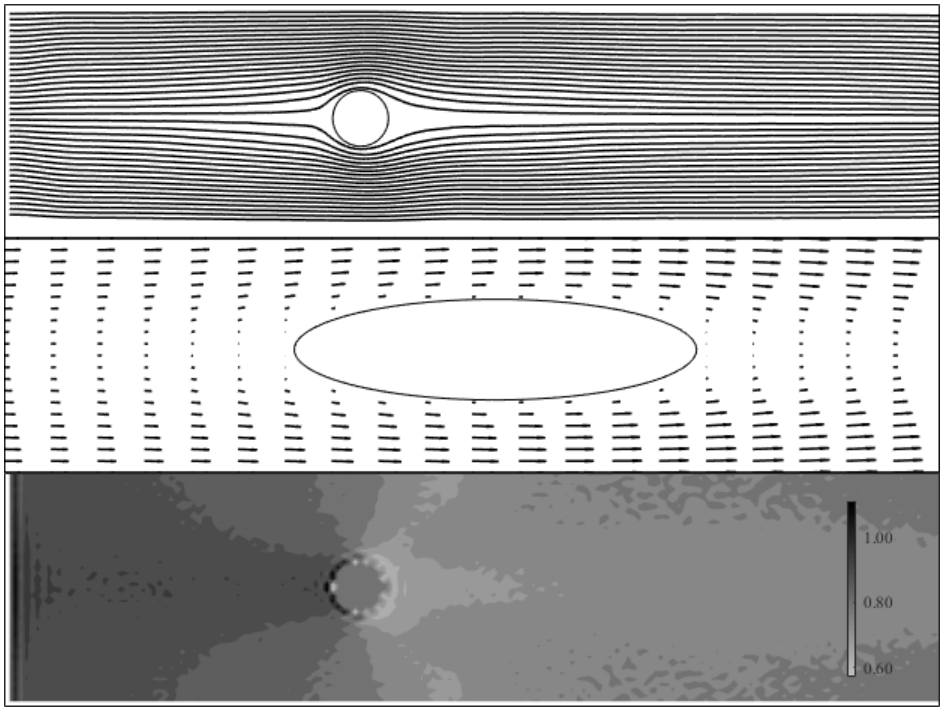

Figure 6.60: Velocity stream line plot, skewed velocity quiver plot, and relative pressure contour plot for case (iii) of flow through an array of cylinders.

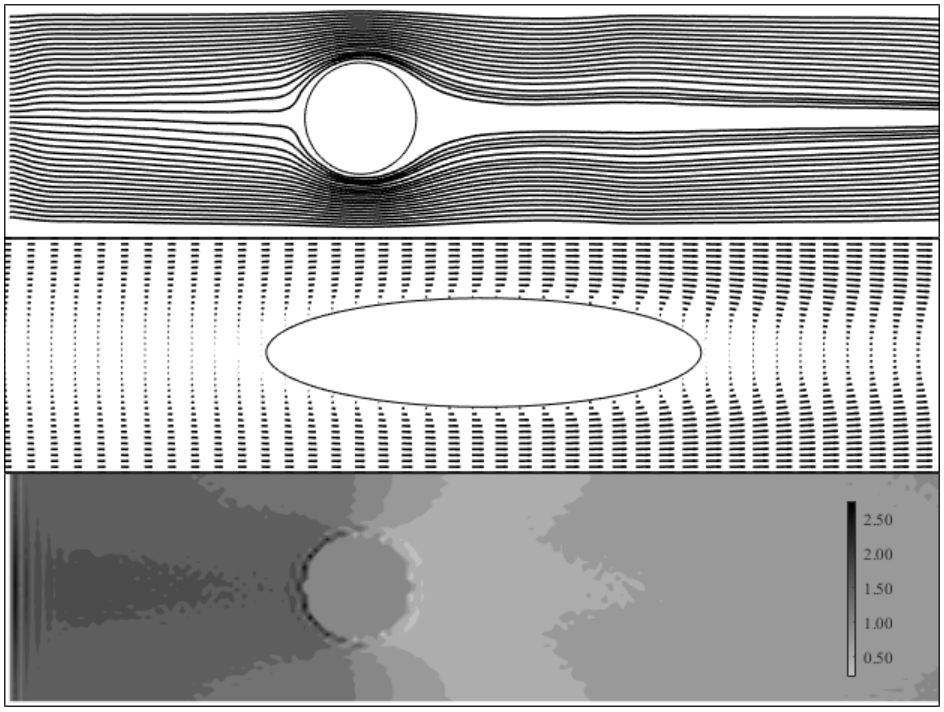

Figure 6.61: Velocity stream line plot, skewed velocity quiver plot, and relative pressure contour plot for case (iv) of flow through an array of cylinders.

The characteristic result and the one for which this study was conducted was to see if the pressure as transmittable action, as suggested by the derivation in the momentum balance, corresponds to what would be observed in an actual system and this is indeed what is observed. The sum of the action inverse action pairs behaves qualitatively as classical pressure does. This can be further seen by looking at the pressure along the surface of the cylinder for case (iv). Figure 6.62 shows the relative pressures of the cells near the surface of the cylinder as a function of the angle, where $\theta = 0$ is the point of the cylinder surface opposite of the inlet flow. These results exhibit qualitative agreement with typical results of the pressure distribution characteristic of flow around cylinders. [98]

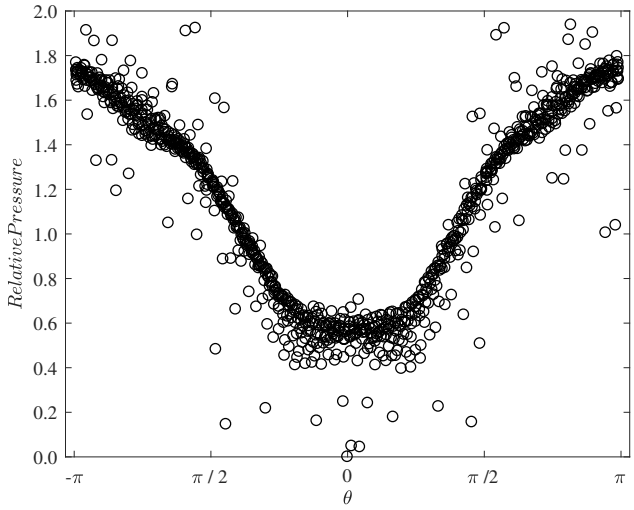

Figure 6.62: Pressure of cells as a function of angle around the cylinder for case (iv) where $\theta = 0$ is the point on the cylinder surface furthest from the inlet of the flow.

6.4 Discussion

The vector formulation of the algorithm proved to work well as a point particle model. The critical feature which differentiates it from other models is that there are two separate components for each momentum which have been consistently referred to as inverse action pairs.

This feature allowed the particles to essentially have both active and passive actions, momenta, or energy, similar to the notions of kinetic and potential energy. One will notice that there was never any reference to potential energy in the development of the event-lattice or objects. This was due to Feynman's condition that a computational method must scale with the space-time volume for

which it simulates, or more directly stated, all interactions are local. Potential energy is completely antagonistic to this ideal and had to be abandoned. Not to say that potential energy cannot describe various phenomena. The ability of having inverse action pairs allows objects to maintain an internal energy or passive action, which is not the typical mass since it can be exchanged but neither is it a potential energy because it is not position dependent. It can however be released through interactions with other objects. Potential energy is itself a non-local concept in that it presupposes a direct spatial relation between objects and an energetic dependence on that spatial relation. Potential energy is originally a notion from Newtonian mechanics which has survived into quantum mechanics. The passive action intrinsic in these objects is similar to potential energy in the fact that both can be transformed into a kinetic form of energy, but only through interaction. If one forgoes the concept of force, since it is only a part of a systematic framework of description, there is plenty of empirical evidence for considering inverse action pairs as a physical reality. For example take the case of a creature standing still then walking to the right and stopping. At first the creature is stationary but soon it will be in a state of translation, thus the momentum which is necessary for the creature's translation is implicit in it while stationary. Secondly, in order to begin the translation process the creature must somehow take the still energy and convert it into rightward momentum. As momentum is conserved it cannot simply create the rightward and only rightward momentum, but must create momenta of both the direction it goes and the opposite. Thus there was in the creature when still both the momenta for the direction it walks and the inverse, or opposite momenta. Third, having released these momenta it discards the leftward into the ground yielding a net momentum and thus translation. Then, in order to stop and become still once again the creature discards that rightward momenta which made the translation possible. Thus the momenta as equal and opposite are separable. Another example would be the problem of describing a rotating collection of objects while translating in space, such that it rotates much faster than it translates. The path of an object on the edge of this rotating object would be far from linear yet could easily be described as a sequence without reference to force or interaction. This is because it admits inverse action pairs. It was not clear at the outset how this pair arrangement would behave for many point particles like in a fluid. The most striking result of all was the form of the velocity distribution function exhibiting such classical properties of the Maxwell Boltzmann distribution even though the collisions of the particles are characteristically different from classical scattering

theory. For instance consider two particles with relatively low velocities but large amounts of transmittable action. If these two particles collide by travelling directly at one another they can both increase in velocity due to the collision. The fact that this still gives the classical velocity distribution at equilibrium was interesting.

Classically the momentum is the product of both the mass of the particle m and its velocity v such that

$$p = mv \tag{6.15}$$

The classical picture of momentum is however incomplete. A prime example is that photons also have momentum but no mass such that the the momentum of a photon is a function of the photon's wave number.

$$p = \hbar k \ , \tag{6.16}$$

where $\hbar$ is the reduced Planck constant and k is the wave number of the photon. It is well known that the wave picture suggested by equation 6.16 also applies to particles of mass as per the de Broglie hypothesis. Consider momentarily the free propagation of a particle in one dimension in the framework of quantum mechanics. The momentum operator may be defined as

$$\hat{p} = \frac{\hbar}{i}\frac{d}{dx} \ , \tag{6.17}$$

while the corresponding kinetic energy operator is

$$T = -\frac{\hbar^2}{2m}\frac{d^2}{dx^2} \ , \tag{6.18}$$

These operators are applied to ψ the wave-function to yield the observables momentum and kinetic energy as eigenvalues. The time independent Schrödinger equation $H\psi = E\psi$ is then

$$-\frac{\hbar^2}{2m}\frac{d^2}{dx^2}\psi = E\psi \ , \tag{6.19}$$

As the particle is free there is no potential energy operator for the Hamiltonian. Equation 6.19 has

the solution

$$\begin{aligned} \psi(x) &= Ae^{ikx} + Be^{-ikx} \\ k &= \left(\frac{2mE}{\hbar^2}\right)^{1/2} \end{aligned} \tag{6.20}$$

An alternative solution in real terms is

$$\begin{aligned} \psi(x) &= C\cos kx + D\sin kx \\ k &= \left(\frac{2mE}{\hbar^2}\right)^{1/2} \end{aligned} \tag{6.21}$$

The momentum operator can be used to obtain the momentum given by the wave function as $\hat{p}\psi = p\psi$. However this can only be obtained when applied to one of the terms of equation 6.20 such that in the case $B = 0$

$$\hat{p}\psi(x) = \frac{\hbar}{i}\frac{d}{dx}Ae^{ikx} = k\hbar Ae^{ikx} = k\hbar\psi \tag{6.22}$$

or in the case where $A = 0$

$$\hat{p}\psi(x) = \frac{\hbar}{i}\frac{d}{dx}Be^{-ikx} = -k\hbar Be^{ikx} = -k\hbar\psi \tag{6.23}$$

Which have the results of a momentum in the positive direction and a momentum in a negative direction respectively. If $A \neq 0$ and $B \neq 0$ then $\hat{p}\psi = p\psi$ does not have an eigenvalue solution. This is however, the linear momentum operator. But linear momentum is actually a highly idealized concept and likely as fictional as perfect circle. Planets are always orbiting other objects in a helical fashion. Atoms constantly shake back and forth, elementary particles all spin and do not have enough of a well defined position to even be travelling in straight line, space-time is itself curved, and the biological world is always wiggling. Not a scientific description for sure, but not devoid of truth either. It is interesting to note then, that the energy operator does have an eigenvalue solution when $A \neq 0$ and $B \neq 0$ as

$$-\frac{\hbar^2}{2m}\frac{d^2}{dx^2}\psi = -\frac{\hbar^2}{2m}\left(\frac{d^2}{dx^2}Ae^{ikx} + \frac{d^2}{dx^2}Be^{-ikx}\right) \tag{6.24}$$

applying the differential once

$$-\frac{\hbar^2}{2m}\frac{d^2}{dx^2}\psi = -\frac{\hbar^2}{2m}\left(\frac{d}{dx}ikAe^{ikx} + \frac{d}{dx}-ikBe^{-ikx}\right) \tag{6.25}$$

and then applying it again

$$-\frac{\hbar^2}{2m}\frac{d^2}{dx^2}\psi = -\frac{\hbar^2}{2m}\left((ik)^2Ae^{ikx} + (-ik)^2Be^{-ikx}\right) \tag{6.26}$$

Since $(-ik)^2 = (ik)^2 = -k^2$ we can factor both $(ik)^2$ and $(-ik)^2$ to get

$$-\frac{\hbar^2}{2m}\frac{d^2}{dx^2}\psi = \frac{\hbar k^2}{2m}\left(Ae^{ikx} + Be^{-ikx}\right) = \frac{\hbar k^2}{2m}\psi \tag{6.27}$$

thus yielding an eigenvalue solution. This net energy does not depend on A nor B and they may be set arbitrarily in terms of the energy. Plotting this function in time where $A > B$ or $B > A$ gives a natural motion of an object such as the translation of a foot while walking, or a worm when slithering.

Another benefit of the inverse action pairs was found in the stability of the simulation technique. Regardless of the initial conditions the mean velocity of the particles was always found to converge to a finite value and fluctuate around it. In the field of molecular dynamics many different techniques are applied to scale the velocity of particles or the size of the system to operate in different ensembles. [99] With inverse action pairs one would be able to easily scale the energy in the system without disrupting the immediate trajectories of the particles. Furthermore the stability was found to be robust through experimenting with atypical parameter settings.

Despite no direct processes being used to ensure that the particles maintain their separation the action exchange process maintained an acceptable degree of spatial separation between the particles. It was already known that the sequence detail algorithm would respect the fact of having at most one particle per cell. This result showed that the generalized interactions also exhibit this behaviour and that their use in the subsequent momentum balance was justified as far as the point particle model is concerned.

The selection of the parameters which consisted of the bulk of the analysis were arbitrary. Experimentation with the w_f parameter confirmed that this selection does not bear any significant

consequences which make the results unreliable due to this arbitrary selection. However, the parameters of action transmission do have important consequences on the emergent behaviours of the system of particles. For example the particles did not exhibit the typical transport properties that would be expected of spherical atomic species. The self-diffusion did not scale like actual gas species and the viscosity of a dense fluid scaled more like a gas, increasing with an increase in mean velocity. In order to obtain the actual behaviour of atomic species would require finding rules of action exchange with these properties. The rules would have to account for changes in behaviour with changes in transmittable action. Of these an infinite variety could be explored. One particular interaction of significant consequence that the generalized interactions and the algorithms considered do not provide any means of implementing is attractive interactions between particles.

It is possible for attraction to be described using inverse action pairs and objects that interact only locally. Consider two objects A and B separated at a distance. If all interactions are entirely local how could the presence of A be known to B such that B can be attracted to A? For B to know about A, or to feel A so to say, there must be a transmission from A to B. However the transmission of something from A to B would require that the something has momentum directed from A to B. If B is to respond to this something attractively then the momentum for this attraction cannot be derived from the something that was transmitted from A to B since the momentum is directed from A to B this momentum would act as a repulsive interaction between A and B, not attractive. If B could however emit momentum, like emitting a photon, pointing in the same direction as the vector from of A to B then the inverse action of this photon would yield a net attraction between A and B.

The particles exhibited a characteristically physical feature that there needs to be energy exchange with the surface in order for the correct form of the Navier-Stokes equation to be obtained. That the particles would not exchange energy with the surface in a real system is non-physical. The objects that make up the surface would have the same action exchange ability as the objects making up the fluid. In forbidding this process and finding the Navier-Stokes equation to be unsatisfied, but then satisfied from allowing this exchange process is a positive result in favour of the algorithm. These results were only done qualitatively as finding the exact form of the solution in the more complex flows would require the derivation of the momentum balance to keep all generalized interaction terms.

It was inferred from the results of the momentum balance that the sum of the inverse action pairs plays the same role as pressure in the Navier-Stokes equation. It is well know that the pressure of fluid drops when flowing through a confined structure such as an orifice or a grating. This same behaviour was seen in the simulations conducted. It is not to say that each particle can have an independent pressure which is solely the sum of its inverse action pairs. This relation to pressure was obtained by summing all the actions over surfaces along an element and so it was derived as a collective property as opposed to a particle property. A more in depth thermodynamic analysis is wanting based on these observations and would justified given the positive results.

Chapter 7

Summary, Conclusions, and Directions for Future Research

The product of this thesis is a set of ideas and an associated mathematical structure constituting a novel framework. The sole conclusion is that frameworks for representing objects may be created. A brief summary of the thesis will be given first, elucidating the process by which the framework was produced. Conclusions relevant to this framework will then be given in terse form. In closing, important directions for further research are presented.

Automata as mathematical models of computation have exceptionally general frameworks for description. Cellular automata in particular can have a structure similar to physical space and so have been used to tackle a variety of physical modelling challenges. Unfortunately there did not yet exist a means for constructing arbitrary objects in cellular automata. Accordingly their applicability to physical modelling has been greatly hindered as they lack this important ingredient for physical description. In an effort to create a framework for objects in cellular automata a conception of objects that did not rely on other objects i.e. substance, was required. Such a conception was found in Whitehead's process philosophy where objects are understood as recognizable forms derived from series of actual occasions. In addition, the history of the lattice gas automaton was reviewed as it is a cellular automaton model which has the ability to represent primitive objects and has found wide application.

A mathematical structure called an event-lattice was developed which uses some of the special

features of the lattice gas automaton. The characteristic feature of the event-lattice was in the definition of an event so that extension in time and extension in space were derivative notions of events as opposed to the converse. It furthermore imposes a symmetry that as there cannot be absolute translation in space with no translation in time, there is no translation in time without translation in space. This result was obtained by reasoning through operational definitions for measuring the passage of time. Investigations of the world-line of objects in a partitioned one dimensional space-time with appropriately chosen spatial and temporal resolutions lead to the conclusion that objects may be represented as finite sequences. The objects that were constructed in the event-lattice were found to have a number of agreeable properties. Using the event-lattice as a basis a cellular automaton with the ability to implement objects was devised.

In order to evaluate the merit of the concept all attention was focused on constructing a sequence model of point particles. A sequence detail algorithm was devised which allowed these objects to maintain identity by virtue of never occupying the same cell. The basic functioning of this model was then generalized so that the interactions of the particles could be put into analytical form. With the generalized interactions in hand a momentum balance could be conducted on a volume element of fluid. Assuming constant density and equal probability of interactions an equation with similar structure to the Navier-Stokes equation was obtained. The characteristic features being that the change in momentum is proportional to the second derivative of the velocity and the negative gradient of transmittable action. An identification was suggested between the transmittable action of the particles and the pressure. This derivation did not require the Boltzmann equation and thus did not require the Chapman-Enskog expansion. These interactions were then put into vector form and it was shown that an algorithm akin to the Lattice Boltzmann Method could be created to investigate the predicted characteristics of the point particle model. A retrofitted Lattice Boltzmann Method was devised and described in detail. Using the retrofitted model simulations could be conducted with particles which should behave like the sequence point particle objects. Various equilibrium properties were obtained. The critical features was that particles always relax to velocity distribution of the Maxwell-Boltzmann family. The mean velocity of the particles was found to be a function of the total transmittable action and the nature by which action was exchanged between particles. The particles remained spatially extended even though no algorithmic processes were in place to forbid it. A characteristic time was found for the interactions and was shown to

exhibit time step invariance with respect to transport coefficients of kinematic viscosity and self-diffusion. The particles were used in conventional flow geometries. Shearing between two plates was used to investigate the effects of different boundary conditions. Flow through an array of cylinders showed that the particles could be used in more complex geometries and that there is a definite association between pressure and the transmittable action of the particles.

The conclusions of this work center upon the mathematical structure which was devised, the main conclusion being that representations of objects in cellular automata are indeed possible to obtain. In general each state of an automaton should have a direct relevance to its neighborhood, otherwise there is no means by which to reduce the complexity of the automaton. The event-lattice is based on this fact. Rejection of the identity element is paramount for actions which are considered as events. Inclusion of an identity action admits asymmetrical treatment of space and time with respect to events and diverges from bare fact. Objects are representable as sequences of actions. It is imperative to not differentiate between the doing of an object and the object itself. Action itself can be a basis of what is conventionally termed substance. Strict differentiation must be maintained between actual occurrences and objects. Topology may be used to describe objects more generally. Free groups generated from the action set may be used for representing the actual occurrences of objects. The length of a sequence as representing an object provides an adequate measure of what is conventionally termed energy and its interpretation in the framework yields many agreeable properties. The fact that there are two degrees of freedom for motion in each dimension does not produce alarmingly divergent results from expected behaviour of massive point particles. An equation of similar form to the Navier-Stokes equation can be obtained from the consideration of these two degrees of freedom granted useful assumptions. Useful simulation techniques can be constructed from these basic notions. Further enquiry into representing objects as sequences is warranted.

The results are stimulating but only preliminary and much more work needs to be conducted on the theoretical aspect of this representation. Relations among sequence objects should be studied in the context of elementary transformations of free groups as found in combinatorial topology. [91] An entirely different avenue of future research may be to utilize sequences in the classical form of cellular automata. The sequence detail algorithm is already sufficient to construct reversible cellular automata which is one of the main challenges in this area of research. In this realm focus

could be placed on searching for rules in which classical objects emerge instead of attempting to define them directly.

The main drawback and perhaps debilitating feature of the sequence representations of common objects i.e. those with mass, is that they require incredibly large sequences. The most important future work directly relevant to the conception outlined in this thesis would be in studying the compact representations of sequences. As much as those studies would be practical they are also fundamental. The sequence representation of objects does not put any constraint on the path that an object follows in the lattice, yet freely propagating objects tend to travel in straight lines. If the composition of the actions which the object consists of were considered to be the informational content about the object, then the straight line path would be the most compact representation of the object. That is, an object travelling in a straight line with a sequence, has the highest rate of information release about the object. Thus an object exhibiting this sequence is in a state of maximal entropy in the sense that a gas at equilibrium has maximum entropy because any part of the gas can be measured to give the properties of the whole gas. In the same way, objects which travel on the same line exhibit the maximum information about the composition of the object in the minimal time. That is, maximal entropy as it relates to a sequence may be summarized by the dictum that the whole may be characterized by the part. This is stimulating in the sense that if there is a principle of maximally compact sequences it could replace the principle of least action in that it causes objects to travel in straight lines in accordance with their momentums. This whole conception can be rephrased in a way sympathetic to quantum mechanics in that the the most observable path an object takes is the path that reveals the most information about the object. Or perhaps on a more human level it is the actions we take that reveal the most about ourselves.

Bibliography

[1] A. N. Whitehead, *An Enquiry Concerning the Principles of Natural Knowledge.* Cambridge: University Press, 1919.

[2] T. Toffoli, "Cellular automata as an alternative to (rather than an approximation of) differential equations in modeling physics," *Physica D: Nonlinear Phenomena*, vol. 10, no. 1, pp. 117 – 127, 1984.

[3] R. P. Feynman, "Simulating physics with computers," *Int. J. Theor. Phys.*, vol. 21, no. 6/7, pp. 467–488, 1982.

[4] G. Hooft, "Equivalence relations between deterministic and quantum mechanical systems," *Journal of Statistical Physics*, vol. 53, no. 1, pp. 323–344, 1988.

[5] E. Fredkin, "An informational process based on reversible universal cellular automata," *Physica D: Nonlinear Phenomena*, vol. 45, no. 1, pp. 254 – 270, 1990.

[6] G. J. Holton, *Thematic Origins of Scientific Thought: Kepler to Einstein.* Harvard University Press, 1988.

[7] C. E. Shannon, "A mathematical theory of communication," *Bell System Technical Journal*, vol. 27, no. 3, pp. 379–423, 1948.

[8] C. H. Bennett, "Logical reversibility of computation," *IBM Journal of Research and Development*, vol. 17, no. 6, pp. 525–532, 1973.

[9] ——, "Notes on the history of reversible computation," *IBM Journal of Research and Development*, vol. 32, no. 1, pp. 16–23, 1988.

[10] J. V. Neumann, *Theory of Self-Reproducing Automata*, A. W. Burks, Ed. Champaign: University of Illinois Press, 1966.

[11] S. Wolfram, "Cellular automata as models of complexity," *Nature*, vol. 311, no. 4, pp. 419–424, 1984.

[12] A. N. Whitehead, *Science and The Modern World*. Cambridge: University Press, 1926.

[13] A. Salomaa, *Theory of Automata*. Oxford: Pergamon Press Ltd., 1969.

[14] P. H. Starke, *Abstract Automata*. Amsterdam: North-Holland Publishing Company, 1972.

[15] B. Trakhtenbrot and Y. M. Barzdin, *Finite Automata Behaviour and Synthesis*. Amsterdam: North-Holland Publishing Company, 1973.

[16] E. F. J. Asmus and J. Florentin, "Algebraic machine theory of machines, languages, and semigroups," in *Algebraic Machine Theory and Logical Design*, M. A. Arbib, Ed. New York: Academic Press, 1968.

[17] A. W. Burks, "Von neumann's self-reproducing automata," in *Essays on Cellular Automata*, A. W. Burks, Ed. Chicago: University of Illinois, 1970.

[18] S. Ulam, "Random processes and transformations," in *Sets, Numbers, and Universes*. MIT Press, 1974.

[19] K. J. Preston and M. J. Duff, *Modern Cellular Automata: Theory and Applications*. New York: Plenum Press, 1984.

[20] E. F. Codd, *Cellular Automata*. New York: Academic Press, 1968.

[21] A. Adamatzky and G. J. Martinez, *Designing beauty: the art of cellular automata.*, ser. Emergence, complexity and computation: volume 20. Cham: Springer, 2016.

[22] C. G. Langton, "Self-reproduction in cellular automata," *Physica D: Nonlinear Phenomena*, vol. 10, no. 1, pp. 135 – 144, 1984.

[23] P. G. Khalatur, D. G. Shirvanyanz, N. Y. Starovoitova, and A. R. Khokhlov, "Conformational properties and dynamics of molecular bottle-brushes: A cellular-automaton-based simulation," *Macromolecular Theory and Simulations*, vol. 9, no. 3, pp. 141–155, 2000.

[24] J. M. Koelman and A. Vianney, "Cellular-automaton-based simulation of 2d polymer dynamics," *Phys. Rev. Lett.*, vol. 64, no. 16, pp. 1915–1918, 1990.

[25] J. M. Greenberg, B. D. Hassard, and S. P. Hastings, "Pattern formation and periodic structures in systems modeled by reaction-diffusion equations," *Bulletin of the American Methematical Society*, 1978.

[26] D. Dab, J.-P. Boon, and Y.-X. Li, "Lattice-gas automata for coupled reaction-diffusion equations," *Phys. Rev. Lett.*, vol. 66, no. 19, pp. 2535–2538, 1991.

[27] S. Cornell, M. Droz, and B. Chopard, "Role of fluctuations for inhomogeneous reaction-diffusion phenomena," *Phys. Rev. A*, vol. 44, pp. 4826–4832, Oct 1991.

[28] R. White and G. Engelen, "Cellular automata and fractal urban form: A cellular modelling approach to the evolution of urban land-use patterns," *Environment and Planning A: Economy and Space*, vol. 25, no. 8, pp. 1175–1199, 1993.

[29] M. Batty, Y. Xie, and Z. Sun, "Modeling urban dynamics through gis-based cellular automata," *Computers, Environment and Urban Systems*, vol. 23, no. 3, pp. 205 – 233, 1999.

[30] I. Santé, A. M. García, D. Miranda, and R. Crecente, "Cellular automata models for the simulation of real-world urban processes: A review and analysis," *Landscape and Urban Planning*, vol. 96, no. 2, pp. 108 – 122, 2010.

[31] G. Sirakoulis, I. Karafyllidis, and A. Thanailakis, "A cellular automaton model for the effects of population movement and vaccination on epidemic propagation," *Ecological Modelling*, vol. 133, no. 3, pp. 209 – 223, 2000.

[32] S. H. White, A. M. del Rey, and G. R. Sánchez, "Modeling epidemics using cellular automata," *Applied Mathematics and Computation*, vol. 186, no. 1, pp. 193 – 202, 2007.

[33] A. Deutsch and S. Dormann, *Cellular Automaton Modeling of Biological Pattern Formation: Characterization, Applications, and Analysis*. Boston: Birkhauser, 2005.

[34] J. W. Wimpenny and R. Colasanti, "A unifying hypothesis for the structure of microbial biofilms based on cellular automaton models," *FEMS Microbiology Ecology*, vol. 22, no. 1, pp. 1–16, 1997.

[35] G. Ermentrout and L. Edelstein-Keshet, "Cellular automata approaches to biological modeling," *Journal of Theoretical Biology*, vol. 160, no. 1, pp. 97 – 133, 1993.

[36] K. Fujibayashi, R. Hariadi, S. H. Park, and S. Murata, "Toward reliable algorithmic self-assembly of dna tiles: A fixed-width cellular automaton pattern," *Nano Letters*, vol. 8, no. 7, 2008.

[37] M. Rubenstein, A. Cornejo, and R. Nagpal, "Programmable self-assembly in a thousand-robot swarm," *Science*, vol. 345, no. 6198, pp. 795–799, 2014.

[38] P. W. K. Rothemund, N. Papadakis, and E. Winfree, "Algorithmic self-assembly of dna sierpinski triangles," *PLOS Biology*, vol. 2, no. 12, pp. 2041–2053, 12 2004.

[39] M. S. Kai Nagel, "A cellular automaton model for freeway traffic," *Journal de Physique I*, vol. 2, no. 12, pp. 2221–2229, 1992.

[40] S. Maerivoet and B. D. Moor, "Cellular automata models of road traffic," *Physics Reports*, vol. 419, no. 1, pp. 1 – 64, 2005.

[41] O. Biham, A. A. Middleton, and D. Levine, "Self-organization and a dynamical transition in traffic-flow models," *Phys. Rev. A*, vol. 46, no. 10, pp. 6124–6127, 1992.

[42] C. Burstedde, K. Klauck, A. Schadschneider, and J. Zittartz, "Simulation of pedestrian dynamics using a two-dimensional cellular automaton," *Physica A: Statistical Mechanics and its Applications*, vol. 295, no. 3, pp. 507 – 525, 2001.

[43] A. Kirchner and A. Schadschneider, "Simulation of evacuation processes using a bionics-inspired cellular automaton model for pedestrian dynamics," *Physica A: Statistical Mechanics and its Applications*, vol. 312, no. 1, pp. 260 – 276, 2002.

[44] C. G. Langton, "Studying artificial life with cellular automata," *Physica D: Nonlinear Phenomena*, vol. 22, no. 1, pp. 120 – 149, 1986.

[45] H. Balzter, P. W. Braun, and W. Köhler, "Cellular automata models for vegetation dynamics," *Ecological Modelling*, vol. 107, no. 2, pp. 113 – 125, 1998.

[46] P. Hogeweg, "Cellular automata as a paradigm for ecological modeling," *Applied Mathematics and Computation*, vol. 27, no. 1, pp. 81 – 100, 1988.

[47] M. J. Simpson, A. Merrifield, K. A. Landman, and B. D. Hughes, "Simulating invasion with cellular automata: Connecting cell-scale and population-scale properties," *Phys. Rev. E*, vol. 76, no. 2, p. 021918, 2007.

[48] S. Bandini, B. Chopard, and M. Tomassini, Eds., *Cellular Automata: 5th International Conference On Cellular Automata for Research and Industry, Geneva, Switzerland, October 9-11, Proceedings.* Berlin: Springer, 2002.

[49] S. El Yacoubi, B. Chopard, and S. Bandini, Eds., *Cellular Automata: 7th International Conference On Cellular Automata for Research and Industry, Perpignan, France, September 20-23, Proceedings.* Berlin: Springer, 2006.

[50] H. Umeo, Ed., *Cellular Automata: 8th International Conference On Cellular Automata for Research and Industry, Yokohama, Japan, September 23-26, Proceedings.* Berlin: Springer, 2008.

[51] S. Bandini and G. C. Sirakoulis, Eds., *Cellular Automata: 9th International Conference On Cellular Automata for Research and Industry, Ascoli Piceno, Italy, September 21-24, Proceedings.* Berlin: Springer, 2010.

[52] G. C. Sirakoulis and S. Bandini, Eds., *Cellular Automata: 10th International Conference On Cellular Automata for Research and Industry, Santorini Island, Greece, September 24-27, Proceedings.* Berlin: Springer, 2012.

[53] J. Was, G. C. Sirakoulis, and S. Bandini, Eds., *Cellular Automata: 11th International Conference On Cellular Automata for Research and Industry, Krakow, Poland, September 22-25, Proceedings.* Berlin: Springer, 2014.

[54] S. El Yacoubi, J. Was, and S. Bandini, Eds., *Cellular Automata: 12th International Conference On Cellular Automata for Research and Industry, Fez, Morocco, September 5-8, Proceedings*. Berlin: Springer, 2016.

[55] M. M. Waldrop, *Complexity: the Emerging Science At the Edge of Order and Chaos*. New York: Simon & Schuster, 1992.

[56] S. Wolfram, *A New Kind of Science*. Wolfram Media, 2002.

[57] S. A. Kauffman, "Emergent properties in random complex automata," *Physica D: Nonlinear Phenomena*, vol. 10, no. 1, pp. 145 – 156, 1984.

[58] A. Watts, "The myopic view of the world," in *Eastern Wisdom, Modern Life - Collected Talks 1960-1969*. Novato: New World Library, 2006.

[59] W. V. O. Quine, *Methods of Logic*, 4th ed. Harvard University Press, 1982.

[60] A. Korzybski, *Science and Sanity an Introduction to Non-Aristotelian Systems and General Semantics*, 4th ed. Lakeville: International Non-Aristotelian Library, Science Press Printing Company, Distributors, 1941.

[61] A. N. Whitehead, *Process & Reality*. New York: The MacMillan Company, 1930.

[62] J. Hardy, Y. Pomeau, and O. de Pazzis, "Time evolution of a two-dimensional model system. i. invariant states and time correlation functions," *Journal of Mathematical Physics*, vol. 14, no. 12, pp. 1746–1759, 1973.

[63] J. Hardy, O. de Pazzis, and Y. Pomeau, "Molecular dynamics of a classical lattice gas: Transport properties and time correlation functions," *Phys. Rev. A*, vol. 13, no. 5, pp. 1949–1961, 1976.

[64] U. Frisch, B. Hasslacher, and Y. Pomeau, "Lattice-gas automata for the navier-stokes equation," *Phys. Rev. Lett.*, vol. 56, no. 14, pp. 1505–1508, 1986.

[65] S. A. Orszag and V. Yakhot, "Reynolds number scaling of cellular-automaton hydrodynamics," *Phys. Rev. Lett.*, vol. 56, no. 16, pp. 1691–1693, 1986.

[66] N. Margolus, T. Toffoli, and G. Vichniac, "Cellular-automata supercomputers for fluid-dynamics modeling," *Phys. Rev. Lett.*, vol. 56, no. 16, pp. 1694–1696, 1986.

[67] G. R. McNamara and G. Zanetti, "Use of the boltzmann equation to simulate lattice-gas automata," *Phys. Rev. Lett.*, vol. 61, no. 20, pp. 2332–2335, 1988.

[68] F. J. Higuera and J. Jiménez, "Boltzmann approach to lattice gas simulations," *EPL (Europhysics Letters)*, vol. 9, no. 7, pp. 663–668, 1989.

[69] F. J. Higuera, S. Succi, and R. Benzi, "Lattice gas dynamics with enhanced collisions," *EPL (Europhysics Letters)*, vol. 9, no. 4, pp. 345–349, 1989.

[70] U. Frisch, D. d'Humieres, B. Hasslacher, P. Lallemand, Y. Pomeau, and J. Rivet, "Lattice gas hydrodynamics in two and three dimensions," *Complex Systems*, vol. 1, no. 4, pp. 649–707, 1987.

[71] P. L. Bhatnagar, E. P. Gross, and M. Krook, "A model for collision processes in gases. i. small amplitude processes in charged and neutral one-component systems," *Phys. Rev.*, vol. 94, no. 3, pp. 511–525, 1954.

[72] Y. H. Qian, D. D'Humières, and P. Lallemand, "Lattice bgk models for navier-stokes equation," *EPL (Europhysics Letters)*, vol. 17, no. 6, pp. 479–484, 1992.

[73] H. Chen, S. Chen, and W. H. Matthaeus, "Recovery of the navier-stokes equations using a lattice-gas boltzmann method," *Phys. Rev. A*, vol. 45, no. 8, pp. R5339–R5342, 1992.

[74] D. d'Humières, "Generalized lattice boltzmann equations," in *Rarefied gas dynamics: theory and simulations*, B. D. Shizgal and D. P. Weaver, Eds. Washington, D.C.: American Institute of Aeronautics and Astronautics, Inc., 1994, pp. 450–458.

[75] I. Ginzburg, M. Krafczyk, P. Lallemand, L.-S. Luo, and D. d'Humières, "Multiple–relaxation–time lattice boltzmann models in three dimensions," *Philosophical Transactions of the Royal Society of London A: Mathematical, Physical and Engineering Sciences*, vol. 360, no. 1792, pp. 437–451, 2002.

[76] X. He and L.-S. Luo, "Theory of the lattice boltzmann method: From the boltzmann equation to the lattice boltzmann equation," *Phys. Rev. E*, vol. 56, no. 6, pp. 6811–6817, 1997.

[77] D. A. Wolf-Gladrow, *Lattice-gas Cellular Automata and Lattice Boltzmann Models : an Introduction*. Berlin: Springer-Verlag, 2000.

[78] S. Succi and R. Benzi, "Lattice boltzmann equation for quantum mechanics," *Physica D: Nonlinear Phenomena*, vol. 69, no. 3, pp. 327 – 332, 1993.

[79] D. Meyer, "From quantum cellular automata to quantum lattice gases," *J Stat Phys*, vol. 85, no. 5/6, pp. 551–574, 1996.

[80] G. Grössing and A. Zeilinger, "Quantum cellular automata," *Complex Systems*, vol. 2, no. 2, pp. 197–208, 1988.

[81] ——, "A conservation law in quantum cellular automata," *Physica D*, vol. 31, no. 1, pp. 70–77, 1988.

[82] ——, "Structures in quantum cellular automata," *Physica B+C*, vol. 151, no. 1, pp. 366 – 369, 1988.

[83] A. N. Whitehead, *The Concept of Nature: Tarner Lectures*. Cambridge: University Press, 2015.

[84] A. Ashtekar, *100 Years of Relativity: Space-time Structure Einstein and Beyond*. Hackensack: World Scientific, 2005.

[85] E. Schrödinger, *The Interpretation of Quantum Mechanics*. Woodbridge: Ox Bow Press, 1995.

[86] Feynman and Hibbs, *Quantum Mechanics and Path Integrals*. New York: cGraw-Hill, 1965.

[87] R. P. Feynman, "The development of the space-time view of quantum electrodynamics," *Science*, vol. 153, no. 3737, pp. 699–708, 1966.

[88] G. 't Hooft, K. Isler, and S. Kalitzin, "Quantum field theoretic behavior of a deterministic cellular automaton," *Nuclear Physics B*, vol. 386, no. 3, pp. 495 – 519, 1992.

[89] G. 't Hooft, *The Cellular Automaton Interpretation of Quantum Mechanics*. Cham: Springer, 2016.

[90] ——, "On the quantization of space and time," in *Proceedings of the Moscow Seminar on Quantum Gravity*, M. Markov, V. Berezin, and V. Frolov, Eds. World Scientific, 1988.

[91] K. Reidmeister, *Einführung in die kombinatorische Topologie*. Darmstadt: Wissenschaftliche Buchgesellschaft, 1932.

[92] M. P. Allen and D. J. Tildesley, *Computer Simulation of Liquids*. New York: Clarendon Press, 1989.

[93] D. Frenkel and B. Smit, "Section 4.4 - molecular dynamics simulation - diffusion," in *Understanding Molecular Simulation*, 2nd ed., D. Frenkel and B. Smit, Eds. San Diego: Academic Press, 2002, pp. 139 – 163.

[94] B. J. Palmer, "Transverse-current autocorrelation-function calculations of the shear viscosity for molecular liquids," *Phys. Rev. E*, vol. 49, no. 1, pp. 359–366, 1994.

[95] T. Toffoli and N. Margolus, *Cellular Automata Machines: A New Environment for Modeling*. Cambridge: MIT Press, 1987.

[96] A. Rahman, "Correlations in the motion of atoms in liquid argon," *Phys. Rev.*, vol. 136, no. 2A, pp. A405–A411, 1964.

[97] J. Naghizadeh and S. A. Rice, "Kinetic theory of dense fluids. x. measurement and interpretation of self-diffusion in liquid ar, kr, xe, and ch4," *The Journal of Chemical Physics*, vol. 36, no. 10, pp. 2710–2720, 1962.

[98] X. He and G. Doolen, "Lattice boltzmann method on curvilinear coordinates system: Flow around a circular cylinder," *Journal of Computational Physics*, vol. 134, no. 2, pp. 306 – 315, 1997.

[99] D. Frenkel and B. Smit, "Chapter 6 - molecular dynamics in various ensembles," in *Understanding Molecular Simulation*, 2nd ed., D. Frenkel and B. Smit, Eds. San Diego: Academic Press, 2002, pp. 139 – 163.